國立交通大學

電子工程學系 電子研究所

博士論文

微型基地台網路之佈局分析與效能估計

Femto Base Station Network Deployment & Performance Analysis

研 究 生：曾勇嵐

指導教授：黃經堯 教授

中 華 民 國 一 0 二 年 五 月

微型基地台網路之佈局分析與效能估計

Femto Base Station Network Deployment & Performance Analysis

研 究 生：曾勇嵐　　Student：Yung-Lan Tseng

指導教授：黃經堯　　Advisor：Ching Yao Huang

國 立 交 通 大 學

電子工程學系 電子研究所

博 士 論 文

A Dissertation

Submitted to Department of Electronics Engineering and

Institute of Electronics

College of Electrical and Computer Engineering

National Chiao Tung University

in Partial Fulfillment of the Requirements

for the Degree of

Doctor of Philosophy

in

Electronics Engineering

May 2013

Hsinchu, Taiwan, Republic of China

中華民國一０二年五月

Femto Base Station Network Deployment & Performance Analysis

Student：Tseng, Yung-Lan Advisor：Dr. Huang, Ching-Yao

Department of Electronics Engineering and Institute of Electronics
National Chiao Tung University

ABSTRACT

In this dissertation, we will analyze how to improve the cellular wireless communication system through the help of femto base station (femto BS) networks. Femto BS is a base station which provides much smaller coverage area and users can deploy femto BSs on locations where they want to improve the Quallity of Service (QoS). To ensure a proper downlink outage probability, design criterion based on a feasible femto base station (BS) density is analyzed. Considering femto BS deployment, a three-dimensional (3-D) Poisson model of random spatial distribution and stochastic geometry are used. From the study, closed forms of feasible femto BS density will be identified. Based on the frame structure of 4G cellular communication system, we also provide a fast approach to estimate the achievable throughput that user will obtain from femto BS networks. The analysis results not only can be used to predict the performance of various femto BS deployment scenarios but also can be used as a design criterion for resource control mechanism designs. Our research results about femto BS network can also be applied to other research topics of wireless communications. In our study, we further extend our study to the *m*-dimensional random networks and the fading figure estimation of Nakagami fading channel.

微型基地台網路之佈局分析與效能估計

學生：曾勇嵐　　指導教授：黃經堯 教授

國立交通大學電子工程學系暨電子研究所 博士班

摘　　要

在這篇論文中，我們將討論如何利用微型基地台網路來增進蜂巢式無線通訊系統的效能。微型基地台可以由一般使用者放置在任何地方，以增加通訊系統覆蓋率或是提升使用者的網路頻寬。但是微型基地台也為蜂巢式通訊系統帶來了新的問題。在我們的研究當中，我們提出提供使用者完整的系統覆蓋率為目標，調整微型基地台在空間當中的"密度"的想法。我們建立一個三維立體空間的隨機網路模型以及四類干擾情況。在每一類干擾情況下，我們分析微型基地台網路所容許的密度區間。在 4G 無線通訊系統的架構之下，我們也提供了一個可以快速估計微型基地台網路傳輸頻寬的估計方法。因此，我們的研究成果可直接應用於無線通訊系統對微型基地台網路的資源配置以及使用者端的服務品質控制。除了微型基地台網路外，我們的研究成果和數學分析還可以延伸應用在無線通訊的其他問題。在我們的論文當中，我們也提出了 1) m 維的隨機網路, 和 2) Nakagami fading channel 的 fading figure 估計方法, 兩項延伸應用。

致 謝

能夠完成這篇論文，真的要感謝出現在我生命周遭的許多人。首先，我要感謝我的父親-曾建友先生以及母親-彭亞娜小姐。謝謝你們在我人生遭遇挫折時，能夠一直持續地相信我，支持我，和幫我加油打氣。另外，還要感謝我的妹妹-映嘉。你是全家的開心果，也祝福妳能順利完成妳的碩士班學業。

感謝我的指導教授-黃經堯教授這些年來的教導，讓我得以順利畢業。在研究的過程中，老師一直給我很大的發揮空間，讓我得以解決難題，往前邁進。也謝謝師母，師母的鼓勵常讓我銘記在心。感謝實驗室的夥伴們，從最初的慧源學長，明原學長、阿坤學長、宜霖學長、文嶽學長、以及振哲學長，和我差不多同時進入實驗室的彥翔、正達、建銘、裕隆、宜鍵、雲懷、大瑜、盟翔、宗奇、昌叡，以及後期的傑堯學長、子宗、明憲、Ensya、烜立、智元、東佑、泓志、仲煒和峻安。因為你們，我才有多采多姿的碩士班和博士班生活。希望即使在大家畢業多年後，還是可以常常見面，聊聊近況。我也要在此感謝交通大學的許多教授，包括王聖智教授、杭學鳴教授、蔣迪豪教授、林大衛教授、陳茂傑教授、等教授，讓我得以一窺無線通訊之美，並了解什麼是做學問應有的態度。

我在資策會工作的同事們，羅耿介顧問，李永台組長、吉隆、志偉、誼學、俊彥、均哲、舒慈、秋紋，以及和我一起在資策會工讀的智元、邵穎、佑賢、盈良，謝謝大家在無線通訊標準活動上給我的協助。參與標準活動讓我收穫豐富。另外，也謝謝宗諭常常討論和我討論數學和大台北美食餐廳情報。謝謝中央大學的許獻聰教授和宜蘭大學的陳懷恩教授常常在標準提案上提供珍貴的建議。

除了感謝學校和工作上的夥伴之外，我也要謝謝 Toastmasters 國際英文演講會的朋友們，包括 Legend Advance club、YZU club、和許多的 sister clubs。英文演講雖然和學術研究沒有直接關係，但卻又是影響深遠。因為在這四年來持續參與英文演講會，讓我不論是在學術會議還是日常生活，都可以有自信地在大眾場合侃侃而談而且條理分明。這一點，是我在參加 Toastmasters 之前所欠缺的。在這裡，我也遇到可以分享日常生活大小事情的好朋友們。未來的日子裡，我還需要向 Toastmasters 的各位多多學習。

我也想要藉由這個機會感謝我在大學以及碩士班時期所參加的交通大學諮商中心志工團。從西元 2000 年到西元 2006 年，我有七年的時間持續投入諮商中心的活動當中。在諮商中心裡，我遇到了許多智慧和專業兼備的諮商老師，包括韶玲老師、鶯珠老師、燦如老師、守謙老師、靜儀老師、景同老師、以及文昭姊等。在交通大學這樣以理工為主的環境當中，諮商中心給我不同的視野來面對人生的課題和選擇。而交通大學諮商中心志工團的好朋友們，十幾年的交情真的是很不容易，有許多朋友已經為人父母了。希望當我們頭髮斑白時，大家還可以一起聚首憶當年。

在這篇論文即將付梓之時，我在劉哲瑜先生的網路部落格上讀到下面這段話:

以前覺得很多夢想自己都達不到，但真的完成其中一項後，才會發現所謂的夢想是「令你害怕的事」。當你願意給自己機會去正視害怕，才有機會達成夢想，如果你不願去正視害怕，連眼前的敵人都不知道在哪，要怎麼擊倒它？要怎麼實現夢想？

我想，這也正是我攻讀博士班的心情寫照。在這幾年的博士班生涯當中，除了專業知識和求學態度的長進之外，也包含如何正視自己夢想，並全力以赴的心情轉變。謝謝在這段期間協助我正視我的夢想的各位。篇幅有限，但要感謝的人真的很多。另外，我還要謝謝郁心，在認識妳的這一年多的時間當中，我真的過得很快樂。也謝謝妳在我心情不好時，能夠適時鼓勵我。

最後，謹以此論文獻給在天上的阿公、阿嬤和爺爺、婆婆 。

曾勇嵐 謹誌

2013 年五月, 交通大學, 新竹, 台灣

I am the master of my fate

I am the captain of my soul

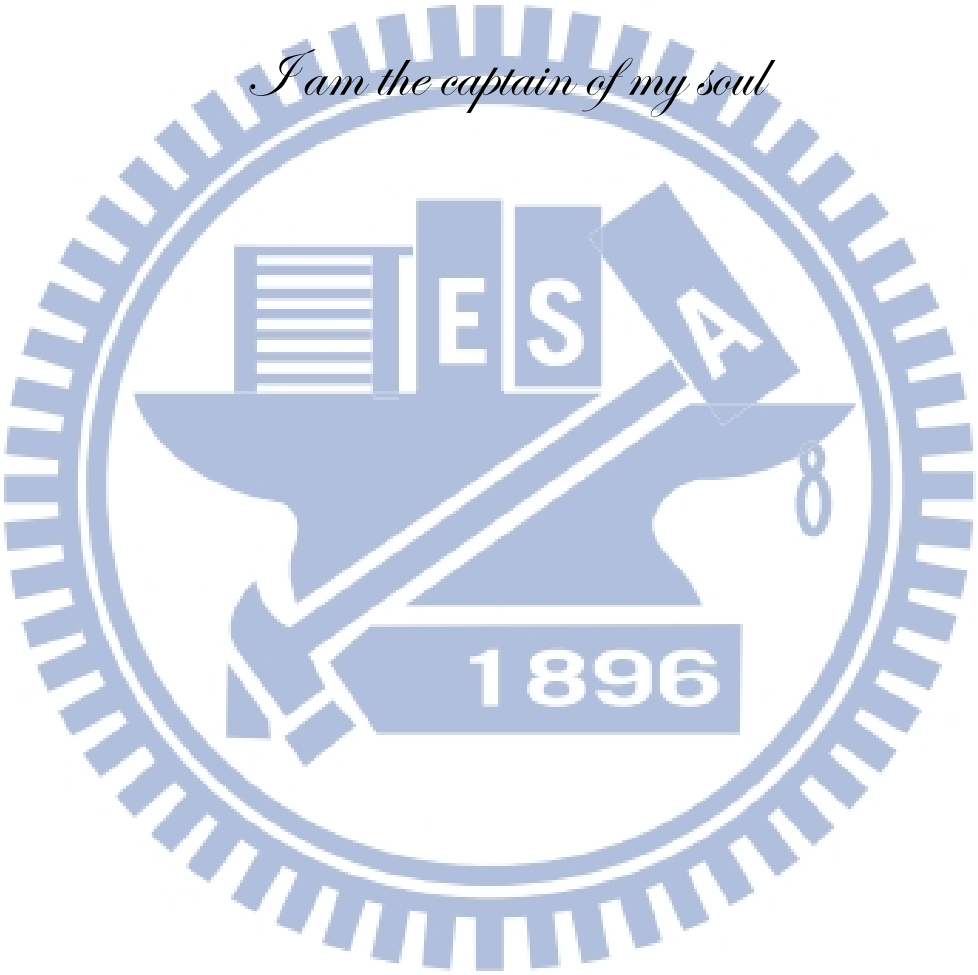

CONTENTS

FIGURES

Chap. 2

Chap. 3

Chap. 4

Chap. 5

TABLES

CHAPTER 1

DISSERTATION OVERVIEW

In this chapter, we will introduce the overview of our dissertation. In section 1.1, we introduce the background of our research. Then, we delineate the outline of our dissertation in section 1.2. In section 1.3, we summarize the definitions and abbreviations of vocabularies that often appear in this dissertation.

1.1 Overview of Dissertation Background

Cellular Wireless Communication network is now widely applied to serve a large part of the population in the world. In the era of first generation cellular network, the cellular network only supports voice service. Now, billions of users around the world require a wide range of data services from the real-time video streaming to the point to point packet transmission. It is expected the requirement towards the bandwidth will keep increasing in a dramatic speed. With the extention of cellular networks, it is already observed the increase of indoor data request. In 2008, more than 50% of voice call and more than 70% of data traffic are generated from the indoor environment [4]. However, because of the characters of signal propagation and complicated indoor surrounding, the cellular network still leaves indoor “coverage holes” in everywhere. To provide ubiquitous coverage, system providers need effective approaches to conquer the indoor coverage holes. Over the past few decades, many candidate technologies were proposed to improve the indoor bandwidth efficiency. Within these candidate approaches, Femto Base Station (Femto BS) is a promising technology which draws a lot of attention from

both the service providers and users.

The basic concept of femto BS is a base station which provides much smaller cell coverage in the cellular netowrks. In the history of cellular netowrks, devices such as micro BS and relay stations were proposed to enhance the signal quality and bandwidth efficiency. However, femto BSs obtain many features which are totally different with previous technologies. The features of femto BS include:

1) Femto BS can be deployed and installed by users.
2) Cell planning is absent in the femto BS networks.
3) Femto BS can provide different Quality of Service (QoS) to different users.
4) Femto BS needs to self-organize and self-optimize their operations.
5) Femto BS needs to cooperate with neighbor BSs automatically.

Because these innovative features and requirements of the femto BS network, femto BS leaves many problems to researchers. First, femto BSs bring flexibility to the cellular network by allowing users to deploy femto BSs by themselves. However, this flexibility makes the cell planning in the femto BS networks complicated. Furthermore, because users can install femto BSs in the location where the Singal to Interference plus Noise Ratio (SINR) needs to be enhanced, it can be expected there will be as many as thousands of femto BSs under the coverage of one macrocell. These femto BSs need to cooperate with each other to optimize the network performance. However, how to improve the efficiency of cellular network by optimizing the performance of femto BS networks is still a pending problem.

To improve the performance of femto BS networks, many studies concentrated on control mechanisms in Physical layer or Medium Access Control layer, such as the power control, resource allocation, or fractional frequency reuse. However, few researches took the random distributions of the femto BS networks, which will influence the system performance, into their consideration.

Besides the locations of femto BS networks, it is also difficult to analyze the throughput that femto BS networks contribute to the users. Most of the studies which analyzed the improvement of femto BS networks were achieved by field test or simulations. However, field test or computer simulations are not efficient in giving us the insight about how femto BS improves the system performance.

1.2 Contribution and Outline

In this dissertation, we will apply the concept of random network to analyze the femto BS networks. First, we use homogenous Poisson Point Process (HPPP) to describe the random distributions of femto BSs. Then, tools of stochastic geometry are applied to model the locations of femto BS networks. Our contributions include:

a) A novel 3-dimensional HPPP space model to analyze the femto BS networks.

In the previous studies about wireless communications, most of the scenarios were based on 2-dimensional (2-D) plane scenario. However, 2-D scenario cannot fulfill our requirement because femto BSs can be deployed by users in anywhere of the buildings. To address the feature of femto BS networks, we provide a novel 3-dimensional (3D) HPPP scenario to analyze the femto BS networks.

b) The range of feasible femto BS density of femto BS networks

Based on the stochastic features of femto BS networks, we will estimate the range of feasible femto BS density which provides fully coverage to the users. In our study, we will analyze the influence of the density of femto BS to the Signal to Interference Ratio (SIR). Then, we analyze how to control the femto BS density to decrease the probability of outage event. The conclusion of our analysis can be a reference of femto BS networks deployment and interference mitigation.

c) Extension to the log value estimation

Derived from our analysis, we also conduct a closed form to analyze the expected value of log value, $E[\ln(R_{n|m})]$. Here, m represents the dimension of HPPP and n represents the nth nearest node observed by the user. $R_{n|m}$ represents the distance between the user and the nth nearest node in the m dimensional space. Both m and n can be any positive integer. In our study, we will show that our closed form expression of $E[\ln(R_{n|m})]$ can be applied to many studies in wireless communications, such as the average signal strength estimation in random network (when $m<3$) and channel estimation of Nakagami fading channels.

d) Femto BS networks achievable throughput estimation

Based on our proposed 3-D HPPP model, we will provide a simple approach to

estimate the achievable throughput of femto BS networks. We will estimate the achievable throughput based on three assumptions: 1) OFDM (Orthogonal Frequency Division Multiplexing) system, 2) Non-cooperated packet transmission and 3) Hybrid Automatic Repeat Request.

The rest of the paper is arranged as follows: In Chap. 2, we will provide a broad introduction about the functions of femto BS and related research topics. In Chap. 3, we will estimate the range of feasible femto BS density under different scenarios. In Chap. 4, we extend our research result of $E[\ln(R_{n|m})]$ to other studies of the wireless communications. In Chap. 5, we propose a closed form for the throughput estimation of femto BS networks. Finally, the conclusions and summaries of this dissertation are summarized in Chap. 6.

1.3 Definitions and Abbreviations

Table 1-1 Definitions of corresponded vocabularies [1]

Vocabulary	Definition
Backhaul	The intermediate links between the core network and base stations.
Base Station	A network element in radio access network responsible for radio transmission and reception in one or more cells to or from the user equipment.
Cell	Radio network object that can be uniquely identified by a user equipment from a (cell) identification that is broadcasted over a geographical area from base station.
Cellular Network	A radio network distributed over land areas called cells, each served by at least one fixed-location transceiver, known as a cell site or base station.
Connection	A communication channel between two or more end-points (e.g. base station, server etc.).
Core Network	The central part of a telecommunication network that provides various services to customers who are connected by the access network.
Coverage Area	An area where services are provided by that cellular network to the level required of that system.
Quality of Service	The collective effect of service performances which determine the

	degree of satisfaction of a user of a service. It is characterized by the combined aspects of performance factors applicable to all services.
Service Provider	A service provider is either a cellular network operator or another entity that provides services to a user.
Throughput	A parameter describing service speed. The number of data bits successfully transferred in one direction between specified reference points per unit time.
User Equipment	Equipment that allows a user to access the network services. For the purpose of wireless communications the interface between the user equipment and the network is the radio interface.

Table 1-2 Abbreviations of the corresponded vocabularies

Vocabulary	Abbreviation
4G	4rd Generation
BS	Base Station
CDF	Cumulative Probability Function
CSG	Closed Subscriber Group
DSL	Digital Subscriber Line
DS-CDMA	Direct Sequence-Code Division Multiple Access
ggd	Generalized Gamma Distribution
HARQ	Hybrid Automatic Repeat reQuest
HPPP	Homogeneous Poisson Point Process
OFDM	Orthogonal Frequency Division Multiplexing
OFDMA	Orthogonal Frequency Division Multiple Access
OSG	Open Subscriber Group
PDF	Probability Density Function
QoS	Quality of Service
SIR	Signal to Interference Ratio
SINR	Signal to Interference plus Noise Ratio
SON	Self-Organization Network
UE	User Equipment

CHAPTER 2
INTRODUCTION OF FEMTO BS

In this chapter, we will introduce the femto BS and research topics derived from femto BS. In section 2.1, we introduce the origin of femto BS. Then, the features & functionalities of femto BS are introduced in section 2.2. In Section 2.3, we list the benefits that femto BSs bring to the cellular network. Although femto BSs benefit the cellular network and users, femto BSs also create new problems. In Section 2.4, we explain the new research topics which are caused by femto BSs and the candidate solutions proposed by preliminary studies.

2.1 The Origin of Femto BS

With the progress of wireless access technology, users' requirements to the cellular wireless communication systems also advance from voice service, short message, to the broadband data communications [2]. Therefore, the bandwidth requirement also grows in a dramatic speed [3]. Because of the popularity of wireless communication, now the users require wireless services in everywhere and so services providers of cellular communication systems need to provide ubiquitous coverage.

However, because of shadowing, multipath phenomenon, and wall penetration of buildings, the cellular network still leaves indoor coverage holes in anywhere. In the past, many candidate technologies were proposed to provide ubiquitous coverage. However, these candidate approaches also have their limits. In recent yeares, femto BS was

proposed to improve the inefficiency of celluar networks in the indoor environment [3]-[10].

The basic concept of femto BS is a base station which provides much smaller cell coverage in indoor areas. In the beginning, operators of cellular netowrks divided one large macro-cell, which is located in the metropolitan area, into many smaller cells. Small cells are applied in the metropolitan area because of two major reasons: First, comparing with suburb areas, areas with dense population have much heavier traffic loading. Under the condition that the backhaul bandwidth in each base station is the same, the cell size in metropolitan areas is shrunk from several kilometers to several hundred meters to guarantee the QoS that users obtains would not be affected by the population of their neighborhood. Second, users in metropolitan areas often suffer from serious signal degradation. Therefore, service providers generated the idea that deploying a base station closer to the end users to conquer the signal degradation. Now, because of more and more indoor traffic requests and strong signal degradation in the indoor areas, the size of base station shrinks further to serve the indoor users.

Before the proposal of femto BS, many candidate technologies were proposed to improve the radio access efficiency in the indoor condition. Here, we will introduce four of the most well known technologies: 1) micro BS, 2) relay station, 3) distributed antenna system, and 4) Wireless Local Area Network Access Point (WLAN AP).

Micro BS

Micro BS, which has been proposed nearly three decade ago [11], can be regarded as a base station with much smaller coverage. Similar to macro BS, micro cell is installed by system operators under careful frequency plan to prevent joint interference with neighbor base stations. The functionality of micro BS is the same with that of macro BS.

Relay Station

Relay station [12] is a signal repeater to receive and re-radiate radio signals from the poor coverage regions. However, their reuse of the licensed spectrum for backhaul limited the system throughput. Therefore, the benefit that relay station provides is limited and not simple to be deployed.

Distributed Antenna System

Distributed antenna (DAS) system [13] is also proposed to solve the signal degradation in the indoor environment. The basic idea of DAS is to install an indoor BS in the building and to deploy the antennas of the BS on different locations in the building. These antennas are connected with the BS through fiber or coaxial cable. DAS could largely improve the spectral efficiency of the network, if both the overlap between the coverage areas of the different antennas is reduced, and the coverage areas of the antennas fit as much as possible to the shape of the building. However, the backhaul connection of the BS is still limited. Furthermore, the deployment and wire connections between the BS and antennas are still complicated.

WLAN AP

Here, we use the IEEE 802.11 series standards [14] as the embodiment of WLAN AP. Comparing with the candidate technologies above, WLAN AP has the follow characters: i) It can be deployed by the users, and ii) Wireless LAN AP uses unlicensed bands to transmit/receive data. WLAN provides robust bandwidth connections in the indoor environment. However, WLAN AP provides service only in the indoor surrounding. Moreover, wireless LAN AP lacks handover and paging processes. So, it is difficult for WLAN AP to support user mobility. Furthermore, lack of joint cooperation between WLAN APs may enhance the mutual interference and so decrease the bandwidth efficiency of the network.

Because of more and more bandwidth requirement towards wireless communications and ubiquitous coverage for wireless broadband connection, these candidate technologies still cannot fulfill the users' requirements. Therefore, femto BS was proposed during the last ten years. From 2007, femto forum, a not-for-profit membership organization, was founded to enable and promote femto BS and femto technology. Furthermore, to improve the system capacity, standard organizations of 4G cellular network, such as 4G LTE (Long Term Evolution) [15] and WiMAX (Worldwide Interoperability for Microwave Access) [16] system, already included femto BSs and the functionalities that femto BS needs in their standard documenets. In the next section, we will introduce the features and functions of femto BSs.

2.2 Features of Femto BS Network

Based on the requirement of 4G cellular network [15]-[16], femto BS is a short range, low cost and low power base station. Femto BS can be deployed and installed by users for better indoor signal quality and bandwidth. This user-installed base station communicates with the cellular network through broadband connection such as DSL, cable modem, or even air link. Femto BS has many features, such as:

(1) Flexibility of deployment

The topology of macro BS network and femto BS network in the cellular network can be expressed through Fig. 2-1. Here, macro BS network represents the company of macro BSs and femto BS network represents the company of femto BSs. In Fig. 2-1, it is clear that the coverage of the femto BS network can be overlapped by the macro BSs or isolates from the macro BS networks. In Fig. 2-1, we call the areas that out of the coverage areas of cellular network as the coverage holes. Femto BSs are deployed to compensate those coverage holes. Besides compensating the coverage holes, femto BSs can also be deployed under the coverage of macro BS network to imoprove the QoS that uer experiences. In this condition, we call it as the macro/femto BS overlapping network. Because femto BSs can be deployed by users in everywhere which needs to improve the user QoS, it is difficult for service providers to optimize the performance of femto BS networks through cell planning.

(2) Huge number of femto BSs

Although femto BS was proposed just few years ago, femto BS already outnumbered traditional base stations by the end of 2010. Furthermore, now femto BSs are deployed at a rate of five millions per year [3]. It can be expected that how to control the huge number of femto BSs in the cellular network would become an important research topic.

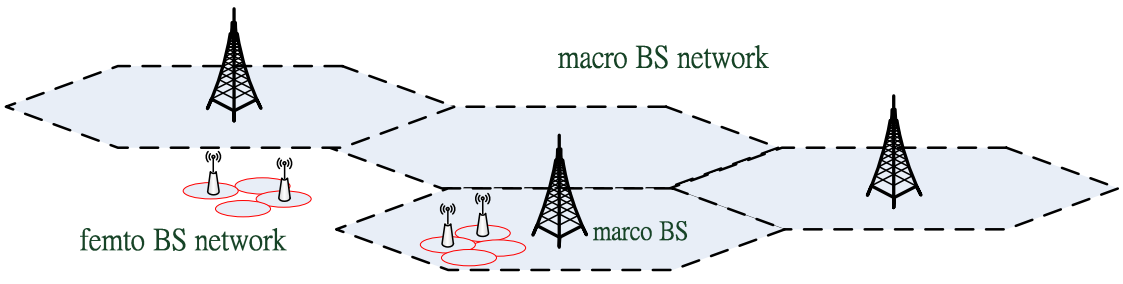

Fig. 2-1 Femto BS networks in the cellular System

(3) User priority

Because the femto BS and the backhaul connection are provided by users, it is reasonable that users will require different user access priorities and QoS requirements when the femto BS is dealing with the access request from different users. Based on the 4G wireless communications standards [15]-[16], three different access modes are supported by femto BS:

a) Closed Subscriber Group (CSG)

A CSG consists of a set of subscribers authorized by the femto BS owner or service provider. The CSG femto BS supports only users in the authorized CSG. A femto BS can belong to many different CSGs.

b) Open access (also known as Open Subscriber Group (OSG))

The open access femto BS supports all users within its coverage.

c) Hybrid access.

A hybrid femto BS supports both the authorized CSG users and non-CSG users, although the non-CSG users have only limited access.

Apparently, femto BSs will have different interference impacts on the surroundings when the associated access modes are different.

(4) Self-Organization Network (SON)

The self-organization Network is a concept that enables the femto BSs to adjust themselves with the minimum human manipulation. Here, we divide the SON into two stages, which are self-configuration and self-optimization.

In the macro BS networks, the radio parameters, such as the operating frequency bands and radiation powers, are set by system providers based on detailed cell planning. However, it would not be possible for users to set the control parameters of femto BSs by themselves. Therefore, femto BSs need the capability to set control parameters automatically. For example, femto BSs need to synchronize with the cellular network at the initialization stage. Moreover, femto BSs should also set its radiation power during the initialization process. The process that femto BSs set all the control parameters at the

initialization stage is called self-configuration.

In addition to self-configuration, the concept of self-optimization was also proposed in the studies of SON. The purpose of self-optimization is to adjust the operation of femto BS dynamically with the changes of the surroundings and users' QoS requirements. Some optimizations need the joint cooperation between neighbor BSs, which include both femto BSs and macro BSs.

(5) Operation Modes

In the cellular network, the macro BS and micro BS are always in the normal operational mode even there is no active user under their coverage. However, femto BS has multiple states during its operation. Based on [15]-[16], the power of femto BSs can be turned on/off by the users or the backhaul connection. Furthermore, femto BSs can step into low duty mode when there is no user under its coverage. Therefore, femto BS changes between multiple states during its operation, as illustrated in Fig. 2-2.

In Fig. 2-2, femto BS enters the initialization state when power on. In the initialization state, procedures such as time/frequency synchronization should be performed. In the end of initialization state, the femto BS should attach with the service provider's core network successfully. It is worthy to note that the femto BS is prohibited from turning on its radio frequency component before it finishes the attachment process with the core network. After attaching with service provider's core network, the femto BS enters the operational state. However, femto BS will revert to the initialization state when it becomes unattached to the service providers core network or fails to meet operational requirements [16].

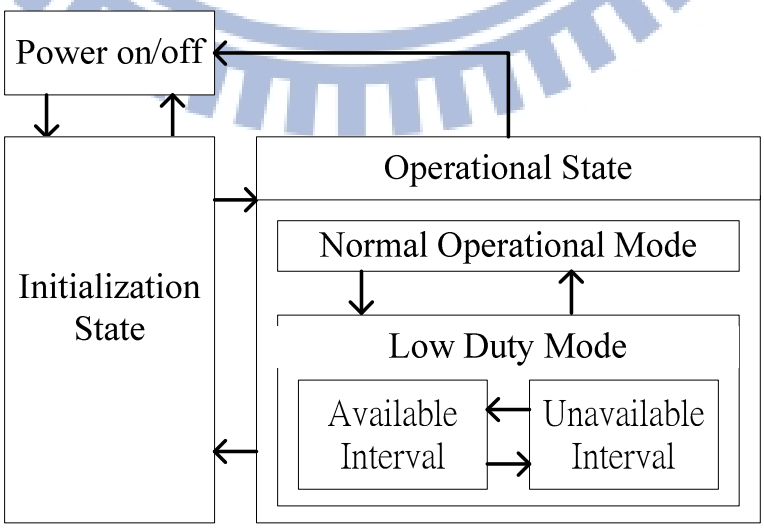

Fig. 2-2 Functional overview of femto BS states and operation modes [16]

Table 2-1 Comparisons of femto BSs with other candidate technologies

	Femto BS	Micro BS	WLAN AP	Relay Station	DAS
Spectrum	Licensed /Unlicensed	Licensed	Unlicensed	Licensed	Licensed
Cell Plan	No	Yes	No	Yes	Yes
Installation	User	Service provider	User	Service provider	Service provider
Backhaul	Cable/DSL	Telephony network	Cable/DSL	No	Telephony network
QoS Guarantee	Hard	hard	Soft	hard	hard
Privileged User	Yes	No	Yes	No	No

In the operational state, femto BS can transfer between normal and low-duty operation mode depending on the traffic loading of femto BS. In low-duty operation, the femto BS alters its operation mode during the available intervals (AI) and unavailable intervals (UAI) respectively. During the AI, the femto BSs may become active on the air interface for activities such as paging, boradcasting system information, and data transmission. During the UAI, femto BS turns off its radiation power to reduce the interference to neighbor cells. Femto BS may also take the chance of UAI to synchronize with the overlaid macro BS or measuring the interference from neighbor cells. Although the low-duty operation may decrease the mutual interference, it is also required that the low-duty operation should not disturb the normal operations of the cellular network and the user QoS [16]. The comparisons of femto BS and candidate access technologies are listed in Table 2-1.

2.3 Benefits of Femto BS

Because of the features that femto BS obtains, femto BS brings many benefits to the cellular networks and the users. The advantages of femto BS include [3]-[10]:

(1) Coverage holes compensation

For the cellular network, the coverage holes in the cellular network can be compensated by the deployment of femto BSs. Because of the isolation of coverage holes from the coverage of cellular network, femto BSs can reuse the frequency spectrum without interfering neighbor BSs and so the area spectral efficiency (bits/s/Hz/m^2) [17] of the cellular network also increases.

(2) Channel quality & spectrum efficiency

The channel qualities between the macro BS and indoor users are always affected by the indoor penetration loss and multipath effects. Because of poor channel quality, macro BSs need to assign more radio resource for indoor users to fulfill the users' QoS. With the deployment of femto BSs, the spectrum efficiency of the whole cellular system will be improved because the channel quality improves.

(3) Load balancing

Femto BS also helps the macro BS network to achieve load balancing. In the macro/femto BS overlapping network, macro BSs can offload the indoor traffic requirement to the femto BSs. Then, macro BSs could save more resource to serve outdoor users, handover users and roaming users. So, outdoor users also benefit from the deployment of femto BSs in both the air link and backhaul connection.

(4) Energy efficiency

To communicate with the macro BS network, indoor UEs need to radiate more radiation power to conquer the weak channel quality. Now, by connecting with the femto BS, UEs consume less power for good connection quality and so both the energy efficiency in packet transmission and the battery life of UEs increase.

2.4 Research Topics of Femto BS

Although femto BS brings many advantages to both the cellular network and the users, femto BS also increases the complexity of cellular network. Without cell planning, femto BS needs intelligent mechanisms to adjust itself based on users' requirements and the surroundings. In this section, we will introduce the preliminary studies about femto BS and their achievements.

2.4.1 Deployment Issue

It is difficult to quantify the influence of the deployment of femto BSs because the randomness of their locations. Many analysis of the femto BSs were achieved through simulations. In [5], a system level simulation was constructed by assuming a hexagonal macro BS network, which was combined with 19 macro BSs. The area of macro BS network was divided into multiple grid areas and the locations of femto BSs were

randomly selected from a grid with 20 m separation. In [18], a detailed apartment model was proposed for the research of femto BS in the LTE system. In [19], the deployment problem was analyzed by selecting the best configuration of femto BSs among many fixed testing points. To maximize the Shannon capacity in the building, the capacity was formulated as an equation related to the locations, radiation powers and channel selections of the femto BSs. Mixed integer programming was used to solve the optimal solution. Xiang *et al.* proposed a joint channel allocation and fast power control scheme [20]. By assuming femto BSs could sense and reuse the frequency spectrum, the downlink spectrum sharing problem in [20] was formulated as a mixed integer nonlinear programming problem and decomposition methods were applied to solve the problem. In [21], Liu *et al.* proposed a mathematical model to capture the unique building features. Based on the model in [21], a set of novel transformation strategies were provided to formulate the deployment issue into a mixed-integer convex program (MICP). Accordingly, an effective global optimization algorithm based on convex relaxation of the formulated MICP within a branch-and-bound framework was applied. Liu‘s works in [21] guaranteed a global optimal solution.

2.4.2 Interference Analysis and Mitigation

Because of the random distributions of femto BS network and different operation modes, femto BSs will produce strong interference if the joint interference is not solved appropriately. In [15], six interference scenarios of femto BS networks are plotted:

1) Femto user -> macro BS
2) Femto BS -> macro user
3) Macro user -> femto BS
4) Macro BS -> femto user
5) Femto user -> femto BS
6) Femto BS -> femto user

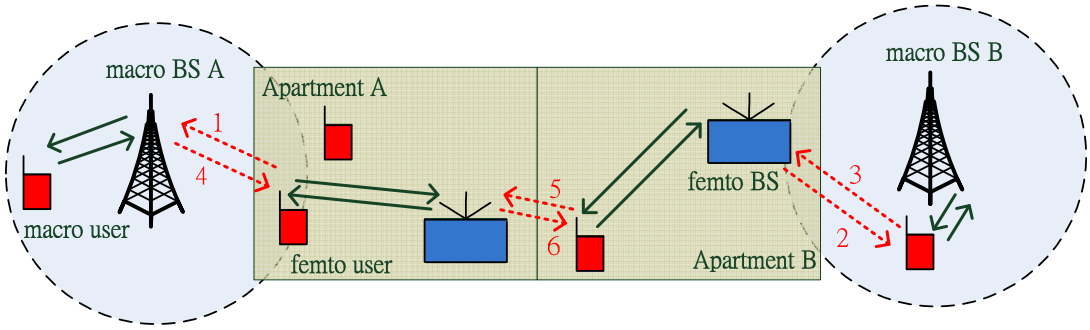

Fig. 2-3 Interference scenarios in the femto BS networks [15]

Macro user is the user who is served by macro BS and femto user is the user who is served by femto BS. In Fig. 2-3, the black solid lines represent data connection and the read dash lines represent interference.

In femto BS interference mitigation algorithm, most of the analyses and proposals are based on two popular radio access technologies: i) CDMA (Code Division Multiple Access) system, and ii) OFDMA system. Here, we will also introduce the preliminary studies based on their access technologies.

2.4.2.1 CDMA System

To analyze the interference that femto BS creates to the macro/femto BS overlapping network, Chandrasekhar and Andrews provided new mathematical models and analysis for the uplink interference problem in the two-tier CDMA-based CSG femto BS networks [22]. In [22], sectoring receiver antennas and time hopping-CDMA mechanism were proposed to be embedded in the femto BS to avoid mutual interference between the macro BS and femto BSs. Das and Ramaswamy investigated the reverse link capacity of femto cells by modeling inter-cell interference as a Gaussian random variable [23]. For CDMA femto cells, power control or saving a “macro BS only” spectrum was proposed by many studies [24]-[26]. In [27], Arulselvan *et al.* proposed a “geo-static scheme”, which to enable the femto BS to adjust power level in radio frequency based on its physical distance to the macro BS. Based on this adaptive power control scheme, the femto BS network locally achieved a target data rate that is centrally computed by the network.

2.4.2.2 OFDMA System

Chu *et al.* proposed a decentralized resource allocation scheme for the OFDMA downlink of a shared spectrum hybrid macro/femto network [28]. In [28], each femtocell randomly selects a subset of OFDMA resources for transmission. The proposed approach in [28] is simple in implementation. However, the random selection approach cannot provide the optimal system performance and QoS guarantee to UEs. To eliminate mutual interference, many studies proposed advanced algorithms baed on different directions, which include: a) Frequency planning, b) Power control, c) SON, d) Optimization problem, and e) Game Theorem.

a) Frequency plan

In [29]-[31], the authors discussed how to assign frequency carriers to femto BSs through the given frequency plan in macro BS networks. In these studies, fractional Frequency Reuse (FFR) was applied in the macro BS network. Then, femto BSs were proposed to reuse the macro BS spectrum to improve the spectrum efficiency. In [32], Ghosh *et al.* analyzed the improvement of FFR in the heterogeneous network. Their results can also be applied to the FFR in the macro/femto BS overlapping network. However, there is one implementation problem in this approach: How to decide if the femto BS could reuse the macro BS spectrum? To solve this problem, G¨uvenc *et al.* proposed a "interference-limited coverage area" (ILCA), which is an area within a contour where the received power levels from the macro BS and femto BS are the same [33] . The ILCA will be compared with a threshold (e.g., the area of a user's premises); if it is larger than the threshold, the femto BS is allowed for co-channel operation (i.e., it is in outer region). Otherwise, femto BS is in the inner region and it cannot reuse the macro BS spectrum. In [34], based on the objective to increase the system spectral efficiency, Bai *et al.* discussed the tendency of macro BS/femto BS to reuse or to partition the spectrum when the serving user is in different locations of the macro BS coverage. Then, a hybrid frequency allocation algorithm was proposed to improve the spectrum efficiency in the macro/femto BS overlapping network.

b) Power control

In [35], Li *et al.* formulated the downlink power control problem for femto BSs that operate in the same frequency carrier with macro BSs. Both centralized and distributed solutions were given jointly with a dynamic channel re-allocation procedure to assure the QoS of users. In [36], a distributed utility-based SINR adaptation was proposed for femto BS networks to alleviate cross-tier interference at the macro BS, which was interfered by overlaid femto BSs.

To briefly summarize, the interference elimination approaches above proposed to eliminate the interference between the macro/femto overlapping network by the popular techniques in the cellular netowrks, such as directional antennas, power control, and frequency participation. Next, we will introduce the studies about how to decrease the mutual interference through SON algorithm.

C) SON algorithm

The approaches of SON algorithms can be divided into three cooperation levels, which are shown in Fig. 2-4. Note that the three levels can co-exist in one control algorithm.

i) Self-Measurement

In self-Measurement, femto BS adjusts its operation parameters by measuring the environment itself. In [37], several heuristic frequency assignment schemes were proposed and compared. Based on their simulations, the LIP (Least Interference Power) scheme, which new femto BS selects the frequency band that has the minimum the received total interference power at the receiver side of itself, is the best practical scheme. However, the performance of LIP scheme is sensitive to the order of femto BSs turning on its radiation power. Furthermore, each femto BS can only access one frequency carrier, which limits the system capacity. To solve this problem, Garcia *et al.* proposed an "autonomous component carrier selection" approach [38]. First, each femto BS selects one least interfered primary carrier from a set of carriers based on its measurement. Then, allocation of additional secondary component carriers is possible if and only if the performance impact on neighboring cells is estimated to be acceptable. In [39], Sundaresan and Rangarajan proposed a distributed random access scheme (DRA). Accoring to DRA, the femto BS decides which resource blocks it occupies based on a hash table. The hash table is generated individually by each femto BS and the size of hash table is decided by the interfering degree, which is also measured by the femto BS itself. Femto BSs will rehash the hash table in the collided resource blocks. The details of resource blocks of OFDM system will be explained in Chap. 5.

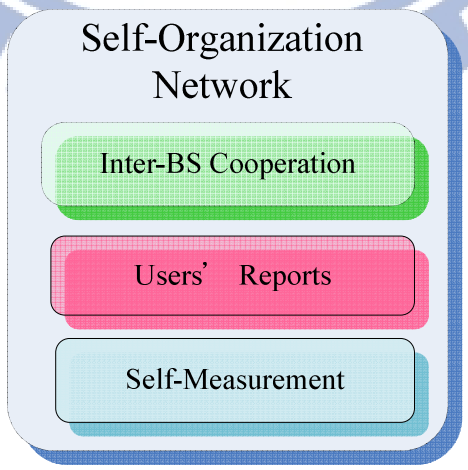

Fig. 2-4 Different cooperation levels of SON algorithms

Many studies also applied cognitive radio technique to realize the SON algorithm [40] -[43]. In [40], Lien *et al.* proposed a cognitive radio resource management (CRRM) scheme for femto BS networks. In CRRM, femto BSs periodically sense the channel to identify which resource block is occupied by the macro BS network. In subsequent data frames, femto BSs only allocate “non-occupied” resource blocks sensed in the sensing phase. To achieve optimal spectrum utility, femto BSs are required to record the following parameters: (i) the traffic loading of the macro BS network, (ii) radio resource allocation correlation probability of the macro BS network, and (iii) percentage of correlated radio resource allocation of the macro BS network. In [41], a localized dynamic spectrum access approach was proposed in a macro BS/femto BS overlapping network. In [41], femto BSs reuse the spectrum for macro-PU/femto-PU, which are primary users served by macro BS and femto BS respectively, by sensing the idle spectrum. Simulation results showed that throughput improves if spectrum sensing is achieved by femto BSs. It is because femto BSs are usually with better sensing capability. In [42], Jin *et al.* proposed to combine cognitive radio and multi-hop cooperative communication in the macro/femto BS overlapping network. By requiring every wireless device to be equipped with frequency-agile spectrum sensing units, Jin *et al.* developed an optimization framework for location-aware cooperative resource management, with jointly employing power control, multi-hop cooperative communication and flow management techniques. Based on stochastic geometry and homogeneous Poisson point process (HPPP), Cheng *et al.* proposed several corresponding downlink spectrum sharing schemes between femto BSs and macro BSs as well as among femto-BSs [43]. Moreover, by requiring femto BS to measure location information and avoidance region, the proposed Distance Sense Multiple Access (DSMA) and controlled-underlay schemes in [43] provided much more throughput than that in traditional interweave and slotted Aloha schemes.

To summatize, the Self-Measurement approach is easy to be implemented. Without information exchange between UEs and other BSs, the femto BS does not produce much control overhead to the backhaul network. However, the drawback of Self-Measurement approach is: the measurement from the femto BSs does not represent the measuremet of users. To fulfill users’ QoS requirements, femto BSs need the measurement reports from users.

ii) Users' Reports

In cellular network, users' reports are already applied in many control algorithms, such as handover process or frequency carrier selection [15]. In the femto BS networks, users' report is extended to modify the control parameters of femto BS network. In [44], Claussen *et al.* proposed a novel mobility-event based self-optimization approach to adjust the femto BS radiation power. In this approach, they tried to minimize the increase of unnecessary mobility events, such as passing and handover events. It was shown that mobility event based self-optimization of coverage can both significantly reduce the total number of mobility events caused by femto cell deployments and improve the indoor coverage. In [45], L´opez-P´erez *et al.* proposed two SON approaches for femto BS in the downlink direction. One is the femto BS selects the least interfered frequency carrier it detects from neighbor BSs. Another one is femto BS selects the least interfered frequency carrier that users measure. Simulations result showed the user based approach gets better performance. Although the femto BS networks can get better performance from the users' report, the number of calculations in each femto BS would increase exponentially with the number of users and the number of carriers. Furthermore, requiring UEs to perform measurements may enhance the power consumptions of UEs, which are typically power limited.

iii) Inter-BS Cooperation

To optimize the bandwidth efficiency and resource allocation, many researches proposed the capability that BSs exchanging information with neighbor cells through air links or backhaul connections [46]-[49]. In [46], Amirijoo *et al.* proposed that network detects an outage area autonomously based on measurements, which from both UEs and neighbor BSs. Then, the network alters the configuration of surrounding BSs to compensate the outage-induced coverage. In [47], Li *et al.* enhanced the joint cooperation of femto BSs by also requiring the information exchange between BSs.

However, even the system performance can be improved by the inter-BS information exchange, the propagation delay of backhaul connection is too long to allow dynamic cooperation between femto BSs and macro BSs [48]. To facilitate the information exchange, information exchange through air links was proposed in many studies. In [49], Adhikary *et al.* proposed a novel approach for the femto BSs to reuse the macro BS spectrum by listening to the resource allocation map, which is broadcasted by macro BS over the time slots. Furthermore, the femto BS also gets the locations information of UEs

through Global Positioning System. Then, femto BS will reuse the macro BS spectrum by limiting joint interference.

To briefly summarize, the inter-BS cooperation improves the system performance futher because of more information gathered during the process. However, it may also increase the signaling overhad and the loading of compulations to the cellular netowrks.

d) Optimization problem

Interference problem can also be solved by using the tools of optimization problem. In [50], L´opez-P´erez *et al.* proposed "dynamic frequency planing" by modeling the frequency allocation problem as a mixed integer programming. In the backhaul network, a centralized controller is responsible to gather all the measurements from users and BSs. Greedy algorithms were used in the simulations and the result showed the macro BS femto BS joint cooperation would conduct the best performance during the simulation. In [51], femto BSs were grouped based on the mutual interference information. Then, a central controller determined the minimum number of orthogonal sub-channels for each group to provide target performance. The transmission power of each femto BS was adjusted based on the received signal strength indication (RSSI) in a distributed manner. However, the above optimization problems require high complexity and centralized computations, which increase the difficulty to be implemented in the femto BS network.

e) Game theorem

Game theorem is also applied by many researchers to analyze spectrum allocation problem in the macro/femto BS overlapping network. In [52], Chen *et al.* proved the existence of the unique optimal solution of the channel allocation problem. Furthermore, they also proposed A DANCE mechanism for a general femtocell channel allocation problem. In [53], Lien *et al.* proposed the cognitive radio resource management scheme for femtocells to mitigate cross-tier interference. Under such cognitive framework, a strategic game was further developed for the intra-tier interference mitigation.

2.4.3 Load Balancing

In the section 2.3, we have introduced that femto BS can share the loadings of macro BS networks. To achieve the objective of load balancing, some studies suggested letting the UEs to prefer the femto BS on the BS selection stage. In [32], [54], the concept of

"range expansion" (also called cell biasing), where a UE may associate with a femto BS even though the received power from the the macro base-station on the downlink is higher, was demonstrated. However, it is obvious that this approach can lead to more interference from the macro BS at the UE which is associated with the femto BS. Therefore, a joint cell-association and scheduling for femto BSs and macro BSs had been discussed for downlink systems [54]. In [32], range expansion was combined with a TDM (Time Division Multiplexing) based interference cancellation approach to improve the overall user experience compared to a macrocell network. In [55], G¨uvenc *et al.* studied the impact of range expansion and number of femto BSs on both sum capacity and fairness of heterogeneous networks. Moreover, a new cell selection method, which adaptively expands the range of femto BSs based on the resource-specific SINR measurements, was proposed.

2.4.4 CSG/OSG Conflict

Different user priorities enhance the complexity of interference problem in femto BS networks. In [56], L´opez-P´erez *et al.* investigated the influence of CSG femto BS network through simulation. In the downlink direction, it had been demonstrated that the CSG femto BS network would decrease the total cell throughput by around 15% with respect to that of OSG femto BS network. Furthermore, CSG femto BS also increases the error reception events of outdoor users. In [57]-[58], Jo *et al.* proposed lemmas which provide expressions of the SINR distribution for various zones within a cell as a function of the macro BS-femto BS distance. Based on their analysis, it showed that indoor users preferring closed access and outdoor users preferring open access. Moreover, the conflict is most pronounced for femtocells near the cell edge of macrocell. To solve this problem, some studies proposed to enable the CSG femto BS to share resource to outdoor users so that a specified minimum data rate can be achieved [56]-[58]. In other words, hybrid mode is preferred to the system in the downlink direction. In the uplink direction, analysis results had shown a more complicated phenomenon [59]. In [59], Xia *et al.* concluded that the best approach depends heavily on whether the multiple access scheme is orthogonal (e.g. OFDMA) or non-orthogonal (CDMA). In a TDMA (Time Division Multiple Access)/OFDMA (Orthogonal Frequency Division Multiple Access) network, CSG is typically preferable at high user densities, whereas in CDMA, OSG provides significant gain of more than 300% for indoor user by reducing the near-far problem

experienced by the femto BS. Therefore, it is suggested that the interests of the femto BS owner and the network operator are more compatible than typically believed, and that CDMA femto BS should be configured for OSG whereas OFDMA or TDMA femto BS should adapt to the density of users.

2.5 Conclusion

In this chapter, we have introduced the background of femto BS. Femto BS has the flexibility to be deployed randomly by users. Femto BS can also provide OSG/CSG/Hybrid access modes to different users. Within the help of femto BS, cellular network can compensate the coverage holes and improve user QoS. Because of better indoor channel quality and frequency reuse factor, the spectrum efficiency also improves. Femto BS can also share the loading of macro BS networks. Moreover, the energy efficiency and battery life of UEs will also be increased.

However, femto BS also brings many challenges to the cellular network. In this chapter, we have introduced four major challenges: 1) Deployment issue, 2) Interference mitigation, 3) Load balancing, and 4) CSG/OSG conflict. To eliminate joint interference problem caused by femto BS networks, traditional approaches such as frequency plan and power control were proposed by many researchers. However, not only traditional approaches, many novel algorithms were constructed based on SON algorithm, optimization problem, and game theorem.

CHAPTER 3
3-D FEMTO BS DEPLOYMENT MODELS AND ANALYSIS

In this chapter, we will analyze how to deploy the femto BS to achieve ubiquitous coverage. In section 3.1, we introduce our analysis model and tools. In section 3.2, we analyze the range of the feasible femto BS density to achieve ubiquitous coverage. In section 3.3, numerical results are provided to prove our analysis model. In section 3.4 we discuss how to apply our analysis model to improve the deployment of femto BSs. Finally, we conclude our contribution in section 3.5.

3.1 Analysis Model

To estimate the performance of femto BS network, we perform two important assumptions in our studies. The first is three-dimensional analysis and the second is applying HPPP in modeling the random distributions of femto BSs.

3.1.1 Three-Dimensional Analysis

In the past, most of the studies about cellular network concentrated on the 2-D analysis model. However, the scenario of femto BS networks is different from that of traditional cellular network because femto BSs are deployed and installed by users to fulfill user

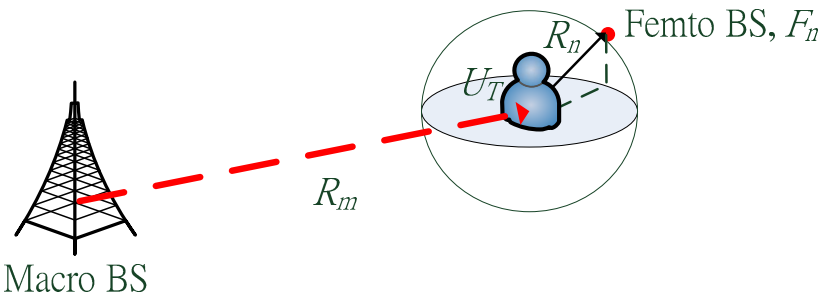

Fig. 3-1 Femto BS network analysis model

QoS in the indoor environment. Furthermore, it is sxpected that most of the femto BSs are deployed in the urban areas, where the complex surroudings create coverage holes in buildings. Therefore, to generate a more realistic analysis, a 3-D special model is more appropriate than the traditional 2-D plane analysis in analyzing the femto BS networks. In our analysis, we create an innovative model by assuming the femto BS networks are deployed in a 3-D space, which is shown in Fig. 3-1. In Fig. 3-1, one target user, U_T, is located under the coverage of one macro BS. We will analze the signal strength and interference that U_T receives. To simplify the analysis, the joint interference from other macro BSs are ignored by considering the macro BS or femto BS network dominates the combination of interference. From the U_T's point of view, by considering the U_T located in the center of a sphere space, femto BSs are randomly deployed around the U_T. R_m is the distance between the user and the macro BS. R_n is the distance between the user and its *n*th nearest femto BS, F_n.

In our works, we apply the PDF of R_n to estimate the signal strength received by U_T. By considering the Hata empirical path loss model, the received signal strength, U_n, can be calculated by (3.1) [60].

$$U_n = P_{fn} - \delta_{fn} - 10\eta_f \log_{10}(R_n) \text{ (dB)}, \quad R_n \geq \varepsilon. \tag{3.1}$$

Here, P_{fn} is the transmission power of femto BS, F_n, and δ_{fn} is the path loss constant between U_T and F_n. η_f is the path loss exponent of femto BS networks and ε is assumed to be small and can be ignored. From (3.1), it is clear that we need to obtain the PDF of $\ln(R_n)$ for the calculation of U_n. In the next section, we provide the details about how to model the random distributions of femto BS networks.

3.1.2 Homogeneous Poisson Point Process

In order to estimate the PDF of R_n and $\ln(R_n)$, we utilize the tools of stochastic geometry [61]-[62] in our works. Stochastic geometry, also known as spatial statistics, which means the statistical modeling of spatial relationships, gives researchers many tools to study the behavior over many spatial realizations of a network whose nodes are placed according to some probability distributions. Stochastic geometry has already applied in many researches about wireless communications [63]-[65]. In CDMA system, Musa *et al*. had published a serious of analysis about DS-CDMA system by using stochastic geometry to model the interference [66]-[69].With the advance of wireless communications, stochastic geometry and related techniques had been widely applied to ad hoc networks [70]-[74], wireless LAN [75], cognitive radio [76], cellular systems [77], relay networks [78]. In Table 3-1, we quoted some popular point processes for wireless network from [65]. In our analysis, we apply homogeneous Poisson point process (HPPP), which is one of the most fundamental models in stochastic geometry, to analyze the distributions of femto BS networks. Next, we will introduce how we apply HPPP in our study.

Homogeneous Poisson point process (HPPP)

HPPP [61] has been widely used in various studies such as the performance of random networks [71]-[72] and stochastic features of interference [80]-[81]. Based on HPPP, we assume that the femto BSs are uniformly distributed around U_T with density λ. Because of uniform distribution in the 3-D space, the PDF of the number of femto BSs in the area can be represented by (3.2) [82].

$$\Pr_X(x,\lambda,\upsilon)=\frac{(\lambda\upsilon)^x\exp(-\lambda\upsilon)}{x!},\quad \upsilon=4\pi r^3/3. \tag{3.2}$$

Table 3-1 Common spatial models [65]

Point Process	Key Properties	Example	Ref.
Poisson (PPP)	Mutual independence between node locations	Ad hoc networks with pure random channel access.	[71]
Binomial	Similar to PPP as far as i.i.d. node locations, but with a fixed number of nodes in a given area.	A known number of relays or mobile users deployed at random in a cell of known size	[79]
Poisson cluster (PCP)	Clustering of nodes, with independence between cluster locations.	Sensor networks, military platoons, an urban network with dense hotspots.	[70]
Poisson plus Poisson Cluster	Independence between the PCP and the PPP. Attraction between nodes.	PPP represents the mobile users in a macrocell and the PCP represents femtocells or hotspots.	[22]
Matern hard Core	Minimum distance between nodes.	Carrier sensing wireless networks with collision avoidance, e.g. WiFi.	[63]
Determinantal	Repulsion between nodes, e.g. Ginibre Process.	Networks with soft minimum distance.	[64]

Here, x is the number of femto BSs in the sphere. r and υ are the radius and volume of the sphere, respectively. From (3.2), it is clear that the complimentary CDF of R_n can be represented by the $\Pr_X(x,\lambda,\upsilon)$.

$$\Pr(R_n \geq r) = \sum_{x=0}^{n-1} \Pr_X(x,\lambda,\upsilon) = \sum_{x=0}^{n-1} \left(\frac{4\pi\lambda r^3}{3}\right)^x \exp(-4\pi\lambda r^3/3)/x!. \tag{3.3}$$

Then, we can obtain the PDF of R_n, denoted by $\Pr_{R_n}(r)$

$$\Pr_{R_n}(r) = \frac{\partial(1-\Pr(R_n \geq r))}{\partial r} = \frac{3(4\pi\lambda r^3/3)^n}{r\Gamma(n)} \exp(-4\pi\lambda r^3/3), \tag{3.4}$$

where $\Gamma(n)$ is gamma function. In the next paragraph, we will show that $\Pr_{R_n}(r)$

follows the generalized gamma distribution.

Generalized gamma distribution (ggd)

The ggd has three parameters, $a\,(>0)$, $d\,(>0)$, and $p(>0)$. For a non-negative random variable, denoted by x, the PDF of ggd is:

$$f(x;\ a, d, p) = \frac{(p/a^{d})x^{d-1}\exp-(x/a)^{P}}{\Gamma(d/p)}. \tag{3.5}$$

By comparing (3.4) with (3.5), it is clear that (3.4) can be obtained by replacing $d = m \cdot n$, $p = m$ and $a = (4\pi\lambda/3)^{-1}$. The first time that ggd appeared in the previous researches is in the Amoroso's paper [83]. Then, it was applied to many fields after the publication of Stacy's work [84]. Therefore, some studies also called ggd the Stacy distribution. In wireless communication, ggd is also known as α-μ distribution because Yacoub proposed the α-μ distribution, a model to analyze the fading in nonlinear environments where the surfaces which cause diffuse scattering are spatially correlated [85]-[86]. The α-μ distribution is proved a rewritten form of the ggd.

After the introduction of ggd, we will continue the analysis of $\Pr_{R_n}(r)$ by replacing R_n with Z_n. Here, we define $Z_n = \ln(R_n)$ and the PDF of Z_n can be calculated from $\Pr_{R_n}(r)$.

$$\Pr_{Z_n}(z_n) \equiv \Pr_{R_n}(\exp(z_n))\left|\frac{\partial R_n}{\partial z_n}\right|,\ \ln(\varepsilon) \le z_n \le \infty$$

$$\Rightarrow \Pr_{Z_n}(z_n) = \frac{3(\frac{4\pi\lambda}{3}\exp(3z_n))^{n}}{\Gamma(n)}\exp(-\frac{4\pi\lambda}{3}\exp(3z_n)) \tag{3.6}$$

Note that $\Pr_{Z_n}(z_n)$ is an approximation because we assume $R_n \ge \varepsilon$. However, this would not detract from the conclusion of this paper because $\Pr(R_n < \varepsilon)$ is very small. In the later analysis, we need to estimate the expected value of the received signal strength. From (3.6), it is clear that to calculate the expected value of the received signal

strength from F_n , denoted as $\mathrm{E}[U_n]$, the $\mathrm{E}[\log_{10}(R_n)]$ needs to be calculated first. Here, we will calculate $\mathrm{E}[\log_{10}(R_1)]$ first and then extend our conclusion to $\mathrm{E}[\log_{10}(R_n)]$. Based on (3.4), the $\Pr_{R_1}(r)$ is given

$$\Pr_{R_1}(r) = 4\pi\lambda r^2 \exp(-4\pi\lambda r^3/3). \tag{3.7}$$

From the definition of expected value, we obtain $\mathrm{E}[\log_{10}(R_1)]$

$$\mathrm{E}[\log_{10}(R_1)] = \frac{\mathrm{E}[\ln(R_1)]}{\ln(10)} = \frac{4\pi\lambda}{\ln(10)} \cdot \int_{\varepsilon}^{\infty} \ln(r) r^2 \exp(-4\pi\lambda r^3/3) dr . \tag{3.8}$$

Then, we obtain the closed form expression of the integral in (3.8) through the help of [87].

$$\int_{\varepsilon}^{\infty} \ln(r) r^2 \exp(-4\pi\lambda r^3/3) dr = \frac{\mathrm{Ei}(-cr^3) - 3\exp(-cr^3)\ln(r)}{9c}\Bigg|_{\varepsilon}^{\infty}$$

$$= \frac{\mathrm{Ex}(c\varepsilon^3) + 3\exp(-c\varepsilon^3)\ln(\varepsilon)}{9c} \approx \frac{\mathrm{Ex}(c\varepsilon^3) + 3\ln(\varepsilon)}{9c}, \; c = \frac{4\pi\lambda}{3}. \tag{3.9}$$

The $3\exp(-c\varepsilon^3)$ is ignored because it is expected that $c\varepsilon^3 << 1$. In (3.9), both $\mathrm{Ei}(c\varepsilon^3)$ and $\mathrm{Ex}(c\varepsilon^3)$ are exponential integrals

$$\mathrm{Ei}(c\varepsilon^3) \equiv \int_{-\infty}^{c\varepsilon^3} \frac{\exp(t)}{t} dt, \; \mathrm{Ex}(z) \equiv \int_{c\varepsilon^3}^{\infty} \frac{\exp(-t)}{t} dt = \text{-Ei}(\text{-}c\varepsilon^3). \tag{3.10}$$

$\mathrm{Ex}(c\varepsilon^3)$ can be transformted to another equation [88]

$$\mathrm{Ex}(z) = -\gamma - \ln(z) + \sum_{k=1}^{\infty} \frac{(-1)^{k+1}(z)^k}{k \cdot k!} . \tag{3.11}$$

where γ is the Euler-Mascheroni constant, which is equal to 0.5772. Because $c\varepsilon^3 << 1$, we can further simplify (3.11)

$$\mathrm{Ex}(c\varepsilon^3) \approx -\gamma - \ln(c\varepsilon^3), \quad c\varepsilon^3 << 1. \tag{3.12}$$

Through this approximation, we identify the closed form of $\mathrm{E}[\ln(R_1)]$

$$\mathrm{E}[\ln(R_1)] = \frac{-\gamma - \ln(4\pi\lambda/3)}{3}. \tag{3.13}$$

After the estimation of $\mathrm{E}[\ln(R_1)]$, we apply the same approach to $\mathrm{E}[\ln(R_n)]$. Similar to (3.9), the closed forms of the integrals to $\mathrm{E}[\ln(R_n)]$ are listed in Table 3-3 for n=1~7. By applying the same pgoress from (3.10)~(3.13), we summarize that $\mathrm{E}[\ln(R_n)]$ for n = 1 to 7 in Table 3-3. According to Table 3-3, we conclude that $\mathrm{E}[\ln(R_n)]$ can be estimated by the following equation for $n \geq 2$.

$$\mathrm{E}[\ln(R_n)] = \mathrm{E}[\ln(R_1)] + \sum_{k=2}^{n} \frac{1}{3(k-1)}, \quad n \geq 2. \tag{3.14}$$

Table 3-2 Closed forms utilized in the integral terms of E [ln(R_n)] [87]

n	$\int \ln(r) r^{3n-1} \exp(-cr^3) dr$
1	$(9c)^{-1}(\mathrm{Ei}(-cr^3) - 3\exp(-cr^3)\ln(r))$
2	$(9c^2)^{-1}\exp(-cr^3)(\exp(cr^3)\mathrm{Ei}(-cr^3) - 3(cr^3+1)\ln(r) - 1)$
3	$(9c^3)^{-1}\exp(-cr^3)(2\exp(cr^3)\mathrm{Ei}(-cr^3) - 3(c^2r^6 + 2cr^3 + 2)\ln(r) - cr^3 - 3)$
4	$(9c^4)^{-1}\exp(-cr^3)(6\exp(cr^3)\mathrm{Ei}(-cr^3) - 3(c^3r^9 + 3c^2r^6 + 6cr^3 + 6)\ln(r)$ $- c^2r^6 - 5cr^3 - 11)$
5	$(9c^5)^{-1}\exp(-cr^3)(24\exp(cr^3)\mathrm{Ei}(-cr^3)$ $- 3(c^4r^{12} + 4c^3r^9 + 12c^2r^6 + 24cr^3 + 24)\ln(r) - c^3r^9 - 7c^2r^6 - 26cr^3 - 50)$
6	$(9c^6)^{-1}\exp(-cr^3)(120\exp(cr^3)\mathrm{Ei}(-cr^3) - 3(c^5r^{15} + 5c^4r^{12} + 20c^3r^9 + 60c^2r^6$ $+ 120cr^3 + 120)\ln(r) - c^4r^{12} - 9c^3r^9 - 47c^2r^6 - 154cr^3 - 274)$
7	$(9c^7)^{-1}\exp(-cr^3)\begin{pmatrix}720\exp(cr^3)\mathrm{Ei}(-cr^3) - 3(c^6r^{18} + 6c^5r^{15} + 30c^4r^{12} + 120c^3r^9 + 360c^2r^6 \\ + 720cr^3 + 720)\ln(r) - c^5r^{15} - 11c^4r^{12} - 74c^3r^9 - 342c^2r^6 - 1044cr^3 - 1764\end{pmatrix}$

Table 3-3 Closed forms of $\mathrm{E}[\ln(R_n)]$

R_n	PDF of R_n	$\mathrm{E}[\ln(R_n)]$
R_1	$4\pi\lambda r_1^2 \exp(-4\pi\lambda r_1^3/3)$	$\frac{-\gamma-\ln(4\lambda\pi/3)}{3}$
R_2	$(16/3)\pi^2\lambda^2 r_2^5 \exp(-4\pi\lambda r_2^3/3)$	$\frac{-\gamma-\ln(4\lambda\pi/3)}{3}+\frac{1}{3}=\mathrm{E}[\ln(R_1)]+\frac{1}{3}$
R_3	$(32/9)\pi^3\lambda^3 r_3^8 \exp(-4\pi\lambda r_3^3/3)$	$\frac{-\gamma-\ln(4\lambda\pi/3)}{3}+\frac{1}{2}=\mathrm{E}[\ln(R_2)]+\frac{1}{6}$
R_4	$(128/81)\pi^4\lambda^4 r_4^{11} \exp(-4\pi\lambda r_4^3/3)$	$\frac{-\gamma-\ln(4\lambda\pi/3)}{3}+\frac{11}{18}=\mathrm{E}[\ln(R_3)]+\frac{1}{9}$
R_5	$(128/243)\pi^5\lambda^5 r_5^{14} \exp(-4\pi\lambda r_5^3/3)$	$\frac{-\gamma-\ln(4\lambda\pi/3)}{3}+\frac{50}{72}=\mathrm{E}[\ln(R_4)]+\frac{1}{12}$
R_6	$(512/3645)\pi^6\lambda^6 r_6^{17} \exp(-4\pi\lambda r_6^3/3)$	$\frac{-\gamma-\ln(4\lambda\pi/3)}{3}+\frac{274}{360}=\mathrm{E}[\ln(R_5)]+\frac{1}{15}$
R_7	$(1024/32805)\pi^7\lambda^7 r_7^{20} \exp(-4\pi\lambda r_7^3/3)$	$\frac{-\gamma-\ln(4\lambda\pi/3)}{3}+\frac{294}{360}=\mathrm{E}[\ln(R_6)]+\frac{1}{18}$

We will verify the estimation result about $\mathrm{E}[\ln(R_n)]$ through simulation.

3.2 Femto BS Density Analysis

In this section, we will analyze how to deploy femto BSs to provide ubiquitous coverage for the U_T in Fig. 3-1. Our objective is to limit the outage probability of cellular network by analyzing the feasible femto BS density under different scenarios. Before the analysis, we need to define the outage event.

Definition I (Outage event)

In the cellular network, the user is in outage state if the received SIR, denoted by ς, is under the minimum target SIR, T_ς.

$$\Pr(\textit{outage}) \equiv \Pr(\varsigma < T_\varsigma), \tag{3.15}$$

where T_ς is given by the cellular system. To keep the QoS requirement, cellular network needs to guarantee that outage probability should be limited by $\Pr_O$ (the

maximum tolerable outage probability of the cellular system).

From session 3.1, it is clear that the signal strength from femto BS to user is influenced by the femto BS density when the distributions of femto BSs follow HPPP. Therefore, we will concentrate on how to limit the outage probability through finding the region of feasible femto BS density, which is the rage of femto BS density to keep the outage probability lower than $\Pr_O$.

In preliminary study, many researches have analyzed the combination of interference when the interferers follow Poisson process [80]-[81], [89]-[91]. By assuming the macro users and femto BSs follow HPPP, Ramaswamy and Das presented an analysis of the uplink capacity of a macro/femto BS network in terms of the number of macro UEs and femto BSs that can be supported such that a certain outage criterion is satisfied for all users [92]. However, these studies were not based on the 3-D environment. Furthermore, the conclusions of these papers are still complicated for us to obtain the insight about how to control the femto BS density to obtain ubiquitous coverage.

To facilitate the analysis of femto BS density, we set an important assumption, which is: the interference is dominated by one major interference source. First, when the interferers follow HPPP, the closest interferer dominates the combination of interference in the region of low outage probability. This is an extension from Mordachev and Loykas' work [93]. Second, when the interferers do not follow HPPP, we can still expect that the pathloss effect is more obvious with the increase of the distance between the target user and the interferer. Therefore, the closest femto BS has more chance to be the dominant interferer than other interferers. The assumption of one dominant interferer helps us to observe the insight about how to control the femto BS density to guarantee coverage. In fact, the feasible femto BS density will also influence the dominaint interferer assumption. In the later analysis, we will also analyze the relationship of each other.

Based on different dominant interferer in the macro/femto BS network, we provide four scenarios:

(a) Macro BS is the serving BS

(b) F_1 is the serving BS

(c) CSG femto BS is the dominant interference source to a non-CSG user

(d) OSG femto BS network

We will estimate the feasible femto BS density under different scenarios in the following sub-sections.

3.2.1 Scenario (a) Macro BS Is the Serving BS

In scenario (a), U_T is served by the macro BS and surrounded by a group of interfering femto BSs. We assume $P_{fn} = P_f, \delta_{fn} = \delta_f, n = 1,2,...$. Based on the assumption that the nearest femto BS dominates the interference when the intereferers follow HPPP, the SIR of the user is simplified by the ratio of the received signal strength from the macro BS, denoted by U_m, and U_1.

Scenario (a)

$SIR(R_m) \approx U_m - U_1$, in the region of low outage probability

$$\varsigma_a(R_m) \equiv U_m - U_1 = (P_m - \delta_m - 10\eta_m \log_{10}(R_m)) - (P_{f1} - \delta_{f1} - 10\eta_f \log_{10}(R_1)). \quad (3.16)$$

Here, ς_a is the function of R_m. P_m is the macro BS power, η_m is the path loss exponent between the macro BS and the user, R_1 is the distance between the user and dominating interference source (the 1st nearest femto BS). In scenario (a), our requirement to outage probability and ubiquitous coverage can be represented by (3.17)

$$\Pr(\varsigma_a(R_m) < T_\varsigma \mid R_m) < \Pr_O. \quad (3.17)$$

In Theorem I, we propose the range of feasible femto BS density under scenario (a).

Theorem I

In order to satisfy the conditional outage probability in (3.17), the feasible femto BS density in scenario (a), denoted by λ^a, should follow

$\lambda^a < -\frac{3}{4\pi}\ln(1-\Pr_O)\exp(-3T_\varsigma^a)$, in the region of low outage probability.

$$T_\varsigma^a = \frac{\ln(10)}{10\eta_f}(T_\varsigma - (P_m - P_{f1}) + (\delta_m - \delta_{f1}) + 10\eta_m \log_{10}(R_m)). \quad (3.18)$$

Proof

From (3.17), the outage event is equivalent to the following inequality.

$$\ln(R_1) < \frac{\ln(10)}{10\eta_f}(T_\varsigma - (P_m - P_{f1}) + (\delta_m - \delta_{f1}) + 10\eta_m \log_{10}(R_m)) \equiv T_\varsigma^a \,. \tag{3.19}$$

By defining $z_1 \equiv \ln(R_1)$, the PDF of z_1 is obtained through (3.6)

$$\Pr_{Z_1}(z_1) = 4\pi\lambda^a \exp(-\frac{4\pi\lambda^a}{3}\exp(3z_1) + 3z_1)\,. \tag{3.20}$$

In addition to $\Pr_{Z_1}(z_1)$, we calculate the CDF of z_1 through the integration of $\Pr_{Z_1}(z_1)$.

$$\Pr_{Z_1}(z_1 < Z) \approx \int_0^Z 4\pi\lambda^a \exp(-\frac{4\pi\lambda^a}{3}\exp(3z_1) + 3z_1)\, dz_1$$

$$= \exp(-4\pi\lambda^a/3) - \exp(-\frac{4\pi\lambda^a}{3}\exp(3Z))$$

$$\approx 1 - \exp(-\frac{4\pi\lambda^a}{3}\exp(3Z))\,. \tag{3.21}$$

Here, we let $\exp(-4\pi\lambda^a/3) \approx 1$ during the analysis of λ^a. Also note the CDF in (3.21) is equivalent to the probability of "infeasibility" for a given λ^a when the threshold is Z. Finally, the upper bound of λ^a can be discovered through the CDF of z_1.

$$\Pr(\varsigma_a(R_m) < T_\varsigma \mid R_m) = \Pr(z_1 < T_\varsigma^a \mid R_m) \approx 1 - \exp(-\frac{4\pi\lambda^a}{3}\exp(3T_\varsigma^a)) < \Pr_O$$

$$\Rightarrow \lambda^a < -\frac{3}{4\pi}\ln(1 - \Pr_O)\exp(-3T_\varsigma^a)\,. \tag{3.22}$$

3.2.2 Scenario (b) F_1 Is the Serving BS

In scenario (b), we discuss the condition that U_T is served by F_1 and the macro BS is the dominant interference source. Without loss of generality, we assume that

$\mathrm{E}[U_k] > \mathrm{E}[U_{k+1}], k \geq 1$. In this scenario, we cannot extend the results of [93] because the interfering nodes do not obey HPPP. In this scenario, the macro BS is the dominant interfering node and a threshold, κ_D^b, is used to decide when the macro BS becomes the dominant interference source.

Definition II (Scenario (b))

Based on the assumption that F_1 is the serving femto BS, macro BS is the dominant interference source when

$$U_m(R_m) - \mathrm{E}[U_2] > \kappa_D^b$$
$$\Rightarrow (P_m - \delta_m - 10\eta_m \log_{10}(R_m)) - (P_{f_2} - \delta_{f_2} - 10\eta_f \mathrm{E}[\log_{10}(R_2)]) > \kappa_D^b. \quad (3.23)$$

From (3.23), we obtain a loose bound even without considering the serving femto BS performance. Eq. (3.23) can be treated as a bound for scenario (b) to be valid. From (3.23), we obtain the requirement to $\mathrm{E}[\log_{10}(R_2)]$,

$$\left(\frac{10\eta_m \log_{10}(R_m) - (P_m - P_{f2}) + (\delta_m - \delta_{f2}) + \kappa_D^b}{10\eta_f} < \mathrm{E}[\log_{10}(R_2)]. \right. \quad (3.24)$$

The closed form expression of $\mathrm{E}[\log_{10}(R_2)]$ is given by (3.14)

$$\mathrm{E}[\log_{10}(R_2)] = \frac{-\gamma - \ln(4\pi\lambda^b/3) + 1}{3\ln(10)}, \quad (3.25)$$

where λ^b is the feasible femto BS density in scenario (b). From (3.24) and (3.25), we find the upper bound of λ^b.

$$\lambda^b < \frac{3}{4\pi}\exp(1 - C_D^b),$$
$$C_D^b = \frac{3\ln(10)}{10\eta_f}(10\eta_m \log_{10}(R_m) - (P_m - P_{f2}) + (\delta_m - \delta_{f2}) + \kappa_D^b) + \gamma. \quad (3.26)$$

Therefore, we obtain a upper bound of λ^b for scenario (b) to be valid.

After finding the upper bound of λ^b, now we want to estimate the requirement of λ^b to ensure that the conditional outage probability in scenario (b) is lower than $\Pr_O$.

Scenario (b)

$$SIR(R_m) \approx U_1 - U_m(R_m) \equiv \varsigma_b(R_m)$$

$$= (P_{f1} - \delta_{f1} - 10\eta_f \log_{10}(R_1)) - (P_m - \delta_m - 10\eta_m \log_{10}(R_m)). \quad (3.27)$$

ς_b is the approximated SIR when the macro BS dominates the joint interference. To keep the conditional outage probability lower than $\Pr_O$, we propose the bounds of λ^b in Theorem II.

Theorem II

In order to guarantee that the conditional outage probability meets the requirement of $\Pr(\varsigma_b(R_m) < T_\varsigma \mid R_m) < \Pr_O$, the feasible femto BS density in scenario (b) should follow

$$\lambda^b > \frac{3}{4\pi} \ln(\Pr_O^{-1}) \exp(-3T_\varsigma^b),$$

$$T_\varsigma^b = \frac{\ln(10)}{10\eta_f}(-T_\varsigma - (P_m - P_{f1}) + (\delta_m - \delta_{f1}) + 10\eta_m \log_{10}(R_m)). \quad (3.28)$$

with the pre-requirement of having the macro BS as the dominating interference source (derived from (3.26)).

$$\lambda^b < 3\exp(1 - C_D^b)/(4\pi),$$

$$C_D^b = \frac{3\ln(10)}{10\eta_f}(10\eta_m \log_{10}(R_m) - (P_m - P_{f2}) + (\delta_m - \delta_{f2}) + \kappa_D^b) + \gamma. \quad (3.29)$$

Proof

Here, we prove only the inequality of (3.28). We start from the definition of outage event $\varsigma_b(R_m) < T_\varsigma$

$$\varsigma_b(R_m) = (P_{f1} - \delta_{f1} - 10\eta_f \log_{10}(R_1)) - (P_m - \delta_m - 10\eta_m \log_{10}(R_m)) < T_\varsigma \,. \quad (3.30)$$

From (3.30), we find the requirement to $\ln(R_1)$

$$\ln(R_1) > \frac{\ln(10)}{10\eta_f}(-T_\varsigma - (P_m - P_{f1}) + (\delta_m - \delta_{f1}) + 10\eta_m \log_{10}(R_m)) \equiv T_\varsigma^b \,. \quad (3.31)$$

In (3.22), we have obtained the closed form of $\Pr(Z_1 < T_\varsigma^a \mid R_m)$, which can also be applied to the inequality, $\Pr(U_1 - U_m(R_m) < T_\varsigma \mid R_m)$, for calculating the requirement of λ^b.

$$\Pr(U_1 - U_m(R_m) < T_\varsigma \mid R_m) = \Pr_{Z_1}(z_1 > T_\varsigma^b \mid R_m) \approx \exp(-4\pi\lambda^b \exp(3T_\varsigma^b)/3) < \Pr_O$$

$$\Rightarrow \lambda^b > \frac{3}{4\pi} \ln(\Pr_O^{-1}) \exp(-3T_\varsigma^b) \,. \quad (3.32)$$

Based on Theorem II, there are feasible values of λ^b in scenario (b) when it is located in the range defined in Theorem II. After combining the Theorem II and the pre-requirement of scenario (b), it is clear that both scenario (b) and its feasible λ^b exist when

$$C_D^b < 1 + 3T_\varsigma^b - \ln(\ln(\Pr_O^{-1})) \,. \quad (3.33)$$

In scenario (a) and scenario (b), we have examined the joint influence between the macro BS and femto BS network. In scenario (c) and scenario (d), we will ignore the macro BS and verify the feasible femto BS density under CSG/OSG femto BS networks.

3.2.3 Scenario (c) CSG Femto BS Is the Dominant Interference Source to A Non-CSG User

In scenario (c), we concentrate on the interference between two different femto BS networks: OSG femto BS network and CSG femto BS network. Both networks are uniformly distributed around a non-CSG user, where $F_{n,O}$ and $F_{n,C}$ are the *n*th

nearest OSG and CSG femto BSs, respectively. The transmission powers and path loss constants of $\{F_{n,O}, F_{n,C}\}$ are $\{P_{fn,O}, P_{fn,C}\}$ and $\{\delta_{fn,O}, \delta_{fn,C}\}$, respectively. The densities of the OSG and CSG femto BS networks are given by $\{\lambda_O^C, \lambda_C^C\}$. In this scenario, we consider the situation that interference is dominated by $F_{1,C}$ when the user is served by $F_{1,O}$. Therefore, we assume $\mathrm{E}[U_{1,C}] > MAX\{\mathrm{E}[U_{2,O}], \mathrm{E}[U_{2,C}]\}$ by giving the Definition III.

Definition III (Scenario (c))

Based on the assumption that $F_{1,O}$ is the serving BS and i) $P_{f2,O} \geq P_{f3,O} \geq \ldots$; ii) $P_{f2,C} \geq P_{f3,C} \geq \ldots$; iii) $\delta_{f2,O} \leq \delta_{f3,O} \leq \ldots$; and iv) $\delta_{f2,C} \leq \delta_{f3,C} \leq \ldots$, $F_{1,C}$ is the dominant interference source when

$$\mathrm{E}[U_{1,C}] - MAX\{\mathrm{E}[U_{2,O}], \mathrm{E}[U_{2,C}]\} > \kappa_D^C, \tag{3.34}$$

$$\begin{cases} \mathrm{E}[U_{1,C}] = P_{f1,C} - \delta_{f1,C} - 10\eta_f \mathrm{E}[\log_{10}(R_{1,C})] \\ \mathrm{E}[U_{2,C}] = P_{f2,C} - \delta_{f2,C} - 10\eta_f \mathrm{E}[\log_{10}(R_{2,C})] \\ \mathrm{E}[U_{2,O}] = P_{f2,O} - \delta_{f2,O} - 10\eta_f \mathrm{E}[\log_{10}(R_{2,O})], \end{cases}$$

where $\{U_{n,O}, U_{n,C}\}$ are the received signal strengths from $\{F_{n,O}, F_{n,C}\}$; $\{R_{n,O}, R_{n,C}\}$ are the distances from $\{F_{n,O}, F_{n,C}\}$ to the non-CSG user. In addition to (3.34), we still need to estimate the requirements of $(\lambda_O^C, \lambda_C^C)$ to ensure that the SIR is larger than T_ς. κ_D^C is the threshold to decide when the $F_{1,C}$ becomes the dominant interference source.

Scenario (C)

$$SIR \approx U_{1,O} - U_{1,C} \equiv \varsigma_c$$

$$= (P_{f1,O} - \delta_{f1,O} - 10\eta_f \log_{10}(R_{1,O})) - (P_{f1,C} - \delta_{f1,C} - 10\eta_f \log_{10}(R_{1,C})). \tag{3.35}$$

However, the closed form of ς_c is not obvious because both $R_{1,O}$ and $R_{1,C}$ are random variables. In order to obtain a clear view of the influence of $(\lambda_O^C, \lambda_C^C)$, we assume that

the outage probability can be controlled when $\mathrm{E}[\varsigma_c] > \kappa_T^C$, which κ_T^C is also a pre-defined threshold. We then propose Theorem III for feasible values of $(\lambda_O^C, \lambda_C^C)$.

Theorem III

In order to guarantee $\mathrm{E}[\varsigma_c] > \kappa_T^C$ in scenario (c), the feasible CSG/OSG femto BS density set $(\lambda_C^C, \lambda_O^C)$ should follow

$$\lambda_C^C < \lambda_O^C \exp(-C_T^C),$$
$$C_T^C = \frac{3\ln(10)}{10\eta_f}(\kappa_T^C + (P_{f1,C} - P_{f1,O}) - (\delta_{f1,C} - \delta_{f1,O})). \tag{3.36}$$

with the pre-requirements of

$$\lambda_O^C \exp(X_2^C) < \lambda_C^C < \lambda_O^C \exp(X_1^C),$$
$$X_1^C = \frac{3\ln(10)}{10\eta_f}((P_{f2,O} - P_{f2,C}) - (\delta_{f2,O} - \delta_{f2,C})),$$
$$X_2^C = \frac{3\ln(10)}{10\eta_f}(\kappa_D^C - (P_{f1,C} - P_{f2,O}) + (\delta_{f1,C} - \delta_{f2,O})) - 1. \tag{3.37}$$

Or

$$\begin{cases} \lambda_C^C > \lambda_O^C \exp(X_1^C), \\ (P_{f1,C} - P_{f2,C}) - (\delta_{f1,C} - \delta_{f2,C}) + \dfrac{10\eta_f}{3\ln(10)} > \kappa_D^C \end{cases}. \tag{3.38}$$

Proof

A). Replacing (3.35) with the closed forms of $\mathrm{E}[\ln(R_{1,C})]$ and $\mathrm{E}[\ln(R_{1,O})]$, we obtain (3.36),

$$\mathrm{E}[\ln(R_{1,C})] - \mathrm{E}[\ln(R_{1,O})] > \frac{\ln(10)}{10\eta_f}(\kappa_T^C + (P_{f1,C} - P_{f1,O}) - (\delta_{f1,C} - \delta_{f1,O})).$$

$$\Rightarrow \lambda_C^C < \lambda_O^C \exp(-C_T^C),\quad C_T^C = \frac{3\ln(10)}{10\eta_f}(\kappa_T^C + (P_{f1,C} - P_{f1,O}) - (\delta_{f1,C} - \delta_{f1,O})). \tag{3.39}$$

B).Then, we examine two cases to analyze the inequality in (3.34). The first case is $\mathrm{E}[U_{2,\mathrm{O}}] > \mathrm{E}[U_{2,\mathrm{C}}]$ and the second one is $\mathrm{E}[U_{2,\mathrm{C}}] > \mathrm{E}[U_{2,\mathrm{O}}]$.

Case 1 $\mathrm{E}[U_{2,\mathrm{O}}] > \mathrm{E}[U_{2,\mathrm{C}}]$

(1.a) If $\mathrm{E}[U_{2,\mathrm{O}}] > \mathrm{E}[U_{2,\mathrm{C}}]$, then $(\lambda_O^C, \lambda_C^C)$ should follow

$$\lambda_C^C < \lambda_O^C \exp(X_1^C),\qquad X_1^C = \frac{3\ln(10)}{10\eta_f}((P_{f2,O} - P_{f2,C}) - (\delta_{f2,O} - \delta_{f2,C})). \tag{3.40}$$

(1.b) When $\mathrm{E}[U_{2,\mathrm{O}}] > \mathrm{E}[U_{2,\mathrm{C}}]$, (3.34) is equivalent to $\mathrm{E}[U_{1,\mathrm{C}}] - \mathrm{E}[U_{2,\mathrm{O}}] > \kappa_D^C$. $(\lambda_O^C, \lambda_C^C)$ should then follow

$$\lambda_C^C > \lambda_O^C \exp(X_2^C),\quad X_2^C = \frac{3\ln(10)}{10\eta_f}(\kappa_D^C - (P_{f1,C} - P_{f2,O}) + (\delta_{f1,C} - \delta_{f2,O})) - 1. \tag{3.41}$$

(1.c) From (1. a) and (1. b), we identify the pre-requirement (3.37) for scenario (c) when $\mathrm{E}[U_{2,\mathrm{O}}] > \mathrm{E}[U_{2,\mathrm{C}}]$.

Case 2 $\mathrm{E}[U_{2,\mathrm{C}}] > \mathrm{E}[U_{2,\mathrm{O}}]$

(2.a) If $\mathrm{E}[U_{2,\mathrm{C}}] > \mathrm{E}[U_{2,\mathrm{O}}]$, then $(\lambda_O^C, \lambda_C^C)$ should follow

$$\lambda_C^C > \lambda_O^C \exp(X_1^C). \tag{3.42}$$

(2.b) When $\mathrm{E}[U_{2,\mathrm{C}}] > \mathrm{E}[U_{2,\mathrm{O}}]$, (3.34) is equivalent to $\mathrm{E}[U_{1,\mathrm{C}}] - \mathrm{E}[U_{2,\mathrm{C}}] > \kappa_D^C$. $(\lambda_O^C, \lambda_C^C)$ should then follow

$$(P_{f1,C} - P_{f2,C}) - (\delta_{f1,C} - \delta_{f2,C}) + \frac{10\eta_f}{3\ln(10)} > \kappa_D^C. \tag{3.43}$$

(2.c) From (2.a) and (2.b), we identify the pre-requirement (3.38) for scenario (c) when $\mathrm{E}[U_{2,\mathrm{C}}] > \mathrm{E}[U_{2,\mathrm{O}}]$.

Therefore, given λ_O^C, the feasible λ_C^C can be found by Theorem III. Next, we will provide a method to decide the appropriate κ_T^C in the Theorem III.

We start the analysis from the PDF of z_1,

$$\Pr_{Z_1}(z_1) = 4\pi\lambda \cdot \exp(\frac{-4\pi\lambda}{3}\exp(3z_1) + 3z_1). \tag{3.44}$$

From (3.44), it is clear that $\exp(3z_1)$ dominates the left tail of $\Pr_{Z_1}(z_1)$ and $\exp(-4\pi\lambda\exp(3z_1)/3)$ dominates the right tail. We approximate the left tail of $\Pr_{Z_1}(z_1)$ by the following equation.

$$\text{Left tail of } \Pr_{Z_1}(z_1) \approx 4\pi\lambda\exp(3Z_1) \approx \frac{1}{\sqrt{2\pi C_{Z_1}^2}}\exp(3Z_1)\exp(-Z_1^2/(2C_{Z_1}^2)),$$

$$C_{Z_1}^2 \equiv (32\pi^3\lambda^2)^{-1} \Rightarrow -\frac{Z_1^2}{2C_{Z_1}^2} \approx 0. \tag{3.45}$$

$C_{Z_1}^2$ is very close to zero and the range of z_1 is small.

Therefore, the attached exponential term, $\exp(-Z_1^2/(2C_{Z_1}^2))$, does not affect the PDF in an obvious way. Thus, we can extend the approximation further.

$$\text{Left tail of } \Pr_{Z_1}(z_1) \approx \frac{1}{\sqrt{2\pi C_{Z_1}^2}} \cdot \exp(3Z_1)\exp(\frac{-Z_1^2}{2C_{Z_1}^2})\exp(\frac{-9C_{Z_1}^2}{2})\exp(\frac{9C_{Z_1}^2}{2})$$

$$= \frac{\exp(9C_{Z_1}^2/2)}{\sqrt{2\pi C_{Z_1}^2}}\exp(-\frac{(Z_1 - 3C_{Z_1}^2)^2}{2C_{Z_1}^2})$$

$$= \exp(9C_{Z_1}^2/2)\Pr(N_{Z_1}), \quad N_{Z_1} \sim N(3C_{Z_1}^2, C_{Z_1}^2). \tag{3.46}$$

Based on observations, the left tails of $\ln(R_{1,C})$ and $\ln(R_{1,O})$ are very similar to that

of the normal distribution. Therefore, we expect the left tail of ς_C to be similar to that of normal distribution because $\exp(3z_1)$ will also dominate the left term during the convolution process. We propose to use the CDF of the normal distribution to find κ_T^C .

$$\Pr(\varsigma_C < T_\varsigma) < \frac{1}{2}\left(1+\operatorname{erf}\left(\frac{T_\varsigma - \bar{\varsigma}_C}{\sqrt{2}\sigma_C}\right)\right) < \Pr_O \Rightarrow \bar{\varsigma}_C > T_\varsigma - \sqrt{2}\sigma_C \operatorname{erf}^{-1}(2\Pr_O - 1) \equiv \kappa_T^C$$

$$\sigma_C^2 = \operatorname{Var}(U_{1,O}) + \operatorname{Var}(U_{1,C}) \tag{3.47}$$

In other words, we can approximate the probability of "infeasibility" of a given λ_C^C by utilizing the CDF of normal distribution. In (3.47), it is observed that κ_T^C also depends on σ_C, which is determined by the variance of z_1, $\operatorname{Var}(z_1)$. $\operatorname{Var}(z_1)$ can be represented by (3.48).

$$\operatorname{Var}(z_1) = \sigma_{z_1}^2 = \mathrm{E}[\ln^2(R_1)] - \mathrm{E}[\ln(R_1)]^2,$$

$$\mathrm{E}[\ln^2(R_1)] = \int_{\varepsilon}^{\infty} 4\pi\lambda r_1^2 \ln^2(r_1)\exp(-4\pi\lambda r_1^3/3)dr_1. \tag{3.48}$$

We can transform the integration in (3.48) through the help of [87]

$$\int \ln^2(x)x^2\exp(-cx^3)dx = \frac{x^3}{3}\left(\frac{2\cdot {}_3F_3(1,1,1;2,2,2;-cx^3)}{9} - \frac{\ln(x)\left((3\exp(-cx^3)-3)\ln(x) + 2(\ln(cx^3)+\gamma) + 2\Gamma(0,cx^3)\right)}{3cx^3}\right) \tag{3.49}$$

Here, σ_{z_1} is the standard deviation of z_1, $\Gamma(0,cx^3)$ is the incomplete Gamma function and ${}_3F_3(1,1,1;2,2,2;-cx^3)$ is the generalized hypergeometric function. It is difficult to obtain a closed form for the integration. However, through our numerical results, we found that σ_{z_1} remains stable when we adjust λ across a wide

range of values. Based on this observation, we assume $\mathrm{Var}(U_{1,O}) = \mathrm{Var}(U_{1,C}) = \mathrm{Var}(U_1)$. It is because both $\mathrm{Var}(U_{1,O})$ and $\mathrm{Var}(U_{1,C})$ would also be stable with the change of the femto BS density. Therefore, we assume $\sigma_C^2 = 2\mathrm{Var}(U_1)$ during the estimation of κ_T^C. $\mathrm{Var}(U_1)$ can be estimated through numerical results.

3.2.4 Scenario (d) OSG Femto BS Network

In scenario (d), we discuss the condition that the user is surrounded by an OSG femto BS network. Here we assume that F_1 is the serving femto BS and F_2 is the dominant interference source. We assume that the outage probability can be controlled when $\mathrm{E}[\mathrm{SIR}] > \kappa_T^d$.

Scenario (d)

$$\mathrm{E}[\mathrm{SIR}] \approx \mathrm{E}[U_1] - \mathrm{E}[U_2] \equiv \bar{\varsigma}_d > \kappa_T^d$$

$$\Rightarrow (P_{f1} - \delta_{f1} - 10\eta_f \mathrm{E}[\log_{10}(R_1)]) - (P_{f2} - \delta_{f2} - 10\eta_f \mathrm{E}[\log_{10}(R_2)]) > \kappa_T^d \quad (3.50)$$

By replacing $\mathrm{E}[\log_{10}(R_1)]$ and $\mathrm{E}[\log_{10}(R_2)]$ with the closed forms in Table 3-3, we obtain the following inequality.

$$(P_{f1} - P_{f2}) - (\delta_{f1} - \delta_{f2}) > \frac{\kappa_T^d - 10\eta_f}{3\ln(10)}. \quad (3.51)$$

It is clear that (3.51) is unrelated with the density of femto BS networks. In other words, we can not improve the outage probability by modifying the femto BS density. In the next section, we will verify this observation and proposed Theorem I ~ Theorem III through simulations.

3.3 Simulations

In this section, we verify above observations and theorems through simulations. In the simulations, parameters are set according to Table 3-4. Before the verification of feasible femto BS density, we first verify the closed forms of estimated $\mathrm{E}[\ln(R_n)]$ in

(3.14). In Fig. 3-2, we compare simulation results of $E[U_n]$ and the closed form of $E[U_n]$ (by using (3.13) and (3.14)), which are represented by $E[U_n]$(Num) and $E[U_n]$(Est) respectively. From Fig. 3-2, it is clear that $E[U_n]$(Num) and $E[U_n]$(Est) match with different femto BS densities. In the following simulations, to accommodate most influential femto BSs, we will select the 10 nearest femto BSs to represent the interference impacts from femto BS network, where the signal strength difference between the first nearest femto BS and the 10th nearest femto BS is about 15dB, shown also in Fig. 3-2.

Table 3-4 Notations and values of femto BS network parameters

Notation	Definition	Value
P_m	Radiation power of macro BS	46 dBm
$\{P_{fn}, P_{fn,C}, P_{fn,O}\}$	Radiation power of $\{F_n, F_{n,O}, F_{n,C}\}$	20 dBm
R_m	Distance from the macro BS to the user	50–700 m
$R_n \quad n=1\sim N$	Distance from F_n to U_T	$\varepsilon \le R_n$
δ_m	Path loss constant of macro BS	50 dB
$\{\delta_{fn}, \delta_{fn,C}, \delta_{fn,O}\}$	Path loss constant of $\{F_n, F_{n,C}, F_{n,O}\}$	35–65 dB
ε	Minimum distance of R_n	1 m
η_m	Path loss exponent of macro BS path	3
η_f	Path loss exponent of femto BS path	3.5
γ	Euler-Mascheroni constant	0.5772
$\Pr_O$	System requirement of the upper bound of outage probability	0.1
T_ς	SIR threshold of the outage event	3 dB
κ_D^b	Dominating threshold of scenario (b)	12.11 dB
κ_T^C	Outage threshold of scenario (c)	14.65 dB
κ_D^C	Dominating threshold of scenario (c)	10 dB
κ_D^d	Dominating threshold of scenario (d)	18 dB

To verify the Theorems, we will compare th simulation results (Num) with the approximation method (App) based on the dominating interference source only and the theorem bounds are calculated for operating at 10% outage probability. For Theorem I, considering different R_m (distance between the user and macro BS), Fig. 3-3 plots the feasible femto BS density, λ^a, with outage probability of Num and App. As shown, when operated at a low outage probability (~ 5%), the approximation in feasible femto BS density, based on the "nearest femto BS only", has good representation of overall interference impact. Also, as expected, when R_m increases, the feasible femto BS density decreases.

In Fig. 3-4, with various R_m, we will show the changes of feasible femto BS densities λ^a and λ^b of Theorem I and Theorem II respectively. Here, instead of considering a fixed path loss constant of 40dB of all in Fig. 3-3, we adjust δ_{f1} to 35dB, 40dB, and 45dB and other δ_{fn} are fixed at 55dB. From Fig. 3-4, for either scenario (a) or (b), the bounds of feasible femto BS density drop more

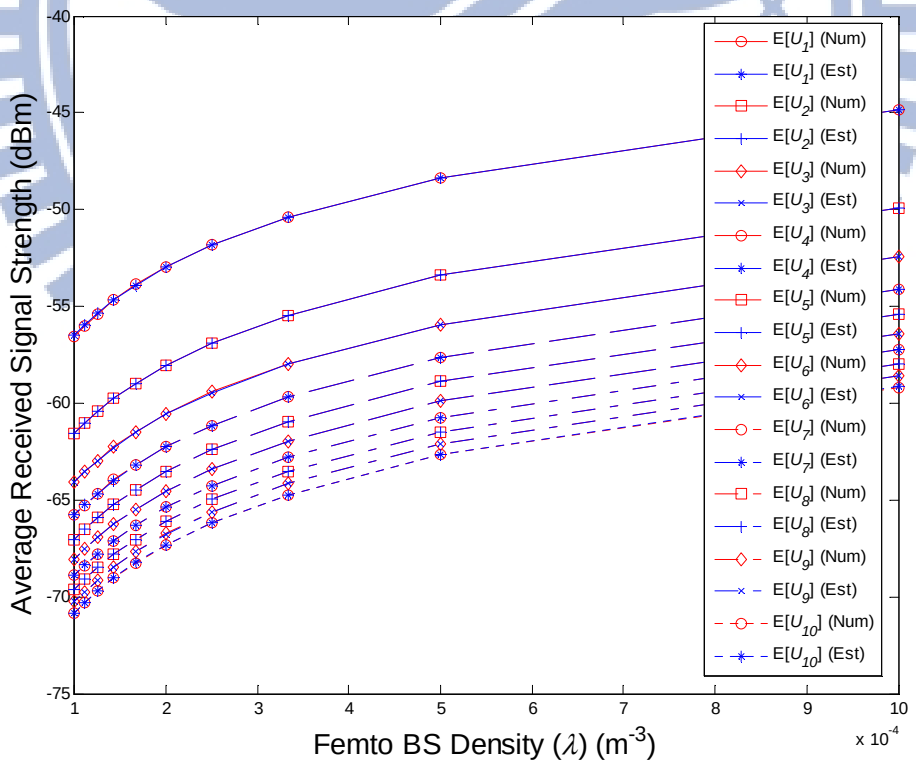

Fig. 3-2 Comparison of $\mathrm{E}[U_n](\mathrm{Num})$ and $\mathrm{E}[U_n](\mathrm{Est})$, $\delta_{f1} = \delta_{f2} \ldots = 40\mathrm{dB}$

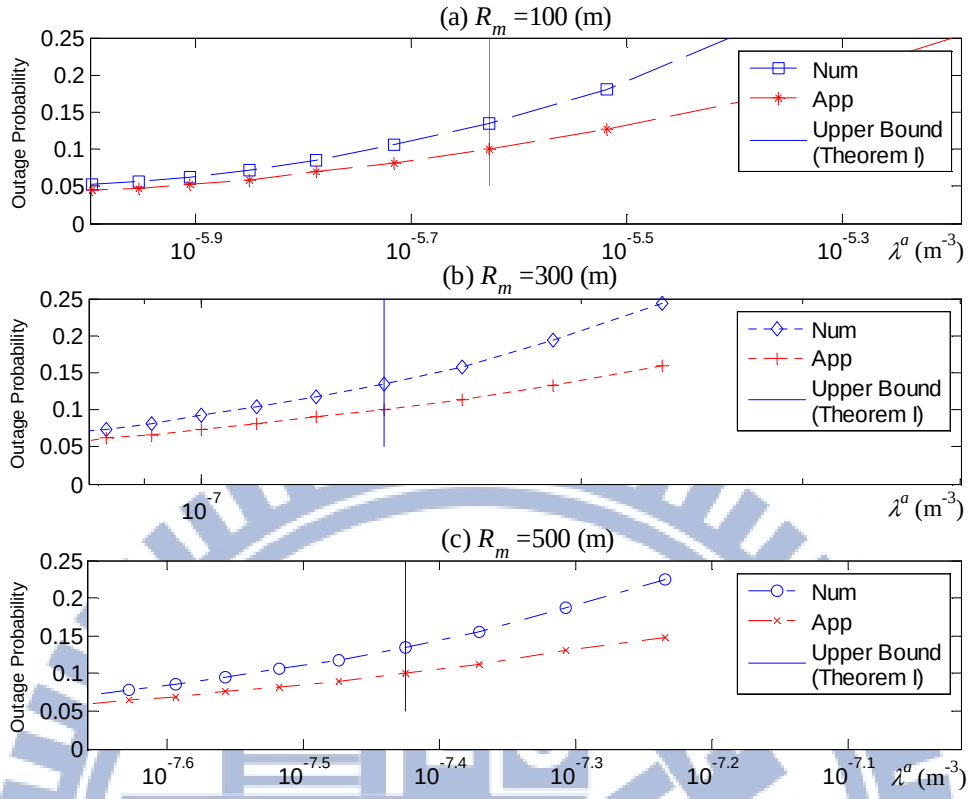

Fig. 3-3 Outage probability estimated with the λ^a in Theorem I, where $\delta_{f1} = \delta_{f2} ... = 40\,\text{dB}$.

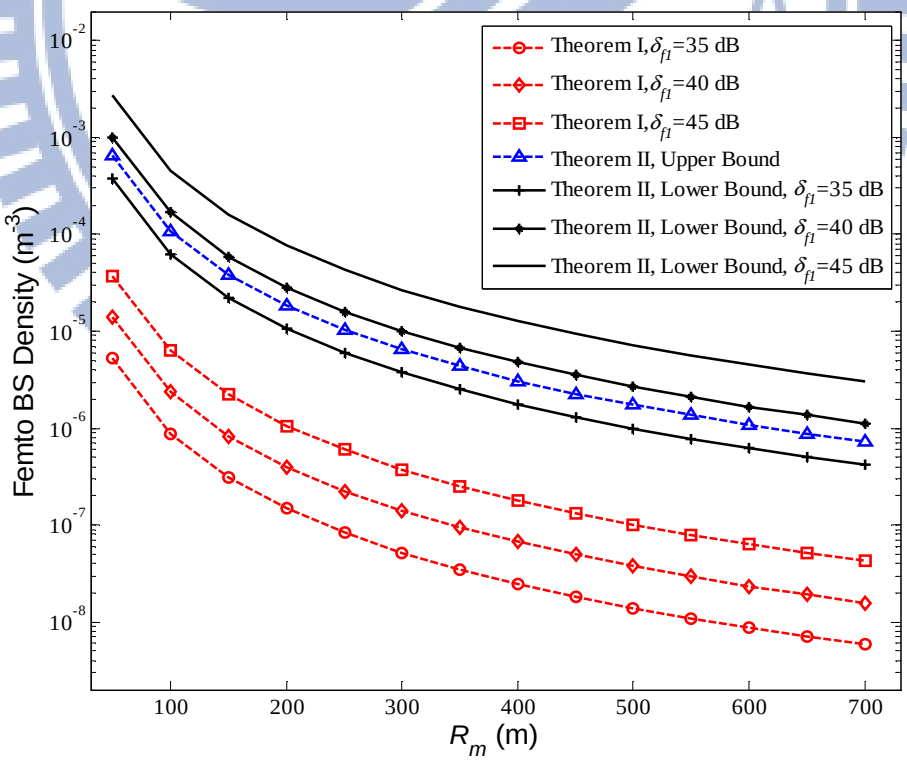

Fig. 3-4 Feasible regions of λ^a and λ^b. Here, we assume $\delta_{f2} = \delta_{f3} ... = 55\text{dB}$ and adjust δ_{f1} from 35 to 45 dB.

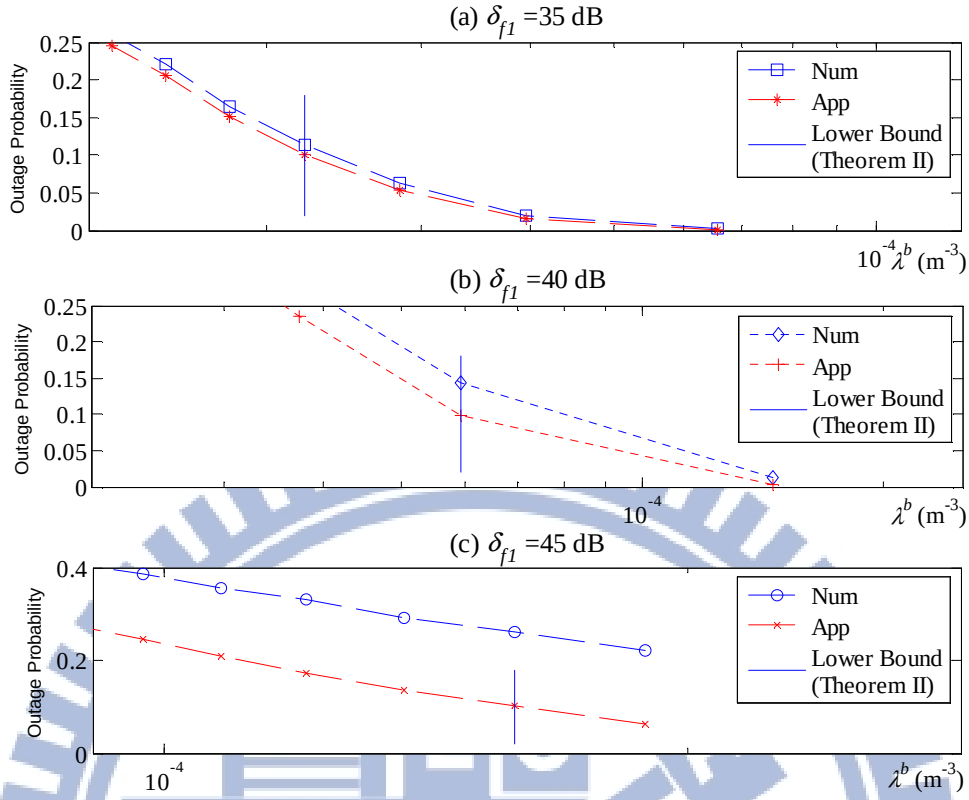

Fig. 3-5 Outage probability when λ^b is located near the lower bound estimated from Theorem II, where $\delta_{f2} = \delta_{f3} ... = 55\text{dB}$ and $R_m = 150\,\text{m}$.

rapidly when R_m < 200m. Then, the tendency slows down when R_m > 200m. For scenario (a), the nearest femto BS is the dominating interference source, the lower path loss constant will decrease the upper bound of the feasible femto BS density. On the contrary, for scenario (b), the nearest femto BS is the serving BS, the lower path loss constant will increase the range of feasible femto BS density. Furthermore, to meet the scenario criterion of having the macro BS as the dominating interference source (calculated as a loose upper bound), the path loss constant of the nearest femto BS should below 40dB (~ 38dB).

In Fig. 3-5, with a fixed value of $R_m = 150\text{m}$, we evaluate the feasible femto BS density with outage probability for Num and App. From Fig. 3-5, it is clear that for δ_{f1} =35dB plot, the App and Num curves match well. For other two, δ_{f1} = 40dB and 45dB, since from Fig. 3-4, the associated lower bounds exceed the upper bound, which violate the assumption of having the macro BS as the dominating interference source, the App and Num departs from each other.

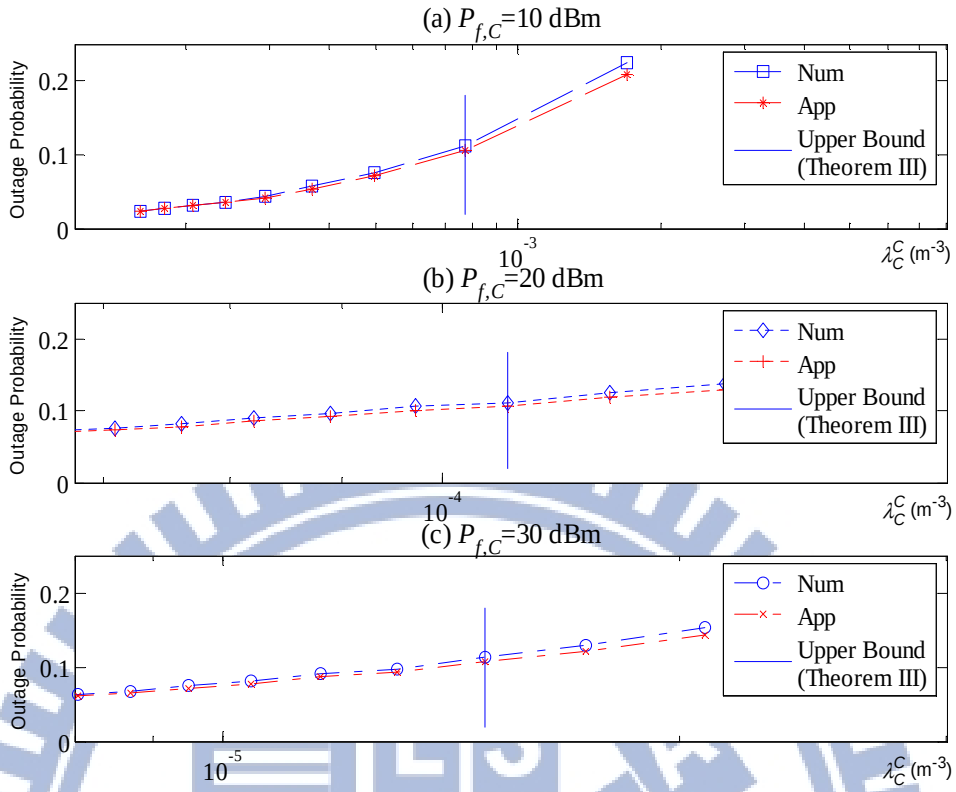

Fig. 3-6 Outage probability when λ_C^C is near the upper bound estimated from Theorem III. Here, $\delta_{f1,O} = 40\,\text{dB}$, $\delta_{f1,C} = 55\,\text{dB}$, $\delta_{f2,O} = \delta_{f3,O} = \delta_{f2,C} = \delta_{f3,C} \ldots = 65\,\text{dB}$, and $\lambda_O^C = 10^{-4}$ m^{-3}

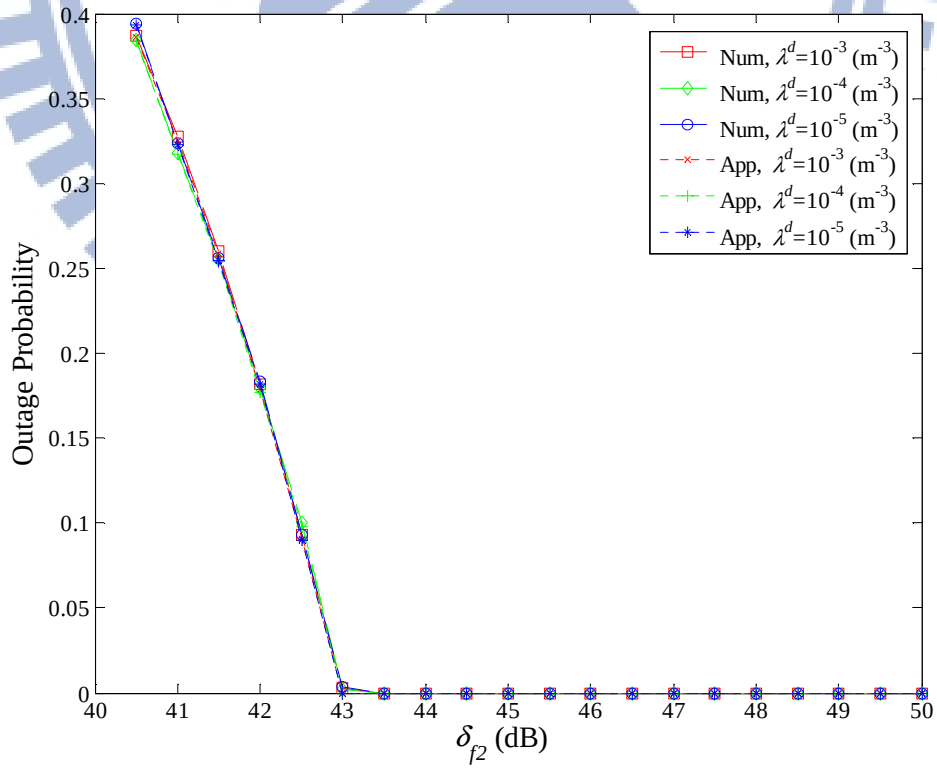

Fig. 3-7 Outage probability of scenario (d). Here, $\delta_{f1} = 40\text{dB}$, $\delta_{f3} = \ldots = 65\text{dB}$, $\delta_{f2} = 41 \sim 50\text{dB}$. It is clear that the outage probability is unrelated to λ^d.

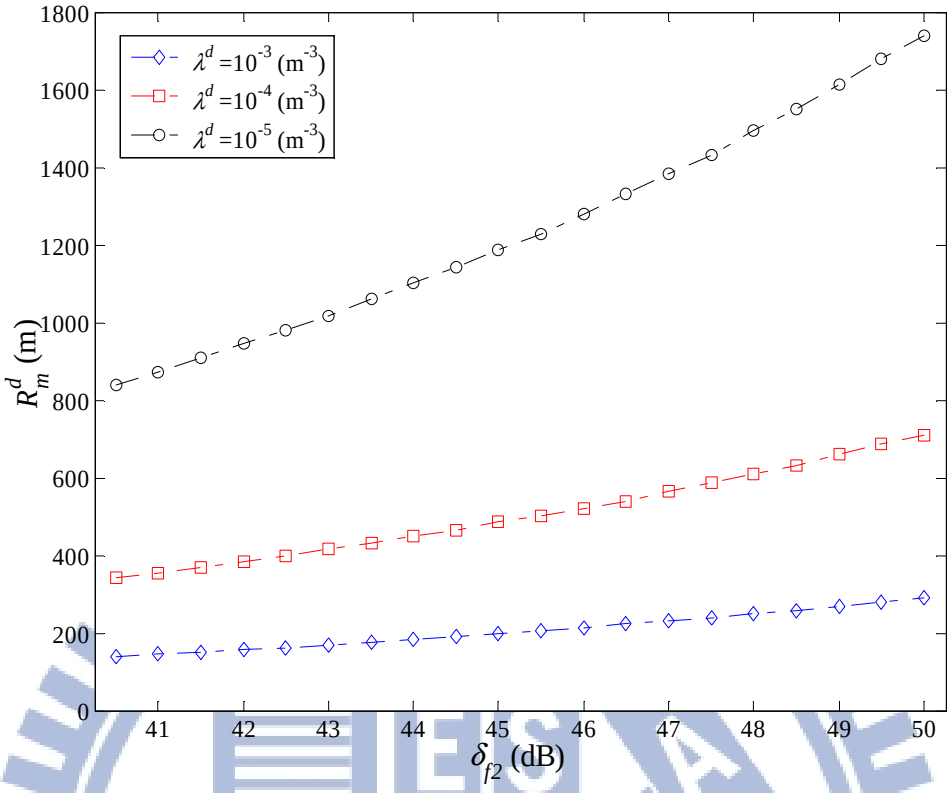

Fig. 3-8 Curves of R_m^d under different δ_{f2} and λ^d. Here, $\delta_{f1} = 40\text{dB}$, $\delta_{f3} = ... = 65\text{dB}$, $\delta_{f2} = 41 \sim 50\text{dB}$.

If considering femto BS as the dominating interference source, from Fig. 3-6, the App and Num curves match well in various operating outage probabilities in the scenario (c), which the nearest CSG femto BS is the dominant interference node to the non-CSG user. In Fig. 3-7, we verify our observation of scenario (d), which both the serving femto BS and the dominating interference node are from the same OSG femto BS network. By adjusting λ^d in the Fig. 3-7, we found that the outage probability is unrelated to the λ^d and this result coincides with our analysis in the scenario (d).

In scenario (d), to ignore the interference from the macro BS, the minimum distance, R_m^d, between the user and macro BS is plotted in Fig. 3-8. Here, we assume the interference from the macro BS can be ignored when $\mathrm{E}[U_2] - U_m(R_m) > \kappa_D^d$. κ_D^d is obtained through numerical results and R_m^d is the minimum value to fulfill the inequality. In Fig. 3-8, we consider different femto BS densities and various path loss constants of the dominating interference femto BS, F_2. As expected, the minimum distance increases with the decrease of femto BS density. When the femto BS density is higher, the minimum distance becomes less sensitive to the change of path loss constant from the

dominating interference femto BS.

3.4 Discussion

Considering four different deployment scenarios, we have identified closed form solutions to analyze related deployment performance of femto BS networks. The results provide a reference for the deployment of femto BS networks.

First, Theorem I and II, corresponding to scenario (a) and (b) respectively, provide the average user performance in a mixed macro BS and femto BS network and the feasible femto BS density when macro BS is either the serving BS or dominating interference source. The resulting feasible femto BS density can be used as design criteria for resource allocation. For example, when the femto BS density exceeds a threshold, the original co-channel resource allocations might need to be switched to orthogonal channel allocations to avoid the further degradation of the system performance due to the excessive interference.

Same concept applies to conditions of a mix of CSG and OSG femto BS network or a complete OSG femto BS network. Based on the observation in the scenario (c) and scenario (d), the feasible femto BS density can be calculated. From that, the operator can use the reference threshold to activate the hybrid access of CSG and OSG or again to consider orthogonal channel allocation scheme to mitigate the interference problems.

In conclusion, the proposed model provides simple approximation of user performance in four different deployment scenarios. Operators can then quickly verify the overall performance and decide proper resource allocation schemes to maintain the QoS of the cellular networks.

3.5 Conclusion

In this chapter, combining stochastic geometry for femto BS deployment and low outage probability criterion for cellular network, we are able to derive closed forms solution for the feasible femto BS density in a 3-D space by assuming the existence of a dominating interference source. To generalize the deployment scenarios, we have considered four different scenarios: (a) macro BS is the serving BS; (b) F_1 is the serving BS; (c) CSG femto BS is the dominant interference source to a non-CSG user; and (d) OSG femto BS network. Results showed that the approximation from the assumption of

dominating interfering source is actually a good representation of user performance in above four different scenarios, which can be used to provide a quick evaluation of the limit in femto BS density under the low outage probability criterion.

CHAPTER 4
EXTENSION OF LOG VALUE ESTIMATION

In this chapter, we extend our work about estimating $\mathrm{E}[\ln(R_n)]$ to the *m*-dimensional HPPP analysis. To distinguish, we use $R_{n|m}$ to represent the distance to the *n*th nearest node in the *m*-dimensional area. In section 4.1, we introduce the background of the *m*-dimensional HPPP and our motivation to extend the study. In section 4.2, we analyze the closed form of $\mathrm{E}[\ln(R_{n|m})]$ and compare our results with preliminary studies. In section 4.3, we extend our study to the estimation of Nakagami fading channel. Numerical results are implemented in section 4.3 to verify our analysis.

4.1 Introduction

In an *m*-dimensional HPPP, the PDF of the location of each random node in a given area *A* is assumed to be uniformly distributed. For generality, we represent the PDF of the number of nodes in an *m*-dimensional area, denoted by *A*, by (4.1) [82]:

$$\Pr_S(s,\lambda,A) = (\lambda\mu(A))^s \exp(-\lambda\mu(A))/s!, \tag{4.1}$$

where S is the number of nodes in A and $\mu(A)$ is the standard Lebesgue measure of A; λ is the average number of nodes in a unit volume of an m-dimensional ball of radius r, and it is called the intensity or density of the HPPP. The volume of the ball is denoted by $C_m r^m$, where C_m varies with m, an integer [82] as

$$C_m = \begin{cases} \pi^{m/2}/(m/2)! & \text{mod}(m,2) = 0, \\ \pi^{(m-1)/2} 2^m ((m-1)/2)!/m! & \text{mod}(m,2) = 1. \end{cases} \quad (4.2)$$

By applying HPPP to the analysis of a random network, the PDF of the Euclidean distance between a point and its nth randomly deployed neighbor, denoted by $R_{n|m}$, also follows the ggd

$$f_{R_{n|m}}(r) = \exp(-\lambda C_m r^m) \frac{m(\lambda C_m r^m)^n}{r\Gamma(n)}. \quad (4.3)$$

Because of the popularity of HPPP and ggd in the wireless communications, our study can be applied to many studies about wireless communications. In Chap. 3, we provided a closed form expression for $\mathrm{E}[\ln(R_{n|m})]$ for $m = 3$

$$\mathrm{E}[\ln(R_{n|3})] = \frac{-\gamma - \ln(4\pi\lambda/3)}{3} + \sum_{k=2}^{n} \frac{1}{3(k-1)}. \quad (4.4)$$

where γ is the Euler-Mascheroni constant and $\gamma \sim 0.5772$. In this study, we continue the analysis with similar approach. In Chap. 3, we have used $\mathrm{E}[\ln(R_{n|3})]$ to estimate the average signal strength when the Hata empirical model is applied. With further study, we can futher extend our result to the m-dimensional random network ($m \le 3$). In section 4.3, we will provide an example about our extension work.

Many researches have concentrated on how to estimate the shape parameters of the ggd. The maximum likelihood approach was proposed in [94] and [95]. In [96], Huang and Hwang proposed a moment approach to estimate the ggd. In [97], Song obtained parameters of the ggd by using scale-independent shape estimation equations. However, these studies did not focus on the estimation of $\mathrm{E}[\ln(R_{n|m})]$. In our previous work, we

obtained the expression in (4.4) by using the definition of expected values directly. In this chapter, we will continue the analysis with a similar approach. Nearly at the same time with our previous works, Reig and Rubio proposed estimators of the ggd that involved the moment function of the log transformation of the ggd [98], which is related to our job. We will compare both works in the next section.

4.2 Log-Value Estimation

On the basis of ggd and HPPP, the expected value of the log distance is defined as

$$\mathrm{E}[\ln(R_{n|m})] \equiv \lim_{\varepsilon \to 0} \int_{\varepsilon}^{\infty} m \ln(r) \exp(-\lambda C_m r^m)(\lambda C_m r^m)^n / (r\Gamma(n)) dr \,. \tag{4.5}$$

In our analysis of the HPPP, we assume that both *m* and *n* are integers. With the help of [87], we find the closed form for different values of *m* and *n*. The closed forms for *n* values from 1 to 5 are listed in Table 4-1. From Table 4-1, it is expected that the closed form of $\mathrm{E}[\ln(R_{n|m})]$ becomes even more complicated for higher values of *m* and *n*. To obtain a general form in the estimation of $\mathrm{E}[\ln(R_{n|m})]$, we apply a generalized closed form, which fully represents $\mathrm{E}[\ln(R_{n|m})]$ for *n* values in the range 1…5:

$$\mathrm{E}[\ln(R_{n|m})] = \lim_{\varepsilon \to 0} \frac{\Gamma(n)\mathrm{Ei}(-\lambda C_m r^m) - m\ln(r)(C_m r^m A_{m,n}(r) + \Gamma(n))\exp(-\lambda C_m r^m)}{\Gamma(n)m} - \frac{B_{m,n}(r) C_m r^m \exp(-\lambda C_m r^m)}{\Gamma(n)m} - K_{m,n}(r) \Big|_{\varepsilon}^{\infty} . \tag{4.6}$$

In (4.6), $A_{m,n}(r)$ and $B_{m,n}(r)$ are polynomials of *r*. Both $A_{m,n}(r)$ and $B_{m,n}(r)$ vary with *m* and *n*. $K_{m,n}(r)$ varies with different (*m*, *n*).

$$\begin{cases} K_{m,n}(r) = 0 & \text{when } n = 1, \\ K_{m,n}(r) = \sum_{k=2}^{n} \frac{\exp(-\lambda C_m r^m)}{m(k-1)} & \text{otherwise.} \end{cases} \tag{4.7}$$

$\mathrm{Ei}(-\lambda C_m r^m)$ is an exponential integral, which is defined as

Table 4-1 Closed forms of $E[\ln(R_{n|m})]$

n	$\int m\ln(r)\exp(-\lambda C_m r^m)(\lambda C_m r^m)^n/(r\Gamma(n))dr$
1	$\frac{1}{m}(\mathrm{Ei}(-\lambda C_m r^m) - m\ln(r)\exp(-\lambda C_m r^m))$
2	$\frac{1}{m}(\mathrm{Ei}(-\lambda C_m r^m) - m\ln(r)\exp(-\lambda C_m r^m)(\lambda C_m r^m + 1) - \exp(-\lambda C_m r^m))$
3	$\frac{1}{2m}(2\mathrm{Ei}(-\lambda C_m r^m) - m\ln(r)(\lambda^2 C_m^2 r^{2m} + 2\lambda C_m r^m + 2)\exp(-\lambda C_m r^m) - \lambda C_m r^m \exp(-\lambda C_m r^m) - 3\exp(-\lambda C_m r^m))$
4	$\frac{1}{\Gamma(4)m}(6\mathrm{Ei}(-\lambda C_m r^m) - m\ln(r)(\lambda^3 C_m^3 r^{3m} + 3\lambda^2 C_m^2 r^{2m} + 6\lambda C_m r^m + 6)\exp(-\lambda C_m r^m) - (\lambda^2 C_m^2 r^{2m} + 5\lambda C_m r^m)\exp(-\lambda C_m r^m) - 11\exp(-\lambda C_m r^m))$
5	$\frac{1}{\Gamma(5)m}(24\mathrm{Ei}(-\lambda C_m r^m) - m\ln(r)(\lambda^4 C_m^4 r^{4m} + 4\lambda^3 C_m^3 r^{3m} + 12\lambda^2 C_m^2 r^{2m} + 24\lambda C_m r^m + 24)\exp(-\lambda C_m r^m) - (\lambda^3 C_m^3 r^{3m} + 7\lambda^2 C_m^2 r^{2m} + 26\lambda C_m r^m)\exp(-\lambda C_m r^m) - 50\exp(-\lambda C_m r^m))$

$$\mathrm{Ei}(z) \equiv \int_{-\infty}^{z} \exp(t)/t\,dt = -\mathrm{Ex}(-z),\ \mathrm{Ex}(z) \equiv \int_{z}^{\infty} \exp(-t)/t\,dt. \tag{4.8}$$

For a general analysis, we will use the generalized closed form when $n \geq 2$ to estimate $E[\ln(R_{n|m})]$.

From (4.6), it is clear that $\exp(-\lambda C_m r^m) = 0$ and $\mathrm{Ei}(-\lambda C_m r^m) = 0$ when $r -> \infty$. Furthermore, both $\ln(\varepsilon) C_m \varepsilon^m A_{m,n}(\varepsilon)$ and $B_{m,n}(\varepsilon) C_m \varepsilon^m$ approach zero when $\varepsilon \to 0$. Therefore, $A_{m,n}(\varepsilon)$ and $B_{m,n}(\varepsilon)$ do not affect the estimation of (4.7). Thus, Eq.(4.6) can be further simplified:

$$E[\ln(R_{n|m})] = \lim_{\varepsilon \to 0}\left(\frac{\mathrm{Ex}(\lambda C_m \varepsilon^m)}{m} + \ln(\varepsilon)\exp(-\lambda C_m \varepsilon^m)\right) + \sum_{k=2}^{n} \frac{1}{m(k-1)}. \tag{4.9}$$

Here, we represent $\mathrm{Ex}(z)$ in another way [88]:

$$\mathrm{Ex}(z) = -\gamma - \ln(z) + \sum_{k=1}^{\infty} \frac{(-1)^{k+1} z^k}{k \cdot k!}. \tag{4.10}$$

Therefore, $\mathrm{E}[\ln(R_{n|m})]$ can be represented by another form:

$$\lim_{\varepsilon\to 0}\left(\frac{\mathrm{Ex}(\lambda C_m \varepsilon^m)}{m}+\ln(\varepsilon)\exp(-\lambda C_m\varepsilon^m)\right)+\sum_{k=2}^{n}\frac{1}{m(k-1)}$$

$$=\frac{-\gamma-\ln(\lambda C_m)}{m}+\sum_{k=2}^{n}\frac{1}{m(k-1)}+\lim_{\varepsilon\to 0}\ln(\varepsilon)(\exp(-\lambda C_m\varepsilon^m)-1). \tag{4.11}$$

In (4.11), it is clear that $\ln(\varepsilon)(\exp(-\lambda C_m\varepsilon^m)-1)$ will also approach zero when $\varepsilon\to 0$. Therefore, we obtain the closed form expression for $\mathrm{E}[\ln(R_{n|m})]$ in the *m*-dimensional space:

$$\begin{aligned}\mathrm{E}[\ln(R_{1|m})]&=\frac{-\gamma-\ln(\lambda C_m)}{m},\\ \mathrm{E}[\ln(R_{n|m})]&=\mathrm{E}[\ln(R_{1|m})]+\sum_{k=2}^{n}\frac{1}{m(k-1)},\ \mathrm{n}\geq 2.\end{aligned} \tag{4.12}$$

In [98], Reig and Rubio proposed estimators to estimate the parameters of the ggd through the moment of the logarithmic transformation of ggd. The logarithmic transformation can be obtained by defining $X\equiv\ln(R_{n|m})$ and relaxing the integer constraints on (*m*, *n*). Using the transformation of variables, the PDF of X can be derived from Eq.(4.3)

$$f_X(x)=\frac{\alpha\Omega^{\beta}}{\Gamma(\beta)}\exp(\alpha\beta x-\Omega\exp(\alpha x)), \tag{4.13}$$

where λC_m is replaced by Ω and (*m*, *n*) are also replaced by (α,β) with the assumptions $\alpha>0$ and $\beta>0$. In their analysis, $\mathrm{E}[X]$ is given by

$$\mathrm{E}(X,\alpha,\beta,\Omega)=(\psi(\beta)-\ln(\Omega))/\alpha. \tag{4.14}$$

$\psi(\beta)$ is the digamma function, and it can be written as $\psi(\beta)\equiv d(\ln(\Gamma(\beta))/d\beta)$. However, $\psi(\beta)$ is a transcendental equation and so (4.14) is difficult to solve directly.

By comparing our closed form in (4.13) with (4.14), we find that (4.14) coincides with

the expressions obtained in our work. This is a consequence of the fact that $\psi(\beta)$ can be further transformed to another representation when β is an integer [88]:

$$\psi(1) = -\gamma,\ \psi(\beta) = -\gamma + \sum_{k=2}^{\beta} 1/(k-1),\ \beta > 1. \tag{4.15}$$

By applying (4.15) to (4.14) and considering our assumptions on (*m*, *n*) and λC_m, we find that $\mathrm{E}(X, m, n, \lambda C_m)$ gives the same result as (4.13). This shows the accuracy of our analysis. In addition, we find the digamma function can be further transformed when β is a half-integer [88]:

$$\begin{aligned} &\psi(1/2) = -\gamma - 2\ln 2, \\ &\psi(n+1/2) = -\gamma - 2\ln 2 + \sum_{k=1}^{n} \frac{2}{2k-1},\ n \geq 1. \end{aligned} \tag{4.16}$$

Therefore, we obtain $\mathrm{E}(X, \alpha, n+1/2, \Omega)$:

$$\begin{aligned} &\mathrm{E}(X, \alpha, 1/2, \Omega) = (-\gamma - 2\ln 2 - \ln(\Omega))/\alpha, \\ &\mathrm{E}(X, \alpha, n+1/2, \Omega) = (-\gamma - 2\ln 2 + \sum_{k=1}^{n} \frac{2}{2k-1} - \ln(\Omega))/\alpha. \end{aligned} \tag{4.17}$$

Both the (4.12) and (4.17) will be utilized in the later analysis.

4.3 Applications

Comparing with the previous works, our contributions in include:

1) We provide a simple approach to the special case (β is an integer or a half-integer) of $\mathrm{E}(X, \alpha, \beta, \Omega)$ when *X* is the log logarithmic transformation of ggd.

2) We apply our work to the *m*-dimensional HPPP. In random networks, along with the HPPP and Hata empirical model, $\mathrm{E}[\ln(R_{n|m})]$ ($m \leq 3$) can be used to estimate the average signal strength (in decibel) at the *n*th nearest node. Furthermore, by assuming the signal to noise ratio (SNR) is much larger than 1, the average Shannon capacity in the

random networks, $C = B \cdot \log_2(1+\xi)$, which ξ is the SNR and B is the frequency bandwidth, can also be approximated by applying the proposed closed-form.

3) In addition to HPPP, the log value estimation can be widely applied to other fields of wireless communication. Next, we further extend our work to the estimation of Nakagami fading channel.

In wireless communications, the channel which the envelope follows Nakagami distribution is called Nakagami fading channel. Nakagami distribution was first proposed by Nakagami [99] to model the ionospheric and tropospheric fast fading channels. Now, it also has been widely adopted for multi-path modeling in wireless communications due to its accuracy and versatility [100]. The PDF of the Nakagami distribution is given

$$f_Y(y) = \frac{2}{\Gamma(M)}\left(\frac{M}{\omega}\right)^M y^{2M-1}\exp(-My^2/\omega), \tag{4.18}$$

where Y represents the envelope of Nakagami fading channel; M is the fading figure and ω is the second moment of Y. Because Nakagami distribution fits very well in the urban and indoor environment [101]-[102], Nakagami distribution can also be applied by the femto BS networks to estimate the multi-path channels. Furthermore, it is well known that Y^2 follows gamma distribution when Y follows Nakagami distribution [103]-[104].

From (4.18), it is clear that the fading figure decide the shape of Nakagami distribution. Therefore, to approximate the fading channel by using the Nakagami distribution, it is necessary to determine the fading figure through samples [103]-[104]. In [103], the log ratio between the arithmetic mean and geometric mean of the samples, Δ, is used in the fading figure estimation :

$$\Delta \equiv \ln\left(\frac{\sum_{i=1}^{N} Y_i^2 / N}{(\prod_{i=1}^{N} Y_i^2)^{1/N}}\right), \tag{4.19}$$

where Y_i^2 is the ith sample of the channel and i = 1…N. Based on the character of gamma distribution, $\sum_{i=1}^{N} Y_i^2$ also follows the gamma distribution when Y_i^2 are identically and independently distributed. In [104], by applying the maximum likelihood approach, the relationship between Δ and the fading figure M is summarized

$$-\psi(M)+\ln(M)\approx\Delta \tag{4.20}$$

However, it is also difficult to find the accurate *M* by (4.20) because the transcendental equation, $\psi(M)$, in (4.20). Furthermore, (4.20) is an approximation, not a closed form expression.

In the preliminary studies, many researchers proposed maximum likelihood (ML) based estimators based on (4.20). In [104], Cheng *et al.* proposed two estimators: $\tilde{m}_1$ and $\tilde{m}_2$ to estimate the fading figure.

$$\tilde{m}_1=\frac{1}{2\Delta};\ \tilde{m}_2=\frac{6+\sqrt{36+48\Delta}}{24\Delta}\ . \tag{4.21}$$

In Zhang's works [105], he showed that a more robust estimator, denoted by $\tilde{m}_{GD}$, had already proposed by Greenwood and Durand.

$$\tilde{m}_{GD}=\begin{cases}(0.5000876+0.1648852\Delta-0.054427\Delta^2)/\Delta, & 0<\mathrm{y}\le 0.5772\\ \dfrac{8.898919+9.059950\Delta+0.9775373\Delta^2}{\Delta(17.79728+11.968477\Delta+\Delta^2)}, & 0.5772<\mathrm{y}<17.\end{cases} \tag{4.22}$$

In [106], Gaeddert and Annamalai also proposed a ML based estimator, denoted as $\tilde{m}_{AMLE}$, which the performance is compariable to $\tilde{m}_{GD}$

$$\tilde{m}_{AMLE}=\frac{b_{AMLE}+\sqrt{b_{AMLE}^2+4(\Delta-a_{AMLE})c_{AMLE}}}{2(\Delta-a_{AMLE})}, \tag{4.23}$$
$$a_{AMLE}=\text{-}5.0428\text{E-}4,\ b_{AMLE}=5.0953\text{E-}1,\ c_{AMLE}=6.5552\text{E-}2.$$

In addition to ML based estimators, a group of estimators, which are called Generalized Moment Estimators, were proposed by Cheng and Beaulieu [107].

$$\tilde{m}_{1/p}=\frac{\hat{\mu}_{1/p}\hat{\mu}_2}{2p(\hat{\mu}_{2+1/p}-\hat{\mu}_{1/p}\hat{\mu}_2)},\ \hat{\mu}_k=\mathrm{E}[Y^{\mathrm{k}}]. \tag{4.24}$$

Here, p is the control parameter. Varying p yields a group of estimators. Generally, the performances of these estimators improve with increasing value of p. However, based on the numerical results in [107], the performance of $\tilde{m}_{1/p}$ can not be better than that of $\tilde{m}_1$ and $\tilde{m}_2$. Moreover, estimating $\hat{\mu}_{1/p}$ and $\hat{\mu}_{2+1/p}$ would increase the computation complexity. Deriving form [107], Gaeddert and Annamalai proposed a group of estimators by replacing the Δ in (4.23) with Δ_{GME} [106]

$$\tilde{m}_{GME} = \frac{b_{GME} + \sqrt{b_{GME}^2 + 4(\Delta_{GME} - a_{GME})c_{GME}}}{2(\Delta_{GME} - a_{GME})}, \tag{4.25}$$

where $\Delta_{GME} = (\hat{\mu}_{1/p})^2 / \hat{\mu}_{2/p}$ and the a_{GME}, b_{GME}, and c_{GME} need to be optimized baed on different values of p. However, the performance of the moment based estimators cannot be better than that of ML based estimators [106], [107]. Therefore, we will compare our proposed approach with the ML based estimators, which include $\tilde{m}_1$, $\tilde{m}_2$, $\tilde{m}_{GD}$, $\tilde{m}_{AMLE}$.

We start the fading figure estimation from the expected value of Δ. Because Y_i^2 and so $\sum_{i=1}^{N} Y_i^2$ follow the gamma distribution, we obtain the expected value of Δ from (4. 19)

$$\mathrm{E}[\Delta] = -\psi(M) - \ln(N) + \psi(M \cdot N), \tag{4.26}$$

by applying (4.12) and (4.17). Furthermore, we obtain closed forms of $\mathrm{E}[\Delta]$ when M is an integer or a half-integer. Therefore, we provide a lookup table to map the fading figure M' and the correspondent $\mathrm{E}[\Delta \mid M']$. Here, M' is an increasing arithmetic progression and M'=0.5, 1, 1.5, 2…. By given the values of $\{M', N\}$, the decision rule of the proposed approach is plotted through the flow chart in Fig. 4-1.

After the construction of lookup table, we will estimate the $\tilde{\Delta}$ through samples. Then, interpolation and extrapolation is utilized to map the $\tilde{\Delta}$ to the estimated fading figure, denoted by $\tilde{M}_{Lin}$. In the next section, we will verify our proposed $\tilde{M}_{Lin}$ with the ML based estimators.

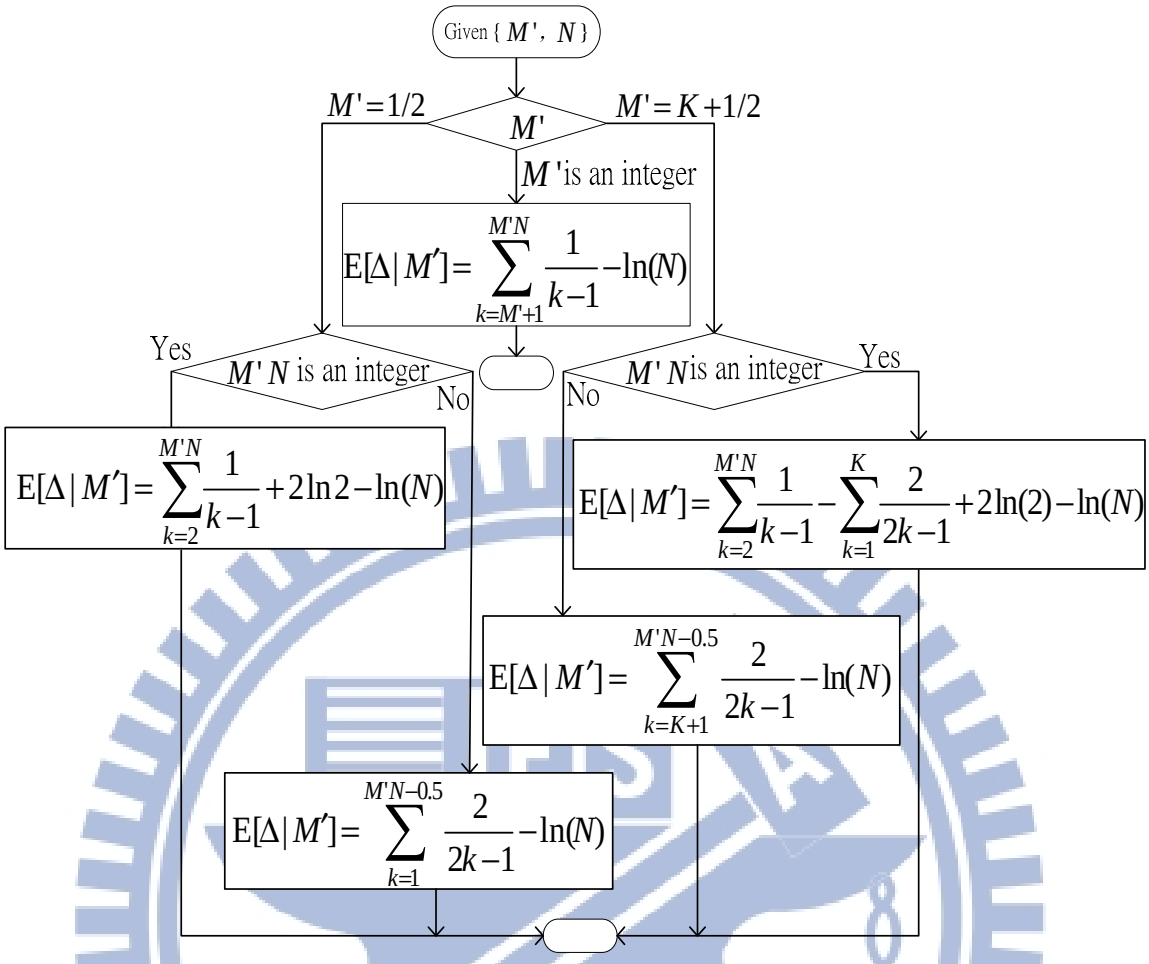

Fig. 4-1 Decision rule to construct the lookup table of $\mathrm{E}[\Delta \mid M']$

4.4 Numerical Results

To verify the closed form model, we compare the numerical results (Num curves) with the estimation results (Est curves). In Fig. 4-2, we verify the proposed closed form in (4.12) and (4.17) by replacing *m* with α. Here, we assume that $\Omega = 0.1$ and α = 1.2, 2.4, and 3.6, respectively.

For the Num curve, we increase β from 0.5 to 12 gradually. The estimation value is obtained from (4.12) when β is an integer; it is obtained from (4.17) when β is a half-integer. As shown in Fig. 4-2, we find that the Est curves fit the Num curves very well. Therefore, it is clear that our proposed closed form facilitates the quick estimation of $\mathrm{E}(X, \alpha, \beta, \Omega)$.

After the verification of the proposed closed forms, we will verify the proposal of estimating the fading figure by applying interpolation approach, denoted by $\tilde{M}_{Lin}$. The Root Mean Square Error (RMSE) is applied to verify the performance of different

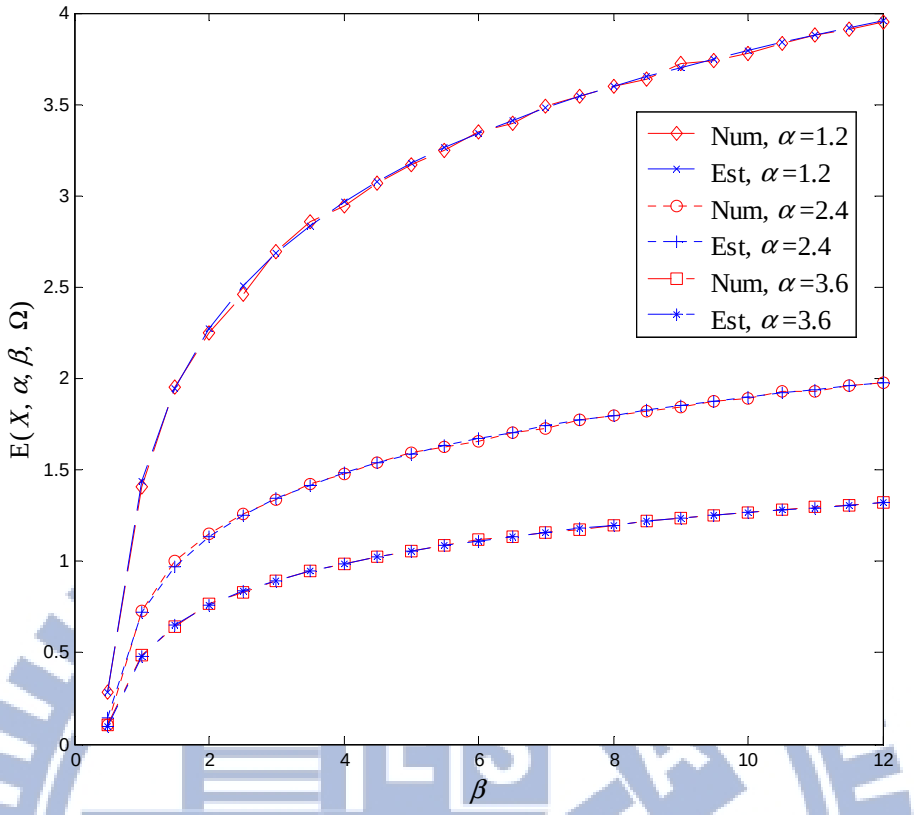

Fig. 4-2 Evaluation of $\mathrm{E}(X,\alpha,\beta,\Omega)$ based on the closed form in (4.12) and (4.17).

estimators. Moreover, the RMSE is normalized by *M* for the convenience of comparison.

In Fig. 4-3, we assume *N*=100 to compare the normalized RMSE of $\tilde{m}_1$, $\tilde{m}_2$, $\tilde{m}_{GD}$, $\tilde{m}_{AMLE}$, and $\tilde{m}_{Lin}$. The assumption of *N*=100 is accepted as small sample size to estimate the fading channels [104]. It is clear that the RMSE of $\tilde{m}_{Lin}$ is the lowest one in the region $M \approx 1 \sim 18$. Although the RMSE of $\tilde{m}_{AMLE}$ is the largest one in the range $M \approx 1 \sim 18$, we find $\tilde{m}_{AMLE}$ is better than $\tilde{m}_{Lin}$ when we keep increase the value of *M*. It is because $\tilde{m}_{AMLE}$ is obtained through Monte Carlo simulations in a wide range of *M* [106]. Therefore, the accuracy of $\tilde{m}_{AMLE}$ improves with the increase of *M*. Even so, $\tilde{m}_{Lin}$ is still better than other estimators when *M* is large. Note that $\tilde{m}_{Lin}$ underperforms when *M*<1. It is because extrapolation may be applied in the region *M*<1. This can be compensated by pre-record the values of $\mathrm{E}[\Delta \mid M']$ which $M'<1$ in the lookup table.

In Fig. 4-4, we adjust the value of *N*=30. From Fig. 4-4, we find the difference between $\tilde{m}_{Lin}$ and other estimators are clearer and the region that $\tilde{m}_{Lin}$ outperforms others is also enlarged. From Fig. 4-3 and Fig. 4-4, we observed

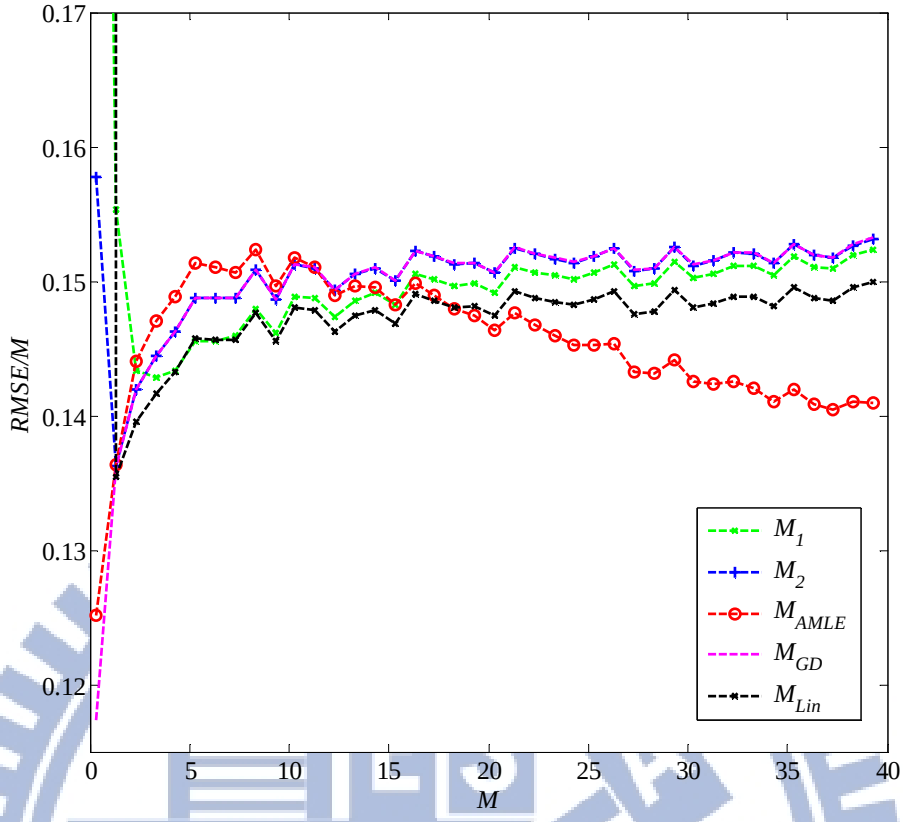

Fig. 4-3 Comparisions with differetent ML based estimators. N=100.

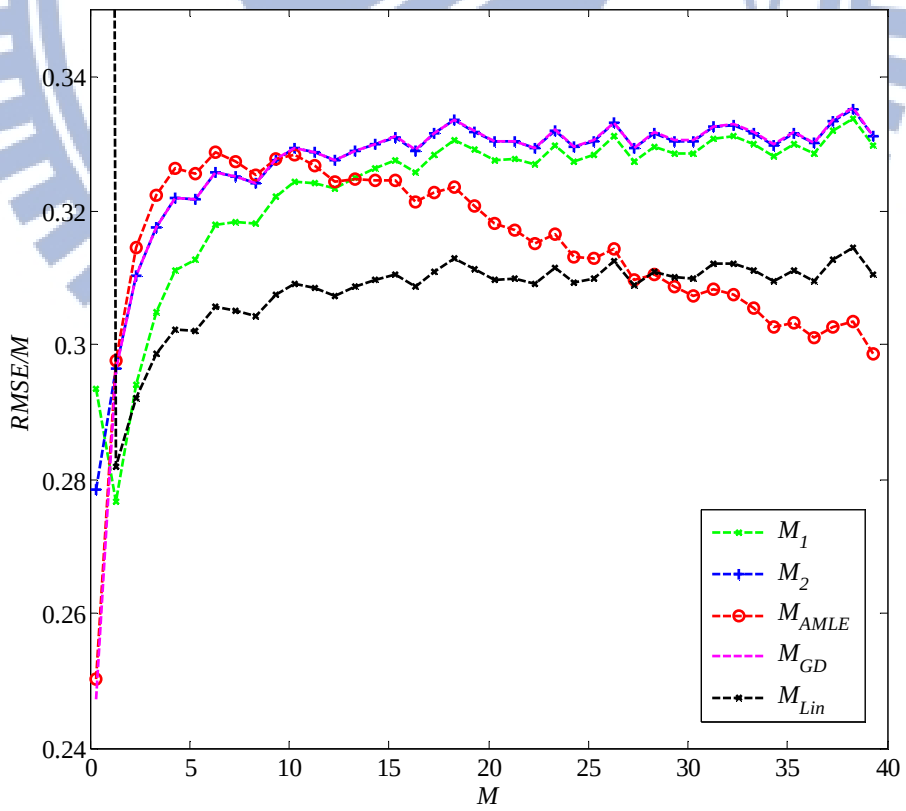

Fig. 4-4 Comparisions with differetent ML based estimators. N=30.

the proposed $\tilde{m}_{Lin}$ is a comparable estimator to other estimators especially when the sample size is small.

4.4 Conclusion

In this chapter, on the basis of the HPPP, we have proposed a closed form for finding $\mathrm{E}[\ln(R_{n|m})]$, where $R_{n|m}$ follows the generalized gamma distribution. Furthermore, we provided closed forms to the special cases of the expected value of logarithmic transformation of ggd, $\mathrm{E}(X,\alpha,\beta,\Omega)$, when β is a integer or an half-integer.

Our results are applicable to many conditions in wireless communications. Here, we have provided two examples: 1) signal power estimation in random networks, and 2) fading figure estimation of the Nakagami channel. Simulation results showed our proposed fading figure estimator is comparable to other estimators.

CHAPTER 5

FEMTO BS NETOWRKS THROUGHPUT ANALYSIS

In this chapter, we will estimate the achievable throughput of femto BS network based on the structure of 4G cellular system, which is designed based on Orthogonal Frequency Division Multiplexing (OFDM) technology. We consider the effects of a) Randomly distributed interference sources, b) Low outage probability, c) Non-cooperated packet transmission, and d) Hybrid automatic repeat request (HARQ). We will identify a closed form estimation of downlink throughput in a femto BS network. The proposed estimation approach is simple and easy to be implemented. Numerical results are also provided to verify our proposal.

This chapter is organized as follows: In section 5.1, we introduce the analysis model. Then, in section 5.2, a closed form expression is proposed to facilitate the estimation process. Numerical results are provided in section 5.3. In section 5.4, we explain how to apply our works to the femto BS networks. Finally, we conclude our observations and contributions in section 5.5.

5.1 Analysis Model

In the analysis model, both the deployment model and transmission protocol are provided to analyze the femto BS networks.

5.1.1 Deployment Model

The deployment model is based on the 3-D model which has proposed in Chap. 3. Based on the 3-D HPPP model, we assume the distance from the target user, U_T, to the serving femto BS , F_S, is fixed. Interfering femto BSs are uniformly distributed around U_T with density, denoted by λ. Hata empirical pathloss model is applied to describe the channel degradation effect.

Extending from our observation in Chap. 3, we assume F_1 , which is the 1st closet interfering femto BS, dominates the combination of interference. From Chap. 3, it is clear the value of λ influences d_n and so the strength of interference. In Chap. 3, we have concluded that λ should follow the following inequality when $\Pr_O$ is very small

$$\lambda < -3\ln(1-\Pr_O)\exp(-3T_\varsigma^{'})/(4\pi) \equiv \lambda_U,$$
$$T_\varsigma^{'} = \frac{\ln(10)}{(10\eta_{f1})}(T_\varsigma - (P_S - P_{f1}) + (\delta_S - \delta_{f1}) + 10\eta_S \log_{10}(d_S)). \quad (5.1)$$

Here, $\{P_S, P_{f1}\}$ are the transmission powers of $\{F_S, F_1\}$ respectively. $\{\delta_S, \delta_{f1}\}$ and $\{\eta_S, \eta_{f1}\}$ are the path-loss constants and path-loss exponents of $\{F_S, F_1\}$. To provide ubiquitous coverage, λ needs to be controlled under the bound of femto BS density. Therefore, we will estimate the achievable throughput of U_T under the condition which (5.1) is fulfilled.

5.1.2 Transmission Protocol

We propose a) non-cooperated femto BS transmission, and b) HARQ, in the transmission protocol of femto BS networks.

a) Non-cooperated packet transmission

In 4G cellular systems, femto BS can transmit data packets by occupying different resource blocks in OFDM system dynamically [16], the resource blocks of OFDM systems are plotted in Fig. 5-1. In the frequency domain, the whole spectrum is divided into multiple frequency carriers. In time domain, the minimum unit is time slot. One resource block (RB) occupies one carrier in the frequency domain and one time slot

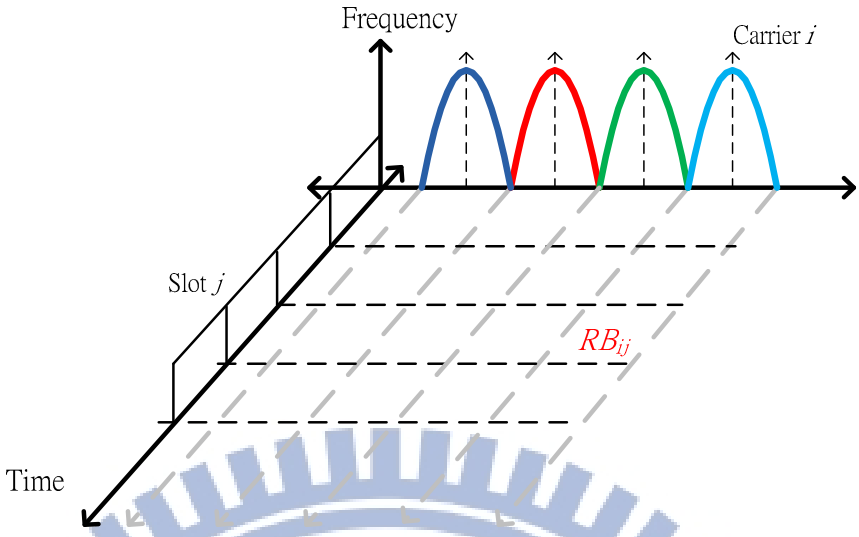

Fig. 5-1 Resource blocks of OFDM system

in the time domain. We assume there is no joint cooperation between the femto BSs and so femto BSs decide to transmit one sub-packet in one resource block randomly with probability $\Pr_T$, which is pre-defined by the system. The sub-packet is the basic unit of HARQ.

b) Hybrid Automatic Repeat Request (HARQ)

Hybrid Automatic Repeat Request (HARQ) is considered in this model because HARQ is well-applied in the 4G communication system [16],[109]. In HARQ, one packet is encoded and divided into many sub-packets. Each sub-packet is transmitted sequentially. U_T decodes a packet by combining all the sub-packets it receives. If successfully decoded, F_S prepares the next packet transmission. Otherwise, F_S keeps transmitting the next sub-packet until the total transmission sub-packet number, m_t, exceeds M_B or N_D. M_B and N_D are the transmission limits because of buffer size and delay limit respectively. In most cases, $N_D > M_B$. During the decoding process, U_T may receive several sub-packets before decoding one packet successfully. To address how many sub-packets are used to decode a packet successfully, the decoding failure probability, $\Pr_f(m_t)$, is applied in the following analysis:

$$\Pr_f(m_t) \equiv \Pr\left(\sum_{k=1}^{m_t} \log_2(1+\varsigma_k) \le R\right). \tag{5.2}$$

$\Pr_f(m_t)$ represents the decoding failure probability after U_T combines m_t sub-packets. Here, $R \equiv b/(W_F T_S)$, where W_F is the bandwidth for each carrier and T_S is the period of one time slot. b is the information bits in each packet. ς_k is the received SINR in each sub-packet transmission.

5.2 Throughput Analysis

In this section, we estimate the achievable throughput of femto BS networks based on Caire and Tuninetti's works [110]. However, their work is achived through numerical results and it is not easy to be applied directly. Based on the assumptions introduced in the last section, we propose an approach to simplify the estimation process and so the achievable throughput of femto BS networks can be estimated directly without numerical simulations.

5.2.1 Closed Form Expression

In our study, we applied the results from Caire and Tuninetti [110]. In [110], the achievable throughput of U_T can be represented by utilizing the *renewal-reward* theorem [110]:

$$D = W_F R \Pr_T \Lambda_A / \Lambda_B,$$

$$\Lambda_A = [1 - \sum_{l=0}^{M_B-1} \binom{N_D}{l} (1-\Pr_T)^{N_D-l} \Pr_T{}^{l} \Pr_f(l) - \sum_{l=M_B}^{N_D} \binom{N_D}{l} (1-\Pr_T)^{N_D-l} \Pr_T{}^{l} \Pr_f(M_B)],$$

$$\Lambda_B = \sum_{m_t=0}^{M_B-1} \Pr_f(m_t)[1 - \binom{N_D}{m_t} (1-\Pr_T)^{N_D-m_t} \Pr_T{}^{m_t+1} - \sum_{l=0}^{m_t} \binom{N_D+1}{l} (1-\Pr_T)^{N_D+1-l} \Pr_T{}^{l}]. \quad (5.3)$$

The closed form expression of *D* is obtained through the following approach.

***Renewal-Reward* Theorem** [111]

First, a *recurrent event* is defined as the event that U_T stops receiving the current packet. Here, we assume the U_T spends *T* time slots in decoding the current packet. When U_T stops the reception, a random reward $\Re$ is associated to the

occurrence of the recurrent event. There are two outcomes for $\Re$

$$\begin{cases} \Re = R & \text{if } U_T \text{ decodes successfully and } T \le \min(N_D, M_B), \\ \Re = 0 & \text{if } U_T \text{ decodes fail and } T > \min(N_D, M_B). \end{cases} \tag{5.4}$$

Based on the Renewal-Reward Theorem, the achievable throughput D can be estimated by the expected value of $\Re$ and T.

$$D = \frac{E[\Re]}{E[T]} \tag{5.5}$$

Moreover, the $E[\Re]$ and $E[T]$ of HARQ protocol can be represented by the following equations[110].

$$\begin{aligned} E[\Re] &= R[1 - \sum_{l=0}^{M_B-1} \binom{N_D}{l} (1-\Pr_T)^{N_D-l} \Pr_T{}^{l} \Pr_f(l) - \sum_{l=M_B}^{N_D} \binom{N_D}{l} (1-\Pr_T)^{N_D-l} \Pr_T{}^{l} \Pr_f(M_B)] \\ &= R\Lambda_A . \end{aligned} \tag{5.6}$$

$$\begin{aligned} E[T] &= \frac{1}{\Pr_T} \sum_{m_t=0}^{M_B-1} \Pr_f(m_t)[1 - \binom{N_D}{m_t} (1-\Pr_T)^{N_D-m_t} \Pr_T{}^{m_t+1} - \sum_{l=0}^{m_t} \binom{N_D+1}{l} (1-\Pr_T)^{N_D+1-l} \Pr_T{}^{l}] \\ &= \frac{\Lambda_B}{\Pr_T} . \end{aligned} \tag{5.7}$$

Based on Renewal-Reward Theorem, Eq. (5.3) provides a formula to estimate the achievable throughput of femto BS networks by applying $E[\Re]$ and $E[T]$. However, it is still difficult to obtain the throughput directly because both $E[\Re]$ and $E[T]$ are related to the decoding failure probability, $\Pr_f(m_t)$. In the previous works, $\Pr_f(m_t)$ is obtained only through numerical calculation [110]. The difficulty of estimating $\Pr_f(m_t)$ makes (5.3) complicated to be utilized directly for throughput estimation. In the next section, we propose a simple model to estimate $\Pr_f(m_t)$ directly.

5.2.2 Approximation of Decoding Failure Probability

In order to estimate D, we have to estimate $\Pr_f(m_t)$. However, it is difficult to find the closed form of $\Pr_f(m_t)$. The reason is because the SINR, ς_k, is a random variable. To solve this dilemma, as mentioned in Chap. 3, if the HPPP femto BS network is operated at a low outage probability, there exists a dominant interferer [93]. Based on our assumption, the dominant interfer is F_1. The observation of F_1 in the HPPP inspired us to simplify the $\Pr_f(m_t)$ by considering the dominance of F_1. Based on the major influence from F_1, we represent ς_k with two variables, $\{\bar{\varsigma}_S, \bar{\bar{\varsigma}}_S\}$, which are calculated as:

$$\bar{\varsigma}_S \equiv \frac{\upsilon_s}{I_{F1}+\Delta I+N_0};\ \bar{\bar{\varsigma}}_S \equiv \frac{\upsilon_s}{\Delta I+N_0};\ \Delta I \equiv \Pr_T \cdot \sum_{n=2} I_{Fn}. \tag{5.8}$$

Here, υ_s is the signal strength from F_S. I_{Fn} is the interference from all other F_n and N_0 is noise power. The influence of other interfering femto BS is captured by ΔI. ΔI is the average interference of all other interfering femto BSs except F_1. Therefore, U_T should be capable of measuring the combination of interference and signal strengths from F_S and F_1 respectively. In realistic communication system, this requirement is also defined in the capability about UE [112]. In (5.8), In each sub-packet transmission, $\bar{\varsigma}_S$ is used to represent the SINR when F_1 transmits a sub-packet simultaneously with F_S and $\bar{\bar{\varsigma}}_S$ is used to represent the SINR when F_1 is idle and F_S transmits one sub-packet. Based on (5.8), we approximate the bandwidth efficiency, β_S, which U_T receives in each sub-packet transmission.

$$\beta_S = \begin{cases} \log_2(1+\bar{\varsigma}_S) \equiv \bar{\beta}_S & \text{with } \Pr_T, \\ \log_2(1+\bar{\bar{\varsigma}}_S) \equiv \bar{\bar{\beta}}_S & \text{with } 1-\Pr_T \end{cases}. \tag{5.9}$$

Then, we need to estimate the influence of F_1 when F_S is transmitting one packet,

which may take m_t sub-packet transmissions. We define x to represent how many times that F_1 transmits sub-packets simultaneously with F_S during the m_t sub-packet transmissions. Based on the proposed protocol, x should follow binomial distribution. It is clear that the summation of bandwidth efficiency in (5.2) decreases with the increase of x. Therefore, we define $X_{\min}^{m_t}$ as the minimum value of x which the summation of bandwidth efficiency in (5.2) is lower than R.

$$X_{\min}^{m_t} \equiv \arg\{\min_x(x\bar{\beta}_S + (m_t - x)\bar{\bar{\beta}}_S < R \mid m_t,\ 0 \le x \le m_t)\} \tag{5.10}$$

Therefore, $\Pr_f(m_t)$ can be approximated with the following equation:

$$\tilde{P}_f(m_t) = \sum_{x=X_{\min}^{m_t}}^{m_t} \binom{m_t}{x} \Pr_T^x \cdot (1-\Pr_T)^{m_t - x} \tag{5.11}$$

In the next section, we will verify our proposal through simulations.

5.3 Simulations

In this section, the pathloss model, packet scheduling, deployment of femto BSs are implemented based on the proposed deployment model and transmission protocol. Simulation parameters are listed in Table 5-1. Based on Table 5-1 and (5.1), the threshold for low outage probability, λ_U, is estimated (~ $10^{-3.34}$ m^{-3}). To simulate the achievable throughput under fully coverage, we assume $\lambda = 10^{-5}$ (m^{-3}) in the first simulation. Then, we decide d_n and the following SINR by applying HPPP with given λ. We will compare the throughput D_{Num} and D_{App}, which the failure probability inside is obtained through simulations and proposed approach respectively.

In Fig. 5-2, we adjust $\Pr_T$ between 0.5, 0.75, and 1 to verify D_{Num} and D_{App}. In Fig. 5-2, it is clear that our model provides close estimation for the throughput of femto BS networks. Furthermore, we find out that D_{Num} and D_{App} match exactly when $\Pr_T$ is close to 1.

Table 5-1 Parameters of simulations

Notation	Value	Definition
$\{P_S, P_{fn}\}$	30 (dBm)	Radiation powers of $\{F_S, F_n\}$
$\{\delta_S, \delta_{fn}\}$	37 (dB)	Path-loss constants of $\{F_S, F_n\}$
$\{\eta_S, \eta_{fn}\}$	3	Path-loss exponents of $\{F_S, F_n\}$
λ	10^{-5},10^{-2} (m^{-3})	Femto BS density
ε	1	Minimum distance of $\{d_S, d_n\}$
N_f	10	Number of interfering femto BSs in the simulation
N_0	-100 (dBm)	Noise power
d_S	3 (m)	Distance between the U_T and F_S
d_n	HPPP	Distance between the U_T and F_n. The values are provided through HPPP.
$\Pr_O$	0.05	Upper threshold of outage probability
T_ς	0 (dB)	SINR bound of outage event
W_F	1 (Hz)	Bandwidth
T_S	1 (s)	Duration of one time slot
M_B	10 (slots)	Transmission limit because of buffer size
N_D	50 (slots)	Transmission limit because of delay limit

Then, we increase the femto BS density to a value much higher than λ_U, $\lambda = 10^{-2}(\text{m}^{-3})$, to see if our approximation is incorrect. Simulation results are plotted in Fig. 5-3. In Fig. 5-3, it is clear that the achievable throughput decreases to a very low level when λ is every high. Even so, we find that D_{Num} and D_{App} still match exactly, which means our proposal also provides an efficient way to estimate the throughput even though the femto BS density is much higher than the feasible density bound λ_U. From Fig. 5-3, we can conclude that the 1st nearest node still dominates $\Pr_t(m_t)$ even the femto BS density locates on the area which the outage probability is very high. Another reason that our approach can also be applied when $\lambda > \lambda_U$ is because we still consider the infleucne of other interferers by taking their average interference in our approach.

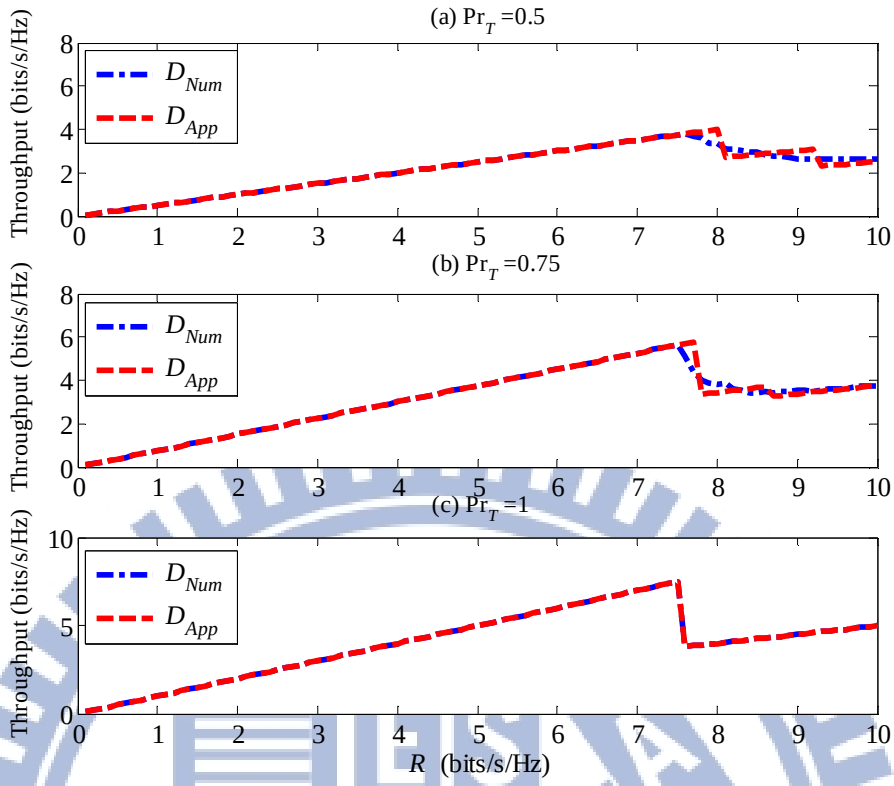

Fig. 5-2 Comparisons of D_{Num} and D_{App} curve when $\lambda = 10^{-5}(\mathrm{m}^{-3})$. It can be found both of the curves are closer when Pr_T increases.

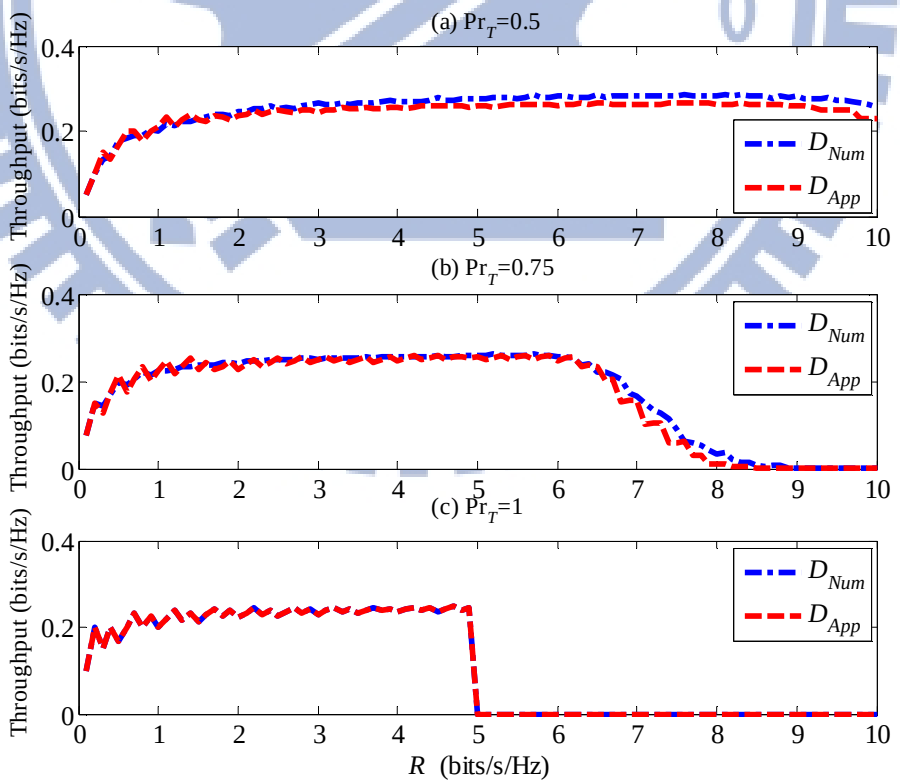

Fig. 5-3 Comparisons of D_{Num} and D_{App} curve when $\lambda = 10^{-2}(\mathrm{m}^{-3})$. It can be found both of the curves are still close to each other.

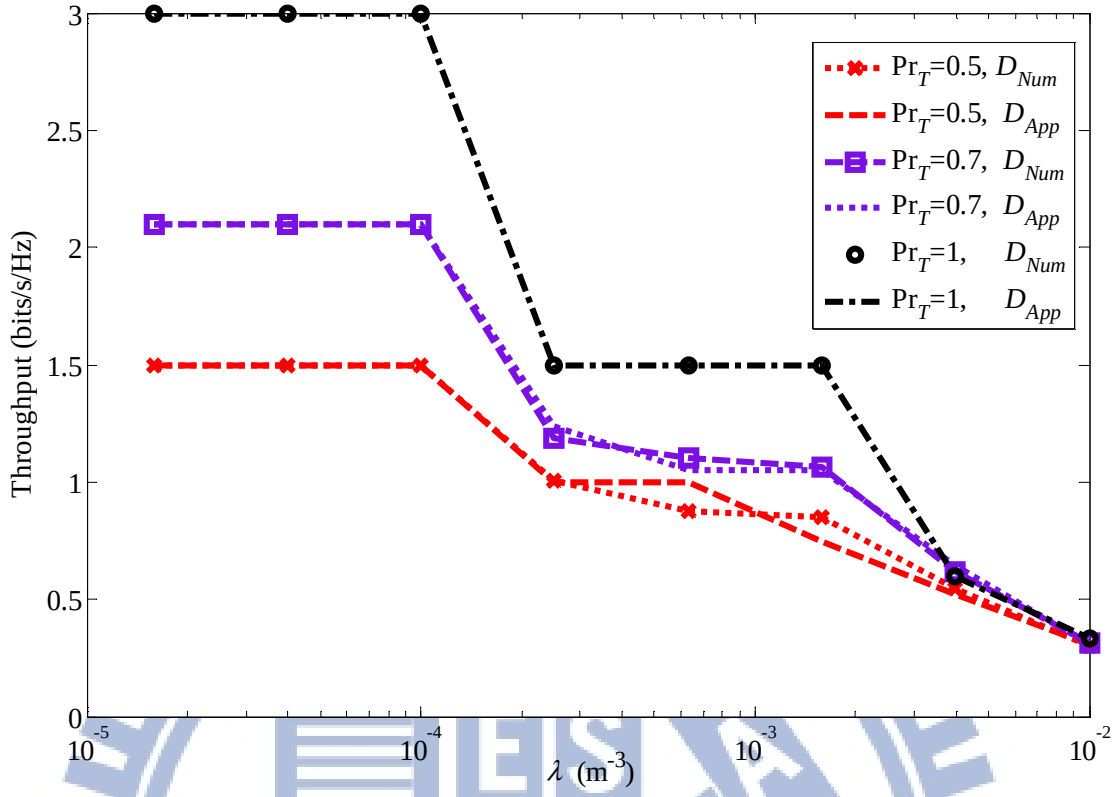

Fig. 5-4 Comparisons of D_{Num} and D_{App} by adjusting the value of λ

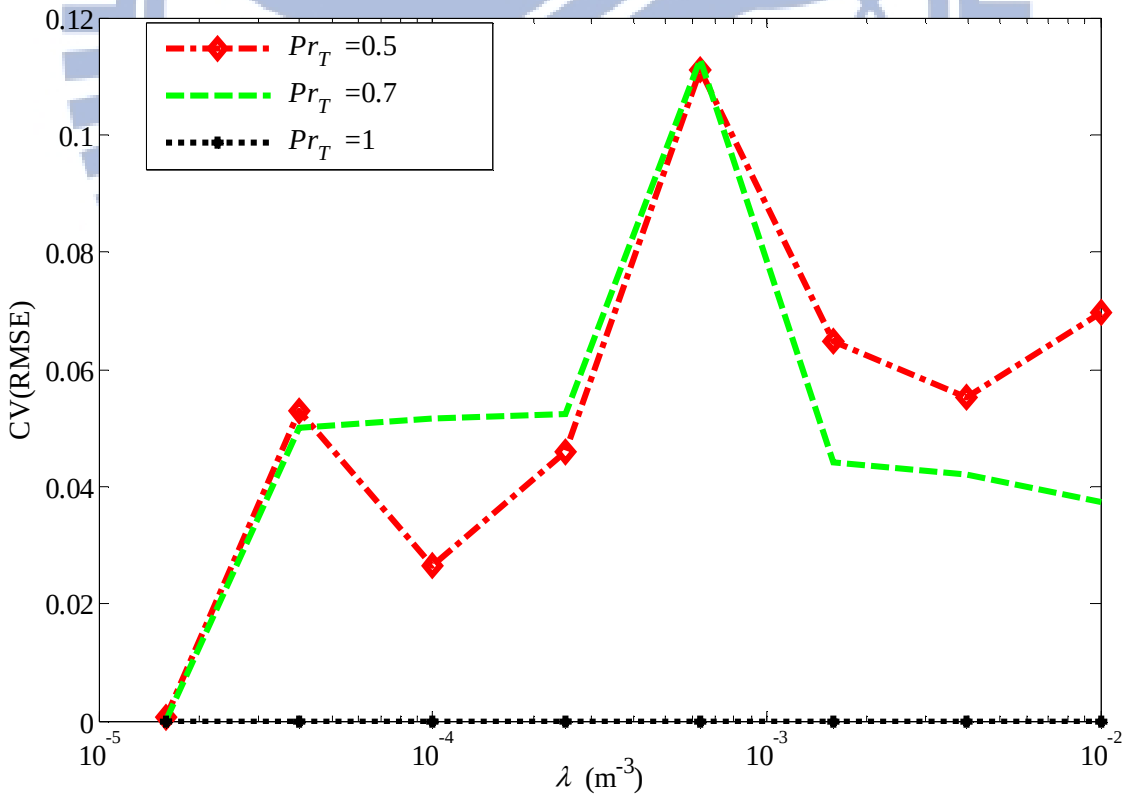

Fig. 5-5 Plot of CV(RMSE) by adjusting the value of λ

In Fig. 5-4, we compare the D_{Num} and D_{App} by giving different values of λ. It is clear that D_{Num} and D_{App} are still close to each other when we adjust λ in a wide range of values. So, we observed that adjusting the value of λ does not affect the accuracy of the proposed estimation approach.

In Fig. 5-5, we clarify the estimation error by plotting the coefficient of variation of the root mean square error, CV(RMSE), which is the ratio of RMSE to the average numerical throughout,

$$\text{CV(RMSE)} \equiv \frac{\sqrt{\text{E}[(D_{App} - D_{Num})^2]}}{\text{Mean}(D_{Num})}. \tag{5.12}$$

Given the value of λ and Pr_T, forty iterations are generated to estimate the estimation error between the numerical throughout and estimated throughout. In each iteration, the values of d_n are decided based on HPPP. During the analysis, we find the maximum value of CV(RMSE) is about 0.11. Furthermore, most of the CV(RMSE) values are lower than 0.07, which means we provide an useful and effective approach to estimate the system throughput in a femto BS network.

5.4 Applications

Based on HPPP, we can apply our study to the femto BS networks of different topologies because femto BS provides the OSG/CSG/Hybrid user priority to different users. With different user priority, the interference caused by femto BSs will be different. Through our proposed model, we can compare the influence of femto BSs to different type of users.

Furthermore, the proposed model can be extended to analyze the throughput of macro BS when interference is from femto BS network. Here, it is assumed that U_T is served by a macro BS with distance, d_m. All the femto BSs follow HPPP. Then, we can estimate the achievable throughput by applying different λ and d_m to verify the influence from the interfering femto BS networks. Moreover, our analysis model can be extended to random networks which the interference sources follow HPPP.

5.5 Conclusion

In this chapter, with the assumptions of uniformly distributed femto BS deployment and low outage probability operation, we simplified the decoding failure probability by considering one dominant interfering femto BS and other interfering femto BSs. Our analytical model estimates the throughout of femto BS netowrks quickly when femto BSs are not cooperated for their data transmission.

Simulation results have been provided to validate our approach. Furthermore, the simulation results showed that the proposed model can also be applied when the outage probability is high. In addition to femto BS networks, the model can be generally applied to different system deployments which follow the assumptions of HPPP random networks.

CHAPTER 6

CONCLUSION

In our dissertation, we have studied the features of femto BS networks and the influence of femto BS towards the cellular network.

In Chap. 2, we broadly introduced the features of femto BSs. The femto BS is different from traditional base stations and other indoor wireless access techonlogies in the following aspects:

1) Flexibility of deployment
2) Huge number of femto BSs
3) User priority
4) Self-Organization Network (SON)
5) Operation Modes.

However, femto BSs also bring new technical problems , which include:

i) Deployment issue
ii) Interference mitigation
iii) Load balancing
iv) CSG/OSG Conflict

In Chap. 2, we have summarized the preliminary studies addressing these technical

problems.

In Chap. 3, we estimated the range of feasible femto BS density to provide ubiquitous coverage for cellular network through the deployments of femto BSs. In the analysis, we proposed a novel 3-D HPPP model to analyze the random locations of femto BS networks. Because of different user priority that femto BS provides and the influence of macro BS, four scenarios were proposed during our analysis:

Scenario a): macro BS is the serving BS;
Scenario b): F_1 is the serving BS;
Scenario c): CSG femto BS is the dominant interference source to a non-CSG user;
Scenario d): OSG femto BS network.

To limit the outage probability observed by the target user under a pre-defined threshold, we have verified the range of feasible femto BS density based on the four scenarios. Numerical results showed that the our conclusion from the assumption of dominating interfering source is actually a good representation of user performance in above four different scenarios, which can be used to provide a quick evaluation of the limit in femto BS density under the low outage probability criterion.

In Chap. 4, we extended our observations about the closed form of $\mathrm{E}[\ln(R_n)]$ in the 3-D space to the *m*-dimensional HPPP. $\mathrm{E}[\ln(R_{n|m})]$ represents the *n*th nearest node in the *m*-dimensional space. Moreover, we further extended our conclusion to the condition which *n* is a half-integer. To extend our works, we proposed a lookup table construction and linear interpolation approach to estimate the fading figure of Nakagami fading channel. Our proposed approach is simple in implementation. The verification results also showed that our proposed estimators outperforms in a wide range when the number of samples is limited. Because Nakagami distribution fits very well in the urban and indoor environment, our proposed approach about fading figure estimation can also be embedded in the femto BS networks for the channel estimation.

In Chap. 5, we proposed a simple approach to estimate the throughput of femto BS networks. Considering the effects of randomly distributed interference sources, low outage probability, non-cooperated packet transmission, and HARQ packet transmission, we have identified a fast estimation approach of downlink throughput in a femto BS network. Simulations were also provided to verify the results. Our proposed approach

can be applied to not only the femto BS networks but also the random networks which the interference sources follow HPPP.

In conclusion, we have created a 3-D HPPP model to estimate the influence and beinfits that femto BS networks bring. Furthermore, we extended our research to the *m*-dimensional HPPP. Our research results can be generally applied to different wireless networks. Moreover, our study about $\mathrm{E}[\ln(R_{n|m})]$ can also be widely applied in the wireless communications.

REFERENCE

[1] *3rd Generation Partnership Project; Technical Specification Group Services and System Aspects; Vocabulary for 3GPP Specifications*, 3GPP TR 21.905 V11.1.0, Jun. 2012.

[2] D. J. Goodman, *Wireless Personal Communications Systems*. Boston, MA: Addison-Wesley, 1997.

[3] J. G. Andrews, H. Claussen, M. Dohler, S. Rangan, and M. C. Reed, "Femtocells: Past, Present, and Future," *IEEE J. Selected Areas Commun.*, vol.30, no. 3, pp.497-508, Apr. 2012.

[4] V. Chandrasekhar, J. G. Andrews, and A. Gatherer, "Femtocell Networks: A Survey," *IEEE Commun. Mag.*, vol. 46, no. 9, pp. 59-67, Sep. 2008.

[5] S. P. Yeh , S. Talwar, S. C. Lee, and H. C. Kim, "WiMAX Femtocells: A Perspective on Network Architecture, Capacity, and Coverage," *IEEE Commun. Mag.*, vol. 46, no. 10, pp. 58-65, Oct. 2008.

[6] D. López-Pérez, A. Valcarce, G.de la Roche, and J. Zhang, "OFDMA Femtocells: A Roadmap on Interference Avoidance," *IEEE Commun. Mag.*, vol. 46, no. 9, pp. 41-48, Sep. 2008.

[7] R. Y. Kim, J. S. Kwak, and K. Etemad, "WiMAX Femtocell: Requirements, Challenges, and Solutions," *IEEE Commun. Mag.*, vol. 47, no. 9, pp. 84-91, Sep. 2009.

[8] H. Claussen, L. T. W. Ho, and L. G. Samuel, "An Overview of the Femtocell Concept," *Bell Labs Technical Journal*, vol. 13, no. 1, pp. 221-245, May, 2008.

[9] S. R. Saunders, S. Carlaw, A. Giustina, R. R. Bhat, V. S. Rao, and R. Siegberg, *FEMTOCELLS*. Hoboken, NJ: Wiley, 2009.

[10] J. Zhang, and G. de la Roche, *FEMTOCELLS: TECHNOLOGIES AND DEPLOYMENT*. Hoboken, NJ: Wiley, 2010.

[11] A. Stocker, "Small-cell mobile phone systems," *IEEE Trans. Veh. Technol.*, vol. 33, no. 4, pp. 269 – 275, Nov. 1984.

[12] J. Sydir, and R. Taori, "An Evolved Cellular System Architecture Incorporating Relay Stations," *IEEE Commun. Mag.*, vol. 47, no. 6, pp.115-121, Jun. 2009.

[13] X. H. You, D. M. Wang, B. Sheng, X. Q. Gao, X. S. Zhao, and M. Chen, "Cooperative distributed antenna systems for mobile communications," *IEEE Wireless Commun. Mag.*, vol. 17, no. 3, pp.35-43, Jun. 2010.

[14] IEEE Xplore Digital Library, [Online]. Available: http://ieeexplore.ieee.org/Xplore/home.jsp

[15] *3rd Generation Partnership Project; Technical Specification Group Radio Access Networks; 3G Home NodeB Study Item Technical Report*, 3GPP TR 25.820 V8.2.0, Sep. 2008.

[16]*IEEE Standard for Local and metropolitan area networks— Part 16: Air Interface for Broadband Wireless Access Systems Amendment 3: Advanced Air Interface*, IEEE Std 802.16m-2011, Nov. 2010.

[17] M.-S. Alouini, and A. J. Goldsmith, "Area Spectral Efficiency of Cellular Mobile Radio Systems," *IEEE Trans. Veh. Technol.*, vol. 48, no. 4, pp.1047-1066, Jul. 1999.

[18] "Simulation assumptions and parameters for FDD HeNB RF requirements," R4-091422, 3GPP TSG RAN WG4 Meeting #50bis, Seoul, Korea, 23 – 27 Mar. 2009.

[19] K. Han, Y. Choi, D. Kim, M. Na, S. Choi, and K. Han, "Optimization of femtocell network configuration under interference constraints," in *Proc. IEEE 7th Int. Symp. Modeling and Optimization in Mobile, Ad Hoc, and Wireless Networks 2009*, Seoul, Korea, 23-27 Jun. 2009, pp. 1-7.

[20] J. Xiang, Y. Zhang, T. Skeie, and L. Xie, “Downlink Spectrum Sharing for Cognitive Radio Femtocell Networks,” *IEEE Syst. J.*, vol. 4, no. 4, pp. 524-534, Dec. 2010.
[21] J. Liu, T. Kou, Q. Chen, and H. D. Sherali, “Femtocell Base Station Deployment in Commercial Buildings: A Global Optimization Approach,” *IEEE J. Selected Areas Commun.*, vol. 30, no. 3, pp. 652–663, Apr. 2012.
[22]V. Chandrasekhar, and J. Andrews, “Uplink capacity and interference avoidance for two-tier femtocell networks,” *IEEE Trans. Wireless Commun.*, vol. 8, no. 7, pp.3498–3509, Jul. 2009.
[23] D. Das and V. Ramaswamy, “On the reverse link capacity of a CDMA network of femto-cells,” in *Proc. IEEE Sarnoff Symp.*, Prineoton, NJ, U.S.A., 28-30 Apr. 2008, pp.1–5.
[24]V. Chandrasekhar, J. Andrews, Z. Shen, T. Muharemovic, and A. Gatherer, “Power control in two-tier femtocell networks,” *IEEE Trans. Wireless Commun.*, vol. 8, no. 8, pp. 4316–28, Aug. 2009.
[25] H. S. Jo, C. Mun, J. Moon, and J.G. Yook, “Interference mitigation using uplink power control for two-tier femtocell networks,” *IEEE Trans. Wireless Commun.*, vol. 8, no. 10, pp. 4906–4910, Oct. 2009.
[26] M. Yavuz, F. Meshkati, S. Nanda, A. Pokhariyal, N. Johnson, B. Raghothaman, and A. Richardson, “Interference Management and Performance Analysis of UMTS/HSPA+ Femtocells,” *IEEE Commun. Mag.*, vol. 47, no. 9, pp. 102-109, Sep. 2009.
[27] N. Arulselvan, V. Ramachandran, S. Kalyanasundaram, and G. Han, “Distributed Power Control Mechanisms for HSDPA Femtocells,” in *Proc. IEEE 69th Veh. Tech. Conf.*, Barcelona, Spain, 26-29 Apr. 2009, pp. 1-5.
[28] X. Chu, Y. Wu, L. Benmesbah, and W. K. Ling, “Resource Allocation in Hybrid Macro/Femto Networks,” in *Proc. IEEE Wireless Commun. and Networking Conf. Workshops 2010*, Sydney, Australia, 18 Apr. 2010, pp.1-5.
[29] C. Y. Oh, M. Y. Chung, H. Choo, and T. J. Lee, “A Novel Frequency Planning for Femtocells in OFDMA-Based Cellular Networks Using Fractional Frequency Reuse,” in *Proc. 2010 Int. conf. Computational Science and Its Applications*, vol. iii, Fukuoka, Japan, 23-26 Mar. 2010, pp. 96-106.
[30] R. T. Juang, P. Ting, H. P. Lin, and D. B. Lin, “Interference Management of Femtocell in Macro-cellular Networks,” in *Proc. IEEE Wireless Telecomm. Symp.*, Tampa, FL, U.S.A., 21-23 Apr. 2010, pp. 1-4.
[31] P. Lee, T. Lee, J. Jeong, and J. Shin, ”Interference Management in LTE Femtocell Systems Using Fractional Frequency Reuse,” in *Proc. IEEE The 12th Int. Conf. Advanced Commun. Tech.*, Phoenix Park, Korea, 7-10 Feb. 2010, pp.1047-1051.
[32]A. Ghosh, N. Mangalvedhe, R. Ratasuk, B. Mondal, M. Cudak, E. Visotsky, T. A. Thomas, J. G. Andrews, P. Xia, H. S. Jo, H. S. Dhillon, and T. D. Novlan, “Heterogeneous Cellular Networks: From Theory to Practice,” *IEEE Commun. Mag.*, vol. 50, no. 6, pp.54-64, Jun. 2012.
[33] I. G¨uvenc¸, M. R. Jeong, F. Watanabe, and H. Inamura, “A Hybrid Frequency Assignment for Femtocells and Coverage Area Analysis for Co-Channel Operation,” *IEEE Commun. Lett.*, vol. 12, no. 12, pp. 880-882, Dec. 2008.
[34] Y. Bai, J. Zhou, and L. Chen, ”Hybrid Spectrum Usage for Overlaying LTE Macrocell and Femtocell,” in *Proc. IEEE Global Telecomm. Conf. 2009*, Honolulu, HI, U.S.A., 30 Nov. - 4 Dec. 2009, pp.1-6.
[35] X. Li, L. Qian, and D. Kataria, “Downlink power control in co-channel macrocell femtocell overlay,” in *Proc. IEEE 43rd Annu. Conf. Inform. Sci. and Syst.*, Baltimore, MD, U.S.A., 18-20 Mar. 2009, pp. 383-388.
[36] V. Chandrasekhar, J. G. Andrews, T. Muharemovic, Z. Shen, and A. Gatherer,

"Power control in two-tier femtocell networks," *IEEE Trans. Wireless Commun.*, vol. 8, no. 8, pp. 4316-4328, Oct. 2009.
[37] H. Zeng, C. Zhu, and W. P. Chen, "System Performance of Self-Organizing Network Algorithm in WiMAX Femtocells," in *Proc. 4th Annu. Int. Conf. Wireless Internet*, no.25, Maui, HI, U.S.A., 17-19 Nov. 2008.
[38] L. G. U. Garcia, K. I. Pedersen, and P. E. Mogensen, "Autonomous Component Carrier Selection: Interference Management in Local Area Environments for LTE-Advanced," *IEEE Commun. Mag.*, vol. 47, no. 9, pp.110-116, Sep. 2009.
[39]K. Sundaresan, and S. Rangarajan, "Efficient Resource Management in OFDMA Femto Cells," in *Proc. 10th ACM Int. symp. Mobile ad hoc networking and computing*, New Orleans, LA, U.S.A., 18-21 May 2009, pp.33-42.
[40] S.Y. Lien, C. C. Tseng, K. C. Chen, and C. W. Su, "Cognitive Radio Resource Management for QoS Guarantees in Autonomous Femtocell Networks," in *Proc. IEEE Int. Conf. Commun. 2010*, Cape Town, South Africa, 23-27 May 2010, pp. 1-6.
[41] G. GÜR, S. BAYHAN, and F. ALAGÖZ, "Cognitive Femtocell Networks: An Overlay Architecture for Localized Dynamic Spectrum Access," *IEEE Wireless Commun. Mag.* vol. 17, no. 4, pp.62-70, Aug. 2010.
[42] J. Jin, and B. Li, "Cooperative Resource Management in Cognitive WiMAX with Femto Cells," in *Proc. IEEE Int. Conf. Comput. Commun. 2010*, San Diego, CA, U.S.A., 15 - 19 Mar. 2010, pp.1-9.
[43] S. M. Cheng, W. C. Ao, F. M. Tseng, and K.C. Chen, "Design and Analysis of Downlink Spectrum Sharing in Two-tier Cognitive Femto Networks," *IEEE Trans. Veh. Technol.*, vol. 61, no. 5, pp. 2194-2207, Jun. 2012.
[44] H. Claussen, L. T. W. Ho, and L. G. Samuel, "Self-optimization of Coverage for Femtocell Deployments,"in *Proc. IEEE Wireless Telecomm. Symp. 2008*, Pomona, CA, U.S.A., 24-26 Apr. 2008, pp. 278-285.
[45] D. L´opez-P´erez, ´A. Lad´anyi, A. J¨uttner, and J. Zhang, "OFDMA femtocells: A self-organizing approach for frequency assignment,"in *Proc. IEEE 20th Int. Symp. Personal, Indoor and Mobile Radio Commun.*, Tokyo, Japan, 13-16 Sep. 2009, pp. 2202-2207.
[46] M. Amirijoo, L. Jorguseski, T. Kürner, R. Litjens, M. Neuland, L. C. Schmelz, and U. Türke, "Cell outage management in LTE networks, " in *Proc. IEEE 6th Int. conf. Symp. Wireless Commun. Systems*, Siena-Tuscany, Italy, 7–10 Sep. 2009, pp. 600-604.
[47] Y. Y. Li, M. Macuha, E. S. Sousa, T. Sato, and M. Nanri, "Cognitive Interference Management in 3G Femtocells," in *Proc. IEEE 20th Int. Symp. Personal, Indoor and Mobile Radio Commun.*, Tokyo, Japan, 13-16 Sep. 2009, pp. 1118-1122.
[48] 3GPP, "3GPP Report of TSG RAN WG1 Meeting," #62, v0.1.0, Oct. 2010.
[49] A. Adhikary, V. Ntranos, and G. Caire, "Cognitive Femtocells: Breaking the Spatial ReuseBarrier of Cellular Systems," in *Proc. IEEE Inform. Theory and Applicat. Workshop 2011*, San Diego, CA, U.S.A., 6-11 Feb. 2011, pp. 1-10.
[50] D. L´opez-P´erez, G. de la Roche, A. Valcarce, A. J¨uttner, and J. Zhang, "Interference Avoidance and Dynamic Frequency Planning for WiMAX Femtocells Networks," in *Proc. IEEE 11th Singapore Int. Conf. Commun. Systems*, Guangzhou, China, 19-21 Nov. 2008, pp. 1579-1584.
[51] H. C. Lee, D.C. Oh, and Y. H. Lee, "Mitigation of Inter-Femtocell Interference with Adaptive Fractional Frequency Reuse," in *Proc. IEEE Int. Conf. Commun.*, Cape Town, South Africa, 23-27 May 2010, pp. 1-5.
[52] C. W. Chen, C. Y. Wang, S. L. Chao, and H. Y. Wei, "DANCE: a game-theoretical femtocell channel exchange mechanism," *ACM SIGMOBILE Mobile Computing and Communications Review*, vol. 14 , no. 1, pp. 13-15, Jul. 2010.

[53] S. Y. Lien, Y. Y. Lin, and K. C. Chen, “Cognitive and Game-Theoretical Radio Resource Management for Autonomous Femtocells with QoS Guarantees,” *IEEE Trans. Wireless Commun.*, vol.10, no. 7, pp.2196-2206, Jul. 2011.
[54] R. Madan, J. Borran, A. Sampath, N. Bhushan, A. Khandekar, and T. Ji, ”Cell Association and Interference Coordination in Heterogeneous LTE-A Cellular Networks,” *IEEE J. Sel. Areas Commun.*, vol. 28, no. 9, pp.1479-1489, Dec. 2010.
[55] I. G¨uvenc¸, M. R. Jeong, I. Demirdogen, B. Kecicioglu, and F. Watanabe, “Range Expansion and Inter-Cell Interference Coordination (ICIC) for Picocell Networks,” in *Proc. IEEE 72th Veh. Technol. Conf.*, San Francisco, CA, U.S.A., 5-8 Sep. 2011, pp.1-6.
[56] D L´opez-P´erez, A. Valcarce, G. De La Roche, E. Liu, and J. Zhang, “Access Methods to WiMAX Femtocells: A downlink system-level case study,” in *Proc. IEEE 11th Singapore Int. Conf. Commun. Systems*, Guangzhou, China, 19-21 Nov. 2008, pp. 1657-1662.
[57] H. S. Jo, P. Xia, and J. G. Andrews, “Open, Closed, and Shared Access Femtocells in the Downlink,” [Online]. Available: http://arxiv.org/abs/1009.3522.
[58] H. S. Jo, P. Xia, and J. G. Andrews, “Downlink Femtocell Networks: Open or Closed?,” in *Proc. IEEE Int. Conf. Commun. 2011*, Kyoto, Japan, 5-9 Jun. 2011, pp. 1-5.
[59] P. Xia, V. Chandrasekhar, and J. G. Andrews, ”Open vs Closed Access FemtoCells in the uplink,” *IEEE Trans. Wireless Commun.*, vol. 9, no. 12, pp.3798-3809, Dec. 2010.
[60] G. L. Stuber, *Principles of Mobile Communication 2nd* ed. Norwell, MA: Kluwer, 2001.
[61] B. D. Ripley, *Spatial Statistics*. Hoboken, NJ: Wiley, Aug. 2004.
[62] G. J. G. Upton and B. Fingleton, *Spatial Data Analysis by Example Volume 1: Point Pattern and Quantitative Data*. Hoboken, NJ: Wiley, Apr. 1985.
[63] F. Baccelli and B. Blaszczyszyn, *Stochastic Geometry and Wireless Networks, Foundations and Trends in Networking*. Paris, France: NOW Publishers, 2011.
[64] M. Haenggi, J. G. Andrews, F. Baccelli, O. Dousse, and M. Franceschetti, ”Stochastic geometry and random graphs for the analysis and design of wireless networks,” *IEEE J. Sel. Areas Commun.*, vol. 27, no.7, pp. 1029-1046, Sep. 2009.
[65] J. G. Andrews, R. K. Ganti, M. Haenggi, N. Jindal, and S. Weber, “A Primer on Spatial Modeling and Analysis in Wireless Networks,” *IEEE Commun. Mag.*, vol. 48, no. 11, pp. 156-163, Nov. 2010.
[66] S. Musa and W. Wasylkiwskyj, “Co-channel interference of spread spectrum systems in a multiple user environment,” *IEEE Trans. Commun.*, vol. 26, no. 10, pp. 1405–1413, Oct. 1978.
[67] E. S. Sousa and J. A. Silvester, “Optimum transmission ranges in a direct-sequence spread-spectrum multihop packet radio network,” *IEEE J. Sel. Areas Commun.*, vol. 8, no. 5, pp. 762–771, Jun. 1990.
[68] E. S. Sousa, “Interference modeling in a direct-sequence spread-spectrum packet radio network,” *IEEE Trans. Commun.*, vol. 38, no. 9, pp. 1475–1482, Sep. 1990.
[69] E. S. Sousa, “Performance of a spread spectrum packet radio network link on a Poisson field of interferers,” *IEEE Trans. Inf. Theory*, vol. 38, no. 6, pp. 1743–1754, Nov. 1992.
[70]R. K. Ganti and M. Haenggi, “Interference and Outage in Clustered Wireless Ad Hoc Networks,” *IEEE Trans. Inf. Theory*, vol. 55, no. 9, pp.4067-4086, Sep. 2009.
[71] A. Hasan, and J. G. Andrews, “The Guard Zone in Wireless Ad hoc Networks,” *IEEE Trans. Wireless Commun.*, vol. 6, no.3, pp.897-906, Mar. 2007.
[72] S. Weber, X. Yang, J. G. Andrews, and G. de Veciana, ”Transmission capacity of wireless ad hoc networks with outage constraints,” *IEEE Trans. Inf. Theory*, vol. 51, no.

12, pp. 4091-4102, Dec. 2005.
[73] S. Weber, and J. G. Andrews, “A stochastic geometry approach to wideband ad hoc networks with channel variations,” in *Proc. IEEE 4th Int. Symp. Modeling and Optimization in Mobile, Ad Hoc and Wireless Networks*, Boston, MA, U.S.A., 3-6 Apr. 2006, pp.1-6.
[74] S. Weber, and J. G. Andrews, “Bounds on the SIR distribution for a class of channel models in ad hoc networks,” in *Proc. IEEE Global Telecommun. Conf. 2006*, San Francisco, CA , U.S.A., 27 Nov. – 1 Dec. 2006, pp.1-5.
[75] H.Q. Nguyen, F. Baccelli, and D. Kofman, “A Stochastic Geometry Analysis of Dense IEEE 802.11 Networks,” in *Proc. IEEE 26th Int. conf. Computer Commun.*, Anchorage, AK, U.S.A., 6-12 May 2007, pp.1199-1207.
[76] C. Lee, and M. Haenggi, “Interference and Outage in Doubly Poisson Cognitive Networks,” in *Proc. IEEE 19th International Conf. Computer Commun. and Networks*, Zurich, Switzerland, 2-5 Aug. 2010, pp.1-6.
[77] V. Chandrasekhar, and J. G. Andrews, “Spectrum allocation in tiered cellular networks,” *IEEE Trans. Commun.*, vol. 57, no. 10, pp. 3059-3068, Oct. 2009.
[78] O. Dousse, M. Franceschetti, and P. Thiran, “On the throughput scaling of wireless relay networks,” *IEEE/ACM Trans. Networking*, vol. 14, no. 6, pp. 2756 – 2761, Jun. 2006.
[79]J. Zhang and J. G. Andrews, “Distributed Antenna Systems with Randomness,” *IEEE Trans. Wireless Commun.*, vol. 7, no.9, pp.3636-3646, Sep. 2008.
[80] P. C. Pinto, and M. Z. Win, “Communication in a Poisson Field of Interferers–Part I: Interference Distribution and Error Probability,” *IEEE Trans. Wireless Commun.*, vol. 9, no.7, pp. 2176-2186, Jul. 2010.
[81] P. C. Pinto, and M. Z. Win, “Communication in a Poisson Field of Interferers–Part II: Channel Capacity and Interference Spectrum,” *IEEE Trans. Wireless Commun.*, vol. 9, no.7, pp. 2187-2195, Jul. 2010.
[82] M. Haenggi, “On distances in uniformly random networks,” *IEEE Trans. Inf. Theory*, vol.51, no.10, pp.3584- 3586, Oct. 2005.
[83] L. Amoroso, “Richerche intorno alla curva dei redditi," *Annali di Matematica Pura ed Applicata*, vol. 2, no.1, pp. 123–159, Dec. 1925.
[84] E. W. Stacy, “A generalization of the gamma distribution," *Ann. Math. Stat.*, vol. 33, no.3, pp. 1187–1192, Sep. 1962.
[85] M. D. Yacoub, “The α-μ distribution: a general fading distribution," in *Proc. IEEE 13th Int. Symp. Personal, Indoor Mobile Radio Commun.*, Lisboa, Portugal, 15-18 Sep. 2002, pp. 629–633.
[86]M. D. Yacoub, “The α-μ distribution: a physical fading model for the Stacy distribution," *IEEE Trans. Veh. Technol.*, vol. 56, no.1, pp. 27–34, Jan. 2007.
[87] Wolfram Mathematica Online Integrator. [Online]. Available: http://integrals.wolfram.com/index.jsp
[88] M. Abramowitz, and I. A. Stegun, *Handbook of Mathematical Functions: with Formulas, Graphs, and Mathematical Tables*. New York: Dover, Jun. 1974, pp. 228-229.
[89]R. Mathar, and J. Mattfeldt, “On the distribution of cumulated interference power in Rayleigh fading channels,” *ACM Journal of Wireless Networks*, vol. 1, no.1, pp.31-36, Feb. 1995.
[90] X. Yang, and A. P. Petropulu, “Co-Channel Interference Modeling and Analysis in a Poisson Field of Interferers in Wireless Communications,” *IEEE Trans. Signal Process.*, vol. 51 , no. 1, pp.64-76, Jan. 2003.
[91] K. Gulati, B. L. Evans, J. G. Andrews, and K. R. Tinsley, “Statistics of Co-Channel Interference in a Field of Poisson and Poisson-Poisson Clustered Interferers,” *IEEE*

Trans. Signal Process., vol. 58 , no. 12, pp.6207-6222, Dec. 2010.
[92]V. Ramaswamy, and D. Das, “Multi-Carrier Macrocell Femtocell Deployment—A Reverse Link Capacity Analysis,” in *Proc. IEEE 70th Veh. Technol. Conf.*, Anchorage, AK, U.S.A., 20–23 Sep. 2009, pp.1-6.
[93] V. Mordachev, and S. Loyka, “On node density - Outage probability tradeoff in wireless networks,” *IEEE J. Selected Areas Commun.*, vol. 27, no. 7, pp. 1120-1131, Sep. 2009.
[94] J. F. Lawless, “Inference in the generalized gamma and log gamma distributions," *Technometrics*, vol. 22, no.3, pp. 409–419, Aug. 1980.
[95] R. L. Prentice, “A log gamma model and its maximum likelihood estimation,” *Biometrika* , vol. 61, no. 3, pp. 539-544, Dec. 1974.
[96] P. H. Huang and T. Y. Hwang, “On new moment estimation of parameters of the generalized gamma distribution using its characterization," *Taiwanese J. Mathematics*, vol. 10, no.4, pp. 1083–1093, Jun. 2006.
[97] K.-S. Song, “Globally convergent algorithms for estimating generalized gamma distributions in fast signal and image processing," *IEEE Trans. Image Process.*, vol. 17, no.8, pp. 1233–1250, Aug. 2008.
[98] J. Reig and L. Rubio, “On simple estimators of the α-μ fading distribution,” *IEEE Trans. Commun.* , vol. 59, no.12, pp. 3254-3258, Dec. 2011.
[99] M. Nakagami, “The *m* distribution: A general formula of intensity distributions of rapid fading,” in *Statistical Methods in Radio Wave Propagation*, W. C. Hoffman, oxford, U.K.: Oxford Univ. Press, 1960, pp. 3–36.
[100] W. Braun and U. Dersch, “Physical mobile radio channel model,” *IEEE Trans. Veh. Technol.*, vol. 40, no. 2, pp. 472–482, Mar. 1991.
[101] H. Suzuki, “A Statistical Model for Urban Multipath Propagation,” *IEEE Trans. Commun.*, vol. 25, no. 7, pp. 673–680, Jul. 1977.
[102] A.U. Sheikh, M. Handforth and M. Abdi, “Indoor Mobile Radio Channel at 946 MHz: Measurements and Modeling,” in *Proc. IEEE 43rd Veh. Technol. Conf.*, Secaucus, NJ, U.S.A., 18-20 May 1993, pp. 73–76.
[103]J. Cheng, N. Wang, and C. Tellambura, “Probability density function of logarithmic ratio of arithmetic mean to geometric mean for Nakagami-*m* fading power,” in *Proc. IEEE 2010 25th Biennial Symp. Commun.*, Kingston, Ontario, Canada, 12-14 May 2010, pp.348-351.
[104] J. Cheng and N. C. Beaulieu, “Maximum-likelihood based estimation of the Nakagami-*m* parameter,” *IEEE Commun. Lett.*, vol.5, no.3, pp. 101-103, Mar.2001.
[105] Q. T. Zhang, “A Note on the Estimation of Nakagami-*m* Fading Parameter,” *IEEE Commun. Lett.*, vol.6, no.6, pp. 237-238, Jun. 2002.
[106] J. Gaeddert and A. Annamalai, “Further Results on Nakagami-m Parameter Estimation,”*IEEE Commun. Lett.*, vol. 9, no. 1, pp.22-24, Jan. 2005.
[107] J. Cheng and N. C. Beaulieu, “Generalized Moment Estimators for the Nakagami Fading Parameter,” *IEEE Commun. Lett.* , vol. 6, no. 4, pp. 144-146, Apr. 2002.
[108] *3rd Generation Partnership Project; Technical Specification Group Radio Access Networks; Evolved Universal Terrestrial Radio Access (E-UTRA);FDD Home eNode B (HeNB) Radio Frequency (RF) requirements analysis (Release 10)*, 3GPP TR 36.921 V10.0.0, Apr. 2011.
[109]3*rd Generation Partnership Project; Technical Specification Group Radio Access Networks; Evolved Universal Terrestrial Radio Access (E-UTRA); Physical layer procedures*, 3GPP TS 36.213 V10.3.0, Sep. 2011.
[110]G. Caire and D. Tuninetti, ”The Throughput of Hybrid-ARQ Protocols for the Gaussian Collision Channel,” *IEEE Trans. Inf. Theory*, vol. 47, no. 5, pp. 1971 - 1988,

Jul. 2001.
[111] Ronald W. Wolff, *Stochastic Modeling and the Theory of Queues*. Upper Saddle River, NJ: Prentice-Hall, 1989.
[112]*3rd Generation Partnership Project; Technical Specification Group Radio Access Networks; Evolved Universal Terrestrial Radio Access (E-UTRA);Physical layer Measurements (Release 10),* 3GPP TR 36.214 V10.1.0, Mar. 2011.

PUBLICATION LIST

Journal Paper

(1) Y. L. Tseng, and C. Y. Huang, "Analysis of Femto Base Station Network Deployment," *IEEE Trans. Veh. Technol.*, vol. 61, no. 2, pp. 748 – 757, Feb. 2012.

Conference Paper

(1) Y. L. Tseng, and C. Y. Huang, "Log-Value Estimation of Random Variable Following Generalized Gamma Distribution in Wireless Communications," Presented in *IEEE International Conference of Information and Communication Technology (ICoICT) 2013.*

(2) Y. L. Tseng, and C. Y. Huang, "Throughput Estimation Model for Uniformly Distributed Femto Base Station Networks," Presented in *IEEE International Conference of Information and Communication Technology (ICoICT) 2013.*

LTE standard Activities

(1) R2-113360 "Extending Barring Time for Delay Tolerant Devices"

(2) R2-114429 "Considerations of EAB"

(3) R2-115453 "Considerations on update of EAB"

(4) R2-116316 "Considerations on Fast EAB Information Update"

IEEE 802.16m standard Activities

(1) IEEE C802.16m-08/1304r1, Femto BS Network Entry Procedure (Kanchei (Ken) Loa, Chun-Yen Hsu, Yi-Hsueh Tsai, Chiu-Wen Chen, Youn-Tai Lee, Chih-Wei Su, Tsung-Yu Tsai, Jiun-Je Jian, Yung-Ting Lee, Hua-Chiang Yin, Shiann-Tsong Sheu, Chih-Cheng Yang, Yih-Guang Jan, Yang-Han Lee, Ming-Hsueh Chuang, Hsien-Wei Tseng, Whai-En Chen, David W. Lin, Ching-Yao Huang, Yung-Lan Tseng; 2008-11-10)
(2) IEEE C802.16m-08/1304r2, Femto BS Network Entry Procedure (Kanchei (Ken) Loa, Chun-Yen Hsu, Yi-Hsueh Tsai, Chiu-Wen Chen, Youn-Tai Lee, Chih-Wei Su, Tsung-Yu Tsai, Jiun-Je Jian, Yung-Ting Lee, Hua-Chiang Yin, Shiann-Tsong Sheu, Chih-Cheng Yang, Yih-Guang Jan, Yang-Han Lee, Ming-Hsueh Chuang, Hsien-Wei Tseng, Whai-En Chen, David W. Lin, Ching-Yao Huang, Yung-Lan Tseng; 2008-11-12)
(3) IEEE C802.16m-08/1321r1, Femto BS Power Adjustment Process (Yung-Lan Tseng, Ching-Yao Huang, Chun-Yen Hsu, Whai-En Chen, Shiann-Tsong Sheu, Chih-Cheng Yang; 2008-11-10)
(4) IEEE C802.16m-09/1561, Quick access message in Femtocell (AWD-Femto) (Kanchei(Ken) Loa, Yi-Ting Lin, Tsung-Yu Tsai, Jiun-Je Jian, Chun-Yen Hsu, Chiu-Wen Chen, Youn-Tai Lee, Yung-Lan Tseng; 2009-07-07)
(5) IEEE C802.16m-09/1561r1, Quick access message in Femtocell (AWD-Femto) (Kanchei(Ken) Loa, Yi-Ting Lin, Tsung-Yu Tsai, Jiun-Je Jian, Chun-Yen Hsu, Chiu-Wen Chen, Youn-Tai Lee, Yung-Lan Tseng; 2009-07-09)
(6) IEEE C802.16m-09/1564, Dedicated periodic/BR preamble assignment in Femtocell (AWD-Femto) (Kanchei(Ken) Loa, Tsung-Yu Tsai, Yi-Ting Lin, Jiun-Je Jian, Chun-Yen Hsu, Chiu-Wen Chen, Youn-Tai Lee, Yung-Lan Tseng; 2009-07-07)

(7) IEEE C802.16m-09/1564r1, Dedicated BR preamble and tile assignment in Femtocell (AWD-Femto) (Kanchei(Ken) Loa, Tsung-Yu Tsai, Yi-Ting Lin, Jiun-Je Jian, Chun-Yen Hsu, Chiu-Wen Chen, Youn-Tai Lee, Yung-Lan Tseng; 2009-07-14)
(8) IEEE C802.16m-09/1573, Comment on CSG ID (AWD-Femto) (Kanchei (Ken) Loa, Yung-Lan Tseng, Chun-Yen Hsu, Youn-Tai Lee, Shiann-Tsong Sheu, Chih-Cheng Yang, Whai-En Chen, Shih-Yuan Cheng; 2009-07-07)
(9) IEEE C802.16m-09/1574, AAI_NBR-ADV message format (15.2.5.4) (Kanchei (Ken) Loa, Yung-Lan Tseng, Chun-Yen Hsu, Youn-Tai Lee; 2009-07-07)
(10) IEEE C802.16m-09/1574r1, Proposed AAI_NBR-ADV message format for femtocell support (AWD-Femto) (Kanchei (Ken) Loa, Yung-Lan Tseng, Chun-Yen Hsu, Youn-Tai Lee; 2009-07-07)
(11) IEEE C802.16m-09/1574r2, Proposed AAI_NBR-ADV message format for femtocell support (AWD-Femto) (Kanchei (Ken) Loa, Yung-Lan Tseng, Chun-Yen Hsu, Youn-Tai Lee; 2009-07-08)
(12) IEEE C802.16m-09/1826, SON Support in AMS Idle Mode (SON) (Chun-Yen Hsu, Yung-Lan Tseng, Chiu-Wen Chen, Kanchei (Ken) Loa, Yi-Ting Lin, Tsung-Yu Tsai, Youn-Tai Lee, Shiann-Tsong Sheu, Chih-Cheng Yang, Whai-En Chen, Shih-Yuan Cheng, Yih-Guang Jan, Yang-Han Lee, Ming-Hsueh Chuang, Hsien-Wei Tseng; 2009-08-28)
(13) IEEE C802.16m-09/1826r1, SON Support in AMS Idle Mode (SON) (Chun-Yen Hsu, Yung-Lan Tseng, Chiu-Wen Chen, Kanchei (Ken) Loa, Yi-Ting Lin, Tsung-Yu Tsai, Youn-Tai Lee, Shiann-Tsong Sheu, Chih-Cheng Yang, Whai-En Chen, Shih-Yuan Cheng, Yih-Guang Jan, Yang-Han Lee, Ming-Hsueh Chuang, Hsien-Wei Tseng; 2009-08-30)
(14) IEEE C802.16m-09/1827, LBS Capability Negotiation (LBS) (Chun-Yen Hsu, Yung-Lan Tseng, Kanchei (Ken) Loa, Youn-Tai Lee; 2009-08-28)
(15) IEEE C802.16m-09/1827r1, LBS Capability Negotiation (Chun-Yen Hsu, Yung-Lan Tseng, Kanchei (Ken) Loa, Youn-Tai Lee; 2009-09-01)
(16) IEEE C802.16m-09/2401, Random frequency selection in femtocell (P80216m/D2-15.4.11) (Kanchei(Ken) Loa, Yi-Ting Lin, Tsung-Yu Tsai, Yung-Lan Tseng; 2009-11-06)
(17) IEEE C802.16m-09/2401r1, An interference mitigation framework in femtocell (Kanchei(Ken) Loa, Yi-Ting Lin, Tsung-Yu Tsai, Yung-Lan Tseng; 2009-11-16)
(18) IEEE C802.16m-09/2401r2, An interference mitigation framework in femtocell (P80216m/D2-15.4.11) (Kanchei(Ken) Loa, Yi-Ting Lin, Tsung-Yu Tsai, Yung-Lan Tseng; 2009-11-17)
(19) IEEE C802.16m-09/2679r1, An interference mitigation framework in femtocell (P80216m/D3-16.4.11) (Kanchei(Ken) Loa, Yi-Ting Lin, Tsung-Yu Tsai, Yung-Lan Tseng, Chun-Yen Hsu, Chiu-Wen Chen; 2010-01-13)
(20) IEEE C802.16m-09/2679r2, An interference mitigation framework in femtocell (P80216m/D3-16.4.11) (Kanchei(Ken) Loa, Yi-Ting Lin, Tsung-Yu Tsai, Yung-Lan Tseng, Chun-Yen Hsu, Chiu-Wen Chen; 2010-01-13)
(21) IEEE C802.16m-09/2769, An interference mitigation framework in femtocell (Kanchei(Ken) Loa, Yi-Ting Lin, Tsung-Yu Tsai, Yung-Lan Tseng, Chun-Yen Hsu, Chiu-Wen Chen; 2009-12-29)
(22) IEEE C802.16m-09/2817, LDM Pattern Parameters Delivery (16.2.3) (Yung-Lan Tseng, Chun-Yen Hsu, Chiu-Wen Chen, Tsung-Yu Tsai, Yi-Ting Lin, Whai-En Chen, Shih-Yuan Cheng, Yih Guang Jan; 2009-12-31)
(23) IEEE C802.16m-09/2817r1, LDM Pattern Parameters Delivery (16.2.3) (Yung-Lan Tseng, Chun-Yen Hsu, Chiu-Wen Chen, Tsung-Yu Tsai, Yi-Ting Lin, Whai-En Chen, Shih-Yuan Cheng, Yih Guang Jan, Andreas Maeder, Linghang Fan; 2010-01-11)
(24) IEEE C802.16m-09/2817r2, LDM Pattern Parameters Delivery (16.2.3) (Yung-Lan

Tseng, Chun-Yen Hsu, Chiu-Wen Chen, Tsung-Yu Tsai, Yi-Ting Lin, Whai-En Chen, Shih-Yuan Cheng, Yih Guang Jan, Andreas Maeder, Linghang Fan, Hassan Alkanani, Nader Zein; 2010-01-11)

(25) IEEE C802.16m-09/2817r3, LDM Pattern Parameters Delivery (16.2.3) (Yung-Lan Tseng, Chun-Yen Hsu, Chiu-Wen Chen, Tsung-Yu Tsai, Yi-Ting Lin, Whai-En Chen, Shih-Yuan Cheng, Yih Guang Jan, Andreas Maeder, Linghang Fan, Hassan Alkanani, Nader Zein; 2010-01-12)

(26) IEEE C802.16m-10/0066r1, Interference mitigation for femtocell (16.4.11) (Kanchei(Ken) Loa, Yi-Ting Lin, Tsung-Yu Tsai, Yung-Lan Tseng, Chun-Yen Hsu, Chiu-Wen Chen, Chun-Che Chien, Youn-Tai Lee, Jong-Kae (JK) Fwu, Hujun Yin, Yi Hsuan, Whai-En Chen, Shiann-Tsong Sheu, Yih Guang Jan, Yang-Han Lee, I.K. Fu, Pei-kai Liao, Paul Cheng, Mihyun Lee, Hokyu Choi, Hyunkyu Yu, Linghang Fan; 2010-03-05)

(27) IEEE C802.16m-10/0066r2, Interference mitigation for femtocell (16.4.11) (Kanchei(Ken) Loa, Yi-Ting Lin, Tsung-Yu Tsai, Yung-Lan Tseng, Chun-Yen Hsu, Chiu-Wen Chen, Chun-Che Chien, Youn-Tai Lee, Jong-Kae (JK) Fwu, Hujun Yin, Yi Hsuan, Whai-En Chen, Shih-Yuan Cheng, Shiann-Tsong Sheu, Chih-Cheng Yang, Yih Guang Jan, Yang-Han Lee, I.K. Fu, Pei-kai Liao, Paul Cheng, Mihyun Lee, Hokyu Choi, Hyunkyu Yu, Linghang Fan, Zheng Yan-Xiu, Chung-Lien Ho, Chang Lan Tsai, Yu-Chuan Fang, Yung-Han Chen; 2010-03-15)

(28) IEEE C802.16m-10/0066r3, Interference mitigation for femtocell (16.4.11) (Kanchei(Ken) Loa, Yi-Ting Lin, Tsung-Yu Tsai, Yung-Lan Tseng, Chun-Yen Hsu, Chiu-Wen Chen, Chun-Che Chien, Youn-Tai Lee, Jong-Kae (JK) Fwu, Hujun Yin, Yi Hsuan, Whai-En Chen, Shiann-Tsong Sheu, Yih Guang Jan, Yang-Han Lee, I.K. Fu, Pei-kai Liao, Paul Cheng, Mihyun Lee, Hokyu Choi, Hyunkyu Yu, Linghang Fan, Zheng Yan-Xiu, Chung-Lien Ho, Chang Lan Tsai, Yu-Chuan Fang, Yung-Han Chen, Feng Xie, Lin Chen, Zhaohua Lu, Yang Liu; 2010-03-16)

(29) IEEE C802.16m-10/0272, Callback HO after femtocell recovery (16.4.8) (Kanchei(Ken) Loa, Yi-Ting Lin, Tsung-Yu Tsai, Yung-Lan Tseng, Chun-Yen Hsu, Chiu-Wen Chen, Chun-Che Chien, Youn-Tai Lee, Jong-Kae (JK) Fwu, Xiangying Yang, Whai-En Chen, Shih-Yuan Cheng, Shiann-Tsong Sheu, Chih-Cheng Yang, Yih Guang Jan, Yang-Han Lee, I.K. Fu, Pei-kai Liao, Paul Cheng, Mihyun Lee, Hokyu Choi, Hyunkyu Yu, Jaehyuk Jang, Ying Li, Jung Je Son; 2010-03-05)

(30) IEEE C802.16m-10/0272r1, Callback HO after femtocell recovery (16.4.8) (Whai-En Chen, Shih-Yuan Cheng, Kanchei(Ken) Loa, Yi-Ting Lin, Tsung-Yu Tsai, Yung-Lan Tseng, Chun-Yen Hsu, Chiu-Wen Chen, Chun-Che Chien, Youn-Tai Lee, Jong-Kae (JK) Fwu, Xiangying Yang, Shiann-Tsong Sheu, Chih-Cheng Yang, Yih Guang Jan, Yang-Han Lee, I.K. Fu, Pei-kai Liao, Paul Cheng, Jaehyuk Jang, Ying Li, Jung Je Son; 2010-03-14)

(31) IEEE C802.16m-10/0272r2, Callback HO after femtocell recovery (16.4.8) (Whai-En Chen, Shih-Yuan Cheng, Kanchei(Ken) Loa, Yi-Ting Lin, Tsung-Yu Tsai, Yung-Lan Tseng, Chun-Yen Hsu, Chiu-Wen Chen, Chun-Che Chien, Youn-Tai Lee, Jong-Kae (JK) Fwu, Xiangying Yang, Shiann-Tsong Sheu, Chih-Cheng Yang, Yih Guang Jan, Yang-Han Lee, I.K. Fu, Pei-kai Liao, Paul Cheng, Jaehyuk Jang, Ying Li, Jung Je Son; 2010-03-15)

(32) IEEE C802.16m-10/0501, Support of Emergency Alert in Sleep Mode (16.2.3) (Chiu-Wen Chen, Chun-Yen Hsu, Kanchei(Ken) Loa, Youn-Tai Lee, Yi-Ting Lin, Tsung-Yu Tsai, Yung-Lan Tseng; 2010-04-30)

(33) IEEE C802.16m-10/0501r1, Support of Emergency Alert in Sleep Mode (16.2.3) (Chiu-Wen Chen, Chun-Yen Hsu, Kanchei(Ken) Loa, Youn-Tai Lee, Yi-Ting Lin,

Tsung-Yu Tsai, Yung-Lan Tseng; 2010-05-11)
(34) IEEE C802.16m-10/0503, Femto ABS IDcell reconfiguration Using Femto Using AAI_NBR-ADV (Tsung-Yu Tsai, Yung-Lan Tseng, Kanchei(Ken) Loa, Chun-Yen Hsu, Chien-Chun Che, Yi-Ting Lin, Chiu-Wen Chen; 2010-04-30)
(35) IEEE C802.16m-10/0504, Femto ABS IDcell Reconfiguration Using AAI_SON-ADV (Yung-Lan Tseng, Tsung-Yu Tsai, Kanchei(Ken) Loa, Yi-Ting Lin, Chiu-wen Chen, Chun-Che Chien, Chun-Yen Hsu; 2010-04-30)
(36) IEEE C802.16m-10/0504r1, Femto ABS IDcell reconfiguration Using AAI_SON-ADV (Yung-Lan Tseng, Tsung-Yu Tsai, Kanchei(Ken) Loa, Yi-Ting Lin, Chiu-wen Chen, Chun-Che Chien, Chun-Yen Hsu; 2010-05-10)
(37) IEEE C802.16m-10/0504r2, Femto ABS IDcell reconfiguration Using AAI_SON-ADV (Yung-Lan Tseng, Tsung-Yu Tsai, Kanchei(Ken) Loa, Yi-Ting Lin, Chiu-wen Chen, Chun-Che Chien, Chun-Yen Hsu; 2010-05-11)
(38) IEEE C802.16m-10/0905, Calibration Sounding Channel with Efficiency Improvement (Tsung-Yu Tsai, Chun-Che Chien, Kanchei(Ken) Loa, Youn-Tai Lee, Yung-Lan Tseng, Yi-Ting Lin, Chun-Yen Hsu, Chiu-wen Chen; 2010-07-09)
(39) IEEE C802.16m-10/0905r1, Calibration Sounding Channel with Efficiency Improvement (Tsung-Yu Tsai, Chun-Che Chien, Kanchei(Ken) Loa, Youn-Tai Lee, Yung-Lan Tseng, Yi-Ting Lin, Chun-Yen Hsu, Chiu-wen Chen; 2010-07-10)
(40) IEEE C802.16m-10/0905r2, Calibration Sounding Channel with Efficiency Improvement (Tsung-Yu Tsai, Chun-Che Chien, Kanchei(Ken) Loa, Youn-Tai Lee, Yung-Lan Tseng, Yi-Ting Lin, Chun-Yen Hsu, Chiu-wen Chen, Yu-Tao Hsieh; 2010-07-13)
(41) IEEE C802.16m-10/0905r3, Calibration Sounding Channel with Efficiency Improvement (Tsung-Yu Tsai, Chun-Che Chien, Kanchei(Ken) Loa, Youn-Tai Lee, Yung-Lan Tseng, Yi-Ting Lin, Chun-Yen Hsu, Chiu-wen Chen, Yu-Tao Hsieh, Ping-Heng Kuo, Pang-An Ting; 2010-07-14)
(42) IEEE C802.16m-10/0985, Calibration Sounding Channel for Multi-BS MIMO with Efficiency Improvement (16.5.1.3.1) (Tsung-Yu Tsai, Chun-Che Chien, Kanchei(Ken) Loa, Youn-Tai Lee, Yung-Lan Tseng, Yi-Ting Lin, Chun-Yen Hsu, Chiu-wen Chen; 2010-08-12)
(43) IEEE C802.16m-10/1136, Calibration Sounding Channel for Multi-BS MIMO with OTA DL/UL Mismatch(16.5.1.3.1) (Tsung-Yu Tsai, Chun-Che Chien, Kanchei(Ken) Loa, Youn-Tai Lee, Yung-Lan Tseng, Yi-Ting Lin, Chun-Yen Hsu, Chiu-wen Chen, ; 2010-09-07)
(44) IEEE C802.16m-10/1149, Clarification on interference mitigation for femtocell (16.4.11) (Yi-Ting Lin, Yung-Lan Tseng, Chun-Yen Hsu, Tsung-Yu Tsai, Chun-Che Chien, Youn-Tai Lee, Chiu-Wen Chen; 2010-09-08)
(45) IEEE C802.16m-10/1149r1, Clarification on interference mitigation for femtocell (16.4.11) (Yi-Ting Lin, Yung-Lan Tseng, Chun-Yen Hsu, Tsung-Yu Tsai, Chun-Che Chien, Youn-Tai Lee, Chiu-Wen Chen, Jin Lee, Anshuman Nigam; 2010-09-13)
(46) IEEE C802.16m-10/1150, Clarification on Femto ABS reselection by AMS (16.4.7.5) (Yung-Lan Tseng, Yi-Ting Lin, Chun-Yen Hsu, Tsung-Yu Tsai, Chun-Che Chien, Youn-Tai Lee, Chiu-Wen Chen; 2010-09-08)
(47) IEEE C802.16m-10/1150r1, Clarification on Femto ABS reselection by AMS (16.4.7.5) (Yung-Lan Tseng, Yi-Ting Lin, Chun-Yen Hsu, Tsung-Yu Tsai, Chun-Che Chien, Youn-Tai Lee, Chiu-Wen Chen; 2010-09-14)
(48) IEEE C802.16m-10/1150r2, Clarification on Femto ABS reselection by AMS (16.4.7.5) (Yung-Lan Tseng, Yi-Ting Lin, Chun-Yen Hsu, Tsung-Yu Tsai, Chun-Che Chien, Youn-Tai Lee, Chiu-Wen Chen; 2010-09-14)

(49) IEEE C802.16m-10/1151, Cell Bar bit limitation towards CSG-Open Femto ABS (16.4.7.3) (Yung-Lan Tseng, Chun-Yen Hsu, Yi-Ting Lin, Tsung-Yu Tsai, Chun-Che Chien, Youn-Tai Lee, Chiu-Wen Chen; 2010-09-08)
(50) IEEE C802.16m-10/1165, Clean-up for interference mitigation trigger condition (16.4.11.1) (Yi-Ting Lin, Yung-Lan Tseng, Chun-Yen Hsu, Tsung-Yu Tsai, Chun-Che Chien, Youn-Tai Lee, Chiu-Wen Chen; 2010-09-08)
(51) IEEE C802.16m-10/1295, Clarification on Femto ABS reselection by AMS (16.4.7.5) (Yi-Ting Lin, Chun-Yen Hsu, Yung-Lan Tseng, Tsung-Yu Tsai, Chun-Che Chien, Youn-Tai Lee, Chiu-Wen Chen; 2010-10-25)
(52) IEEE C802.16m-10/1295r1, Clarification on Femto ABS reselection by AMS (16.4.7.5) (Yi-Ting Lin, Chun-Yen Hsu, Yung-Lan Tseng, Tsung-Yu Tsai, Chun-Che Chien, Youn-Tai Lee, Chiu-Wen Chen, Yu-Tao Hsieh, Pang-An Ting; 2010-11-08)
(53) IEEE C802.16m-10/1295r2, Clarification on Femto ABS reselection by AMS (16.4.7.5) (Yi-Ting Lin, Chun-Yen Hsu, Yung-Lan Tseng, Tsung-Yu Tsai, Chun-Che Chien, Youn-Tai Lee, Chiu-Wen Chen, Yu-Tao Hsieh, Pang-An Ting; 2010-11-09)
(54) IEEE C802.16m-10/1296, Clarification on Femto ABS reselection by AMS (16.4.7.5) (Yi-Ting Lin, Yung-Lan Tseng, Chun-Yen Hsu, Tsung-Yu Tsai, Chun-Che Chien, Youn-Tai Lee, Chiu-Wen Chen; 2010-10-25)
(55) IEEE C802.16m-10/1296r1, Clarification on Femto ABS reselection by AMS (16.4.7.5) (Yi-Ting Lin, Yung-Lan Tseng, Chun-Yen Hsu, Tsung-Yu Tsai, Chun-Che Chien, Youn-Tai Lee, Chiu-Wen Chen, Yu-Tao Hsieh, Pang-An Ting; 2010-11-08)
(56) IEEE C802.16m-10/1296r2, Clarification on Femto ABS reselection by AMS (16.4.7.5) (Yi-Ting Lin, Yung-Lan Tseng, Chun-Yen Hsu, Tsung-Yu Tsai, Chun-Che Chien, Youn-Tai Lee, Chiu-Wen Chen, Yu-Tao Hsieh, Pang-An Ting; 2010-11-09)
(57) IEEE C802.16m-10/1425, Figure Clarification of PHS Signaling (5.2.3.2) (Chun-Yen Hsu, Yung-Lan Tseng; 2010-12-16)